Improvements to the design methodology and control of semicontinuous distillation

IMPROVEMENTS TO THE DESIGN METHODOLOGY AND CONTROL OF SEMICONTINUOUS DISTILLATION

By Pranav Bhaswanth MADABHUSHI,

A Thesis Submitted to the School of Graduate Studies in the Partial Fulfillment of the Requirements for the Degree Doctor of Philosophy

McMaster University
Doctor of Philosophy (2020)
Hamilton, Ontario (Department of Chemical Engineering)

TITLE: Improvements to the design methodology and control of semicontinuous distillation
AUTHOR: Pranav Bhaswanth MADABHUSHI (McMaster University)
SUPERVISOR: Dr. Thomas Alan ADAMS II
NUMBER OF PAGES: xvii, 99

Abstract

Distillation technology has been evolving for many decades for a variety of reasons, with the most important ones being energy efficiency and cost. As a part of the evolution, semicontinuous distillation was conceived, which has the advantages of both batch and continuous distillation. The economic benefits of this intensified process compared to batch and continuous distillation were expounded in many of the previous studies. Semicontinuous distillation of ternary mixtures, which is the main focus of this thesis, is carried out in a single distillation column with a tightly integrated external middle vessel and the operation is driven by a control system. The system operation does not include any start-up or shut-down phases of the column and has three periodically repeating operating modes.

In the status quo design procedure, called the 'sequential design methodology,' an imaginary continuous distillation system design was used to design the semicontinuous distillation system. In this methodology, dynamic simulations of the process were used to find the values of the controller tuning parameters based on the design of the continuous system. Afterwards, black-box optimization was used to find better controller tuning parameter values that minimized cost. However, after analyzing the dynamics of the system for different cases, it was found that the heuristics used in this design methodology yielded suboptimal designs. Therefore, the primary goal of the thesis is to improve these heuristics by incorporating more knowledge of the system and thereby develop a better design methodology.

Firstly, the setpoint trajectories generated by the ideal side draw recovery arrangement for side stream flowrate control, which was standard in most semicontinuous distillation studies, was modified. In this thesis, the performance of the status quo as compared to the modified version, based on the criteria, cycle time and cost for different case studies, was presented. Results showed that the modified-ideal side draw recovery arrangement for side stream flowrate control performed better with a 10-20% lower separating cost while maintaining

product purities. Furthermore, to reap more cost benefits, dynamic optimization was used to seek the flow rate trajectory that minimized cost. However, it was found that the additional cost savings, which is in addition to the benefits gained by using the modified version, were at the most 2% from different case studies.

Subsequently, the impact of changing the imaginary continuous distillation system design on the nature of the semicontinuous distillation limit cycle, specifically, its period was studied. Results revealed the necessity for a new design procedure, and thus the back-stepping design methodology was proposed. This design methodology was used to find better limit cycles of zeotropic ternary semicontinuous distillation using the aspenONE Engineering suite. The proposed methodology was applied to three different case studies using feed mixtures with different chemical components. A comparison with the sequential design methodology for the two case studies indicates that the new method outperforms the state-of-the-art by finding limit cycles that were 4% to 57% lower in terms of cost. Furthermore, the designs obtained from this procedure were guaranteed to have feasible column operation with stable periodic steady-state behaviour.

Semicontinuous distillation design using the design methodology with heuristic components involves guessing, checking and then using black-box optimization to find the values of the design variables to meet some performance criteria. Furthermore, mathematical guarantees of either local or global optimality of the designs obtained from the design procedure do not exist. Therefore, to address these issues, in this thesis, the application of using the shooting method for designing the semicontinuous distillation process was demonstrated using two case studies, which involve the separation of hexane, heptane and octane. This method has the potential to be combined with gradient-based optimization algorithms for optimization of the process design in the future.

Acknowledgements

I am deeply indebted to my supervisor Dr. Thomas Adams II, for playing a fundamental role in shaping my doctoral work. Dr. Adams provided the guidance, assistance, and expertise that I needed during the time I was lost and at the same time gave the freedom to branch out into uncharted territories of semi-continuous distillation. I cannot perceive a better supervisor. I am grateful for the feedback given by my committee members Dr. Mhaskar and Dr. Davidson to improve the research quality of the thesis.

I am delighted to be a part of the McMaster Advanced Control Consortium (MACC), where friendships were struck, discussions prevailed, and valuable lessons were learnt. My special thanks to Ikenna Okeke, Anthony Quarshie, Leila Hoseinzade, and many others who later joined for the stimulating conversations we have had and keeping a lively workplace environment. Encouragement from Gowtham Kotam, Lakshmi Narayana Battigiri, Ravi Chander Dutta, and Sashank Kasiraju during the times when it was needed is something that I cannot forget. And finally, my gratitude to some of the close family members who played a crucial role in supporting me while I completed the thesis.

This thesis is dedicated to my parents, wife, siblings, and the loving memory of my grandparents.

"Yasyāmatam Tasya Matam. Matam Yasya Na Veda Sah.
Avijñātam Vijānatām. Vijñātam Avijānatām"

Those who think they know, do not know. Those who think they do not know, really know. Know that which is not known. Ignore what you think you know.

— Kenopanishad – 2-3

Contents

List of Figures

List of Tables

Declaration of Authorship

I, Pranav Bhaswanth MADABHUSHI, declare that I was the primary investigator in this thesis titled, "Improvements to the design methodology and control of semicontinuous distillation" and the work presented in it are my own research contributions. I confirm that:

- the published scholarly work that presented as a reprint in Chapter 2 has my full contribution to project conceptualization, investigation and analysis, model development and simulation, and manuscript preparation. In this work, a new heuristic model is proposed for side stream flowrate control, which leads to cost savings of almost 20% when compared to the status quo.

- the published scholarly work presented as a reprint in Chapter 3, Section 3.1 has my contribution as a supervisor to an undergraduate summer research student, Edgar Iván Sánchez Medina, which involves project conceptualization, investigation and analysis, and manuscript preparation. In this work, simulation experiments were conducted by the student under my guidance. The outcome from this work confirmed the hypothesis that the design of the hypothetical continuous distillation system design affects the characteristics of the limit cycle in which the semicontinuous distillation system operates.

- the published scholarly works which are presented as reprints in Chapter 3, Sections 3.2 and 3.3 has my full contribution to project conceptualization, investigation and analysis, model development and simulation, and manuscript preparation. In this work, a new design methodology was proposed to find cost-effective semicontinuous distillation designs. Application of the design methodology to three case studies produced designs with cost savings of 4 to 57% compared to the best-known cases.

- the work presented in Chapter 4, which is a manuscript draft, has my full contribution to project conceptualization, investigation and analysis, model development and simulation, and manuscript preparation. The application of the single shooting method to precisely find the location of the limit cycle is demonstrated using two case studies in this work. This work is a precursor to devising a systematic design procedure to obtain an optimal semicontinuous distillation design.

Chapter 1

Introduction

1.1 Semicontinuous distillation

Distillation, which is a thermal separation process, is generally categorized into continuous distillation (steady-state operation), and batch distillation (time varying operation) based on the distillation column operation. In the steady-state operation of continuous distillation, the feed mixture is constantly supplied to the distillation column while the top and bottoms products are continually removed. Contrastingly, in conventional batch distillation, the feed is fed to the reboiler at the beginning of the column operation. During the operation, the top product is continuously withdrawn depleting the content in the reboiler over time, thus making the process operation unsteady. Continuous distillation is primarily implemented in bulk chemical and petrochemical industries because it is economical when processing large production volumes (Kim and Diwekar 2005). Specialty chemical, biochemical, and pharmaceutical industries are places where batch distillation is primarily implemented. This is because ordinary batch distillation is flexible in handling uncertainties in raw material and product specifications and is economical at small production volumes (Kim and Diwekar 2005).

Continuous distillation of zeotropic mixtures with n components into n product streams (each enriched in a component) is carried out in a sequence of distillation columns, called the 'distillation configuration' (Jiang and Agrawal 2019).

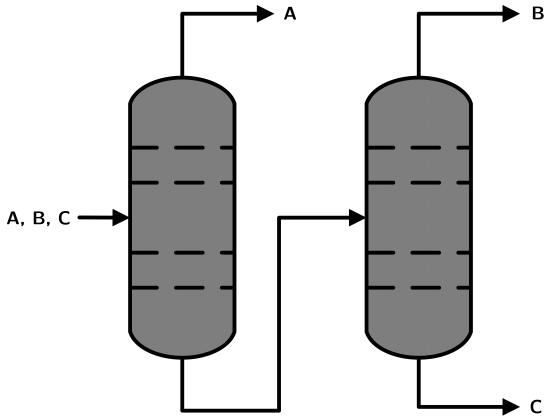

FIGURE 1.1: The continuous distillation of ternary mixtures. A = High volatile component, B = Intermediate volatile component, C = Low volatile component.

As an example, Figure 1.1 illustrates the continuous distillation of ternary mixtures using two distillation columns. However, the operational flexibility and the unsteady behaviour of batch distillation are features that are exploited to create different 'distillation column configurations' such as multifraction batch distillation column (Diwekar 2011; Kim and Diwekar 2005). Multicomponent mixtures distilled using multifraction batch distillation requires only one distillation column, unlike continuous distillation that requires $n - 1$ columns (Diwekar 2011; Kim and Diwekar 2005). Apart from multifraction batch distillation, specifically, for distilling ternary mixtures, which is the focus of this thesis, the batch operation of the middle-vessel column (Figure 1.2) was proposed as an attractive alternative compared to ordinary batch distillation and stripping columns (Davidyan et al. 1994; Robinson et al. 1930; Hasebe et al. 1996).

The middle-vessel is a single process vessel that combines the stripping and rectifying columns (Kim and Diwekar 2005). In the middle-vessel column, the light and heavy components in the mixture were withdrawn from the top and the bottom of the column while the intermediate component concentrates in the middle-vessel (Hasebe et al. 1996). The feed mixture is supplied to the middle-vessel, which is, in turn, pumped to the feed stage of the column, while material from this stage is recycled back to the middle-vessel (Hasebe et al. 1996).

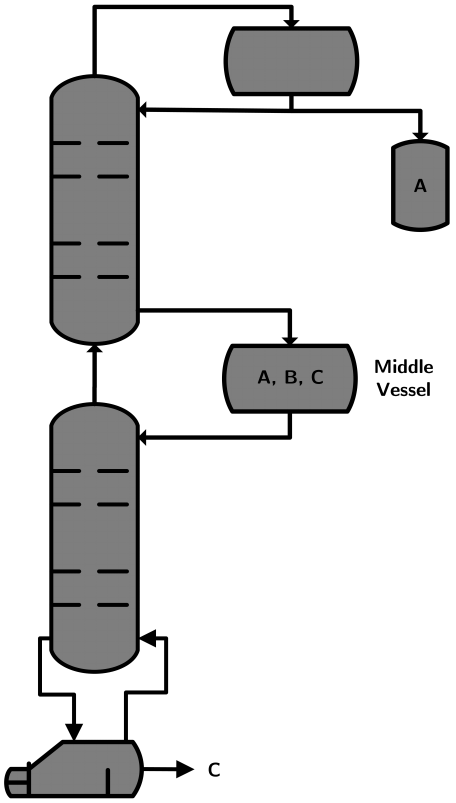

FIGURE 1.2: The batch middle-vessel distillation of ternary mixtures. A = High volatile component, B = Intermediate volatile component, C = Low volatile component.

This system was concluded to be superior compared to ordinary batch distillation for binary separations and ternary separations (under certain conditions) based on separation time as performance criteria (Hasebe et al. 1996; Meski and Morari 1995). Soon after, a natural generalization of the middle-vessel column with total reflux batch operation was proposed by Hasebe et al. (1995), with further generalizations suggested by Skogestad et al. (1997) for multi-component separations. Later, Phimister and Seider (2000), introduced the semicontinuous operation of the middle-vessel column for separation of ternary mixtures, which was subsequently called semicontinuous distillation. A multi-vessel extension of this system was also later simulated for multicomponent separations by Wijesekera and Adams (2015a) and Wijesekera and Adams (2015b).

Since a significant portion of a chemical or refining plant's energy requirement is associated with distillation, innovations surrounding the base distillation configuration are essential to becoming more energy efficient (Sholl and Lively 2016; Humphrey and Siebert 1992; Jiang and Agrawal 2019). Typically, process intensification principles are used to devise energy-efficient distillation configurations with heat integration and thermal couplings (Rong and Turunen 2006; Jiang and Agrawal 2019). Semicontinuous distillation is known to incorporate these principles by including some of the advantages of both batch and continuous distillation (Phimister and Seider 2000; Adams and Pascall 2012). It has a lower capital cost requirement than continuous distillation because multicomponent separation is carried out using only one distillation column and $n-2$ process vessels, which are cheaper than the distillation units (Adams II and Seider 2009). A comparative analysis indicated that this process is economical compared to continuous distillation in terms of annualized cost per annual production rate (separating cost) at the intermediate production scale considering a small payback period. This is because, at the intermediate production scale, the lower total direct costs of the process offsets the increase in operating costs (Pascall and Adams 2013a; Pascall and Adams 2013b; Wijesekera and Adams 2015a; Wijesekera and Adams 2015b; Meidanshahi and Adams II 2015; Meidanshahi and Adams II 2016).

The capital cost of semicontinuous distillation is however comparable to batch distillation since the number of pieces of equipment in both cases is about the same. Similar to batch distillation, the process is inherently flexible (Phimister and Seider 2000). Also, the energy requirements in semicontinuous distillation is typically lower than batch distillation because it does not have the column startup or shutdown phases during operation. With these advantages, the process is ideal for implementation in industries that are scaling up their production capacities from the small scale to a larger scale. Also, industries operating at the intermediate production scale, for example specialty chemicals production and biorefineries (Phimister and Seider 2000; Adams and Pascall 2012) can reap the benefits that this process has to offer. There are also other applications for the semicontinuous operation of the middle-vessel column, namely,

pressure-swing azeotropic distillation, extractive distillation, and semicontinuous distillation with integrated reaction (Adams and Pascall 2012). In this thesis, the focus is entirely on the semicontinuous distillation of ternary zeotropic mixtures, except for a case of the separation of the quaternary zeotropic mixture in Chapter 2.

1.2 Brief process description

For separating ternary mixtures, semicontinuous distillation operation has three different operating modes that were classified based on the state of the middle-vessel (Adams and Pascall 2012). The three operating modes were called the separating mode, the discharging mode, and the charging mode (Adams and Pascall 2012). In the separating mode, the middle-vessel is enriched gradually with the intermediate volatile component of the ternary mixture by recycling a side stream from the distillation column to the middle-vessel. Upon reaching the desired purity, the separating mode ends, and the discharging mode begins. As this mode begins, instantaneously, the material in the middle-vessel is discharged through the discharge stream until a pre-determined lower limit of the liquid height is reached. The lower limit was chosen such that the pump that transports material from the middle-vessel to the distillation column does not cavitate. The instance that the discharging mode ends, the charging mode begins. At this point, material flow through the discharge stream is stopped, and fresh feed to be separated is charged to the middle-vessel through the charging stream. The charging mode ends when the liquid height in the middle-vessel reaches a pre-determined upper limit, which was chosen to operate the process within the safety constraints. At this moment, material flow through the charging stream is stopped, triggering the start of a new separating mode, thus, making the process operation periodic.

The process operation within each mode is dynamic; however, the overall process operates in a periodic steady-state called the 'limit cycle' because of its periodic behaviour. To distinguish between different kinds of steady-states, in this thesis, the limit cycle is specifically referred to as a periodic steady-state.

A decentralized control system drives the process operation described in the above paragraph (Figure 1.3). This control system is used to maintain the mass-averaged top and bottoms product purities, the reflux drum and sump levels, and the column pressure at the desired setpoint values (Pascall and Adams 2013a). It also has a feedback loop to control the flowrate side stream that is recycled to the middle-vessel to follow a desired setpoint trajectory (Pascall and Adams 2013a).

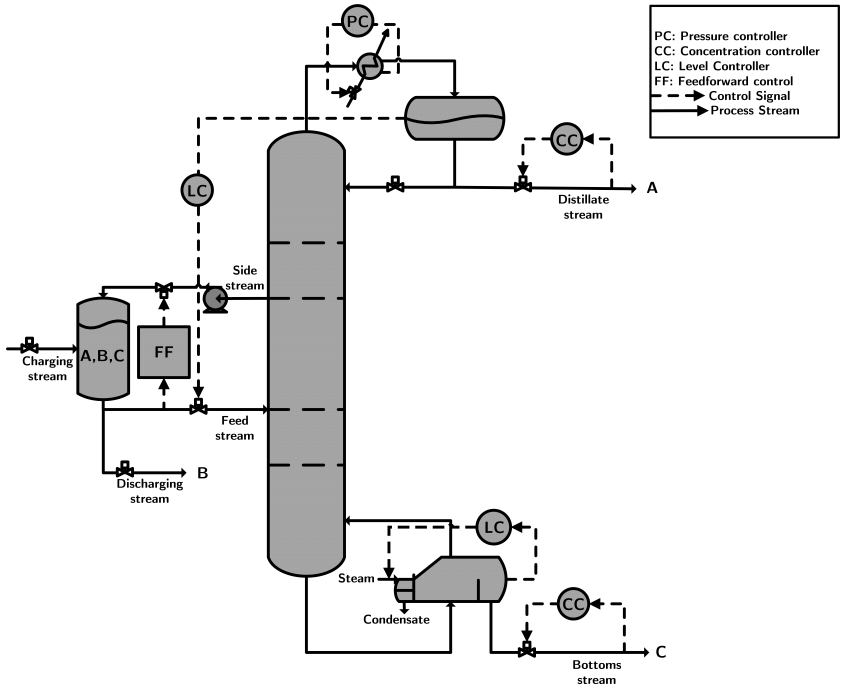

FIGURE 1.3: The semicontinuous distillation of ternary mixtures. Reprinted with permission from Madabhushi, Pranav Bhaswanth, and Thomas A. Adams II. "Side stream control in semicontinuous distillation." Computers & Chemical Engineering 119 (2018): 450-464. Copyright 2018 Elsevier.

1.3 The sequential design methodology

In semicontinuous distillation, the intention is to design the system to separate the components in the ternary mixture to the desired purity requirements while maintaining the column operation within feasible limits. Furthermore, there

can be many designs that meet these requirements, and therefore the goal is to find a cost-effective design among them. To this end, semicontinuous distillation design has two essential steps, the design of the column and the middle-vessel, and the design of the control system. The degrees of freedom available these steps can be classified as time-invariant design variables, and time-varying design variables (or control variables). Since feedback control is used to meet the desired setpoint values or trajectories, these become the degrees of freedom instead of the control variables. The time-invariant design variables of the system are, equipment sizes, the number of trays, feed stage location, side stream stage location, reflux rate, and controller tuning parameters. The side stream flowrate trajectory alone is a time-varying design degree of freedom.

The simultaneous design of the process and the tightly integrated decentralized control system is quintessential because the process is control-driven. However, in most of the previous studies, a sequential design methodology (heuristic-based) was followed because the simultaneous approach is complex (Meidanshahi and Adams II 2016). In this design procedure, instead of designing a semicontinuous distillation system, a hypothetical continuous distillation system is designed. This system was designed to distill the ternary feed mixture to the desired values of top and bottoms product purities, respectively. In this continuous distillation system, which has its basis in the semicontinuous distillation system, the side stream from the distillation column is not recycled to the middle-vessel. The values of the time-invariant design variables (except the controller tuning parameters) of the semicontinuous distillation system, were determined by designing this hypothetical continuous distillation system.

Moreover, the steady-state of this continuous distillation system was used as the initial state to simulate the periodic steady-state of the semicontinuous distillation process. The setpoints of the controllers were provided to meet the design objectives, while a model gave the setpoint trajectory of the side stream flowrate controller. The model was derived to reduce the loss of intermediate volatile component through the distillate and bottoms streams of the column (Adams and Seider 2008). Simulations are carried out for various combinations of the controller tuning parameter values found using a trial-and-error method

until the system operates in a desirable limit cycle. Then, a derivative-free optimization routine is used to find the controller tuning parameter values that minimized the separating cost.

1.4 Contributions

Evidently, from the above description of the sequential design methodology, it is clear that heuristics formed the basis for its development. Furthermore, these heuristics did not have a firm theoretical foundation, being arbitrary in nature. Thus, the main contribution of this thesis is to develop a better heuristics, which can give improved designs in terms of cost compared to the state-of-the-art. Chapters 2 and 3 primarily focus on incorporating better heuristic knowledge to find designs that are more economical than the best-known. Although the heuristic design method proposed in Chapter 3 is convenient because of the simplicity involved in its application, there are challenges. To overcome the drawbacks, in Chapter 4 of this thesis, the single shooting method for semicontinuous distillation design is introduced. This method paves the way for the future development of an systematic (relies on minimal/no heuristic knowledge) design methodology, which can yield an optimal design. In the final chapter, suggestions for future work, conclusions and closing remarks are outlined.

1.4.1 Model-based approach to side stream flowrate control

In the sequential design methodology, the flowrate of the material that is recycled through the side stream to the middle-vessel is controlled by a PI controller to follow a setpoint trajectory, which was given by the 'Ideal Side draw recovery arrangement' (Pascall and Adams 2013a; Pascall and Adams 2013b; Meidanshahi and Adams II 2016; Wijesekera and Adams 2015a; Wijesekera and Adams 2015b). In these studies, this is referred to as the 'Ideal Side draw recovery arrangement' feedforward control law since the process was perceived to be at a pseudo steady-state at each time step with the concentration changes in the column feed considered to be disturbances. In Chapter 2, however, the feedforward control law is specifically referred to as the control model because it is only

a means to generate side stream flowrate trajectories that are followed by the PI controller, which uses the PI control law. The 'Ideal Side draw recovery arrangement' feedforward control law was derived from the mathematical model of the column by assuming that it operates at a pseudo steady-state at all times during the dynamic operation in each mode. Additional assumptions were made to ensure that the loss of intermediate volatile component through the distillate and bottoms streams of the column is reduced (Adams and Seider 2008). Although the extra assumptions that were imposed on the system were reasonable, removing some of them and re-deriving the model was found to generate setpoint trajectories with much higher recycling rates, which ultimately lead to lower separating cost limit cycles than the status quo. The new feedforward control law was called the 'Modified-Ideal Side draw Recovery arrangement.' Case studies indicate that the systems operated in a periodic steady-state where the reduction in separating cost is 10-20% lower than the best-known. All the simulations and optimization runs were carried out in Aspen V10 simulation environment.

Furthermore, the discovery that "Ideal Side draw Recovery arrangement" limits the flowrate range in the setpoint trajectories that it generates led to the search for optimal trajectories. Dynamic optimization was therefore carried out to find a better side stream flowrate trajectory that minimizes the separating cost than the best trajectory from the 'Modified-Ideal Side draw Recovery arrangement', while meeting all the enforced constraints. The results from different cases indicate that the additional cost reduction obtained as a consequence of the optimization is negligible. Moreover, it was speculated that the design of the hypothetical continuous distillation system might influence the periodic steady-state in which the semicontinuous distillation system operates.

The results from this research contribution were published in the peer-reviewed journal Computers and Chemical Engineering, and is presented in Chapter 2 of this thesis.

The full citation of the paper is – Madabhushi, Pranav Bhaswanth, and Thomas A. Adams II. "Side stream control in semicontinuous distillation." Computers & Chemical Engineering 119 (2018): 450-464.

1.4.2 The back-stepping design methodology

As a consequence of the speculation that the design of the hypothetical continuous distillation system has an influence on the characteristics (particularly cycle time) of the periodic steady-state of the semicontinuous distillation system, simulation experiments were conducted. Analysis of the results from the experiments concludes that the sequential design methodology inherently produced sub-optimal semicontinuous distillation designs. Specifically, it was found that the reflux rate and the sizing of the side stream pump and valve played an essential role in leading to an economical periodic steady-state operation of the process. The results were published as conference proceedings in Computer Aided Chemical Engineering, and is presented in Chapter 3 of this thesis. The full citation of the conference proceeding is – Madabhushi, Pranav Bhaswanth, Edgar Iván Sánchez Medina, and Thomas Alan Adams II. "Understanding the dynamic behaviour of semicontinuous distillation." In Computer Aided Chemical Engineering, vol. 43, pp. 845-850. Elsevier, 2018.

Consequently, a new design methodology, called the "Back-stepping design methodology," which iteratively changes the hypothetical continuous distillation design was proposed. The iterations ensured that a hydraulically feasible (meeting flooding, weeping and weir loading limits) semicontinuous distillation design is obtained, while choosing a suitable side stream pump and valve size. Similar to the sequential design methodology, this design procedure uses a derivative-free optimization routine to find cost-effective designs by varying the reflux rate, controller tuning parameters, and the initial state, which is the steady-state of the hypothetical continuous distillation system. This design procedure was used to design the semicontinuous distillation of two different ternary mixtures, where better designs were found (4-16% lower separating cost) compared to the state-of-the-art. The results from this research contribution were published in the peer-reviewed journal Industrial & Engineering Chemistry Research, and is presented in Chapter 3 of this thesis.

The full citation of the paper is – Madabhushi, Pranav Bhaswanth, and Thomas Alan Adams. "Finding Better Limit Cycles of Semicontinuous Distillation. 1.

Back Stepping Design Methodology." Industrial & Engineering Chemistry Research 58, no. 36 (2019): 16654-16666.

The back-stepping design methodology is augmented for cases when points in the design space (space of design variables) exhibit different types of steady-state behaviour. The steady-state behaviours displayed were an undesired fixed point (the system operates in steady-state where the desired mass-averaged product purities are not obtained), or the desired limit cycle (the system operates in periodic steady-state where the desired mass-averaged product purities are achieved). This extension to the design procedure is necessary because *a priori* knowledge of the systems' steady-state behaviour in the design space does not exist. The extended methodology was used to design the semicontinuous distillation of dimethyl ether, methanol, and water. The design obtained from the new design procedure outperforms the status quo design in terms of cost (57% lower in separating cost). The results from this research contribution were published in the peer-reviewed journal Industrial & Engineering Chemistry Research and is presented in chapter 3 of this thesis.

The full citation of the paper is – Madabhushi, Pranav Bhaswanth, and Thomas A. Adams. "Finding Better Limit Cycles in Semicontinuous Distillation. 2. Extended Back-Stepping Design Methodology." Industrial & Engineering Chemistry Research 58, no. 36 (2019): 16667-16675.

1.4.3 Single shooting method for semicontinuous distillation design

In the sequential and back-stepping design methodologies many simulations of the semicontinuous distillation system are performed to find a feasible design, and then an optimal design is sought after using a derivative-free optimization routine. Although better heuristic knowledge is incorporated to yield better designs in terms of cost in the back-stepping design methodology, ultimately the method is still a guess and check procedure. A large number of otherwise avoidable simulations are necessary to reject undesirable parts of the design space, thus needing a significant amount of CPU time (typically of the order of

weeks) for design optimization. Moreover, the meta-heuristic based optimization procedure does not guarantee that the design obtained in finite CPU time is a global optimum. And most often, the assurance that the design is a local optimum is also slim.

The simulation of semicontinuous distillation entails numerical integration of the accurate dynamic model of the system that includes operating mode transitions. The numerical integration is started from an initial state (steady-state of the hypothetical continuous distillation system) that does not lie on the limit cycle. Termination of the numerical integration is based on visual confirmation that a limit cycle is reached by visually tracking trajectories of some state variables. Thus, ascertaining that a limit cycle is attained is impossible in the black-box optimization (Audet and Hare 2017) phase, which necessitates having a heuristically chosen termination criterion. Note here that in this thesis, black-box optimization is used interchangeably with derivative-free optimization because the particle swarm algorithm was used to carry out the optimization of the black-box objective and constraint functions.

Therefore, to address these problems, for the first time, the use of shooting method to precisely locate the limit cycle of the semicontinuous distillation system is demonstrated in this thesis. To this end, a two-point boundary value formulation of the semicontinuous distillation system with non-separable periodic boundary conditions (Ascher and Petzold 1998) is presented. This boundary value problem is solved numerically using the shooting method, which converts it into an initial value problem. Newton's method is then used to calculate the zeros of the boundary conditions to iteratively converge to a point on the limit cycle (Ascher and Petzold 1998; Parker and Chua 2012). In Chapter 4, the method is applied on two different cases to illustrate the contrasts between the shooting method for semicontinuous distillation design and the previous methods. A draft manuscript of the full paper containing contributions from this work is submitted to the journal Chemical Engineering Research & Design – Madabhushi, Pranav Bhaswanth, and Thomas A. Adams. "On the application of shooting method for semicontinuous distillation design."

References

Adams II, T. A. and Seider, W. D. (2009). Design heuristics for semicontinuous separation processes with chemical reactions. *Chemical Engineering Research and Design* 87(3), 263–270.

Adams, T. A. and Pascall, A. (2012). Semicontinuous thermal separation systems. *Chemical Engineering & Technology* 35(7), 1153–1170.

Adams, T. A. and Seider, W. D. (2008). Semicontinuous distillation for ethyl lactate production. *AIChE journal* 54(10), 2539–2552.

Ascher, U. M. and Petzold, L. R. (1998). *Computer methods for ordinary differential equations and differential-algebraic equations*. Vol. 61. Siam.

Audet, C. and Hare, W. (2017). *Derivative-free and blackbox optimization*. Springer.

Davidyan, A. G., Kiva, V. N., Meski, G. A., and Morari, M. (1994). Batch distillation in a column with a middle vessel. *Chemical Engineering Science* 49(18), 3033–3051.

Diwekar, U. (2011). *Batch distillation: simulation, optimal design, and control*. CRC Press.

Hasebe, S., Kurooka, T., Aziz, B. B. A., Hashimoto, I., and Watanabe, T. (1996). Simultaneous separation of light and heavy impurities by a complex batch distillation column. *Journal of chemical engineering of Japan* 29(6), 1000–1006.

Hasebe, S., Kurooka, T., and Hashimoto, I. (1995). Comparison of the separation performances of a multi-effect batch distillation system and a continuous distillation system. In: *Dynamics and Control of Chemical Reactors, Distillation Columns and Batch Processes (Dycord'95)*. Elsevier, 249–254.

Humphrey, J. and Siebert, A. (1992). Separation technologies: an opportunity for energy savings. *Chemical Engineering Progress* 88 (3). ISSN: 0360-7275.

Jiang, Z. and Agrawal, R. (2019). Process intensification in multicomponent distillation: A review of recent advancements. *Chemical Engineering Research and Design* 147, 122–145.

Kim, K.-J. and Diwekar, U. (2005). Batch distillation. In: *Batch processes*. CRC Press, 119–162.

Meidanshahi, V. and Adams II, T. A. (2015). A new process for ternary separations: Semicontinuous distillation without a middle vessel. *Chemical Engineering Research and Design* 93, 100–112.

Meidanshahi, V. and Adams II, T. A. (2016). Integrated design and control of semicontinuous distillation systems utilizing mixed integer dynamic optimization. *Computers & Chemical Engineering* 89, 172–183.

Meski, G. A. and Morari, M. (1995). Design and operation of a batch distillation column with a middle vessel. *Computers & chemical engineering* 19, 597–602.

Parker, T. S. and Chua, L. (2012). *Practical numerical algorithms for chaotic systems*. Springer Science & Business Media.

Pascall, A. and Adams, T. A. (2013a). Semicontinuous Separation of Bio-Dimethyl Ether from a Vapor–Liquid Mixture. *Industrial & Engineering Chemistry Research* 53(13), 5081–5102.

Pascall, A. and Adams, T. A. (2013b). Semicontinuous separation of dimethyl ether (DME) produced from biomass. *The Canadian Journal of Chemical Engineering* 91(6), 1001–1021.

Phimister, J. R. and Seider, W. D. (2000). Semicontinuous, middle-vessel distillation of ternary mixtures. *AIChE journal* 46(8), 1508–1520.

Robinson, C. S. et al. (1930). Elements of Fractional Distillation.

Rong, B.-G. and Turunen, I. (2006). Synthesis of new distillation systems by simultaneous thermal coupling and heat integration. *Industrial & Engineering chemistry research* 45(11), 3830–3842.

Sholl, D. and Lively, R. (2016). Seven chemical separations to change the world. *Nature* 532, 435–437.

Skogestad, S., Wittgens, B., Litto, R., and Sørensen, E. (1997). Multivessel batch distillation. *AIChE Journal* 43(4), 971–978.

Wijesekera, K. N. and Adams, T. A. (2015a). Semicontinuous distillation of quaternary mixtures using one distillation column and two integrated middle vessels. *Industrial & Engineering Chemistry Research* 54(19), 5294–5306.

Wijesekera, K. N. and Adams, T. A. (2015b). Semicontinuous distillation of quintenary and N-ary mixtures. *Industrial & Engineering Chemistry Research* 54(51), 12877–12890.

Chapter 2

Improvements to side stream control

The content of this chapter is a **published reprint** of the following peer-reviewed publication,

Madabhushi, Pranav Bhaswanth, and Thomas A. Adams II. "Side stream control in semicontinuous distillation." Computers & Chemical Engineering 119 (2018): 450-464.

Computers and Chemical Engineering 119 (2018) 450–464

Contents lists available at ScienceDirect

Computers and Chemical Engineering

journal homepage: www.elsevier.com/locate/compchemeng

Side stream control in semicontinuous distillation

Pranav Bhaswanth Madabhushi, Thomas A. Adams II*

Department of Chemical Engineering, McMaster University, 1280 Main St. West, Hamilton, Ontario L8S 4L8, Canada.

ARTICLE INFO

Article history:
Received 11 April 2018
Revised 27 August 2018
Accepted 1 September 2018
Available online 25 September 2018

Keywords:
Semicontinuous distillation
side stream control
dynamical system analysis
dynamic optimization

ABSTRACT

The idea to reduce cycle time (T), by controlling the side stream flow rate using a feedforward control model – the ideal side draw recovery arrangement (ISR) – was standard in most semicontinuous distillation studies. However, its effect particularly on 'T' and more broadly on the system dynamics was not clearly understood. In the current study, we compare the performance of using a modified form of ISR model with the status quo based on the criteria T and separating cost (SC) on different case studies. Results show that the modified control model performed better with a 10-20% reduction in SC while maintaining product purities. Furthermore, the side stream flow rate trajectory that minimizes SC was found by using dynamic optimization and it did not differ a lot from the trajectory generated by the modified control model. The improvement in SC was at most 2%.

1. Introduction

Distillation in process industries is a common separation technology with a major portion of plant operating costs associated with it (Adams and Pascall, 2012). Distillation systems are typically operated either in batches or continuously, where the choice is based on the production volume, feed composition, and product demand variability (Phimister and Seider, 2000a). Batch distillation is used in situations where the production demand is low or for high process flexibility, for example, pharmaceutical industries and biofuel production plants. Conversely, continuous distillation typically involves high volume production with low process flexibility—a common situation in petrochemical production facilities.

Alternatively, an atypical process for the separation of multicomponent mixtures is semicontinuous distillation. It is ideal for industries that are scaling up their production capacities from the batch mode, such as in pharmaceutical industries (Pascall and Adams, 2013). There are different categories of semicontinuous distillation, namely, zeotropic distillation, pressure-swing azeotropic distillation, extractive distillation, and semicontinuous distillation with integrated reaction (Adams and Pascall, 2012). In this article, the focus is on the semicontinuous distillation of multicomponent zeotropic mixtures, hereafter referred to as just semicontinuous distillation. Semicontinuous distillation is carried out using middle vessels (MVs) tightly integrated with a distillation column through side stream recycle. This process was demonstrated to have a lower capital investment when compared to an equivalent continuous distillation process for intermediate production ranges in many different case studies (Meidanshahi and Adams, 2015; Pascall and Adams, 2014,2013; Wijesekera and Adams, 2015a,b). Unlike the continuous counterpart that ideally operates at a steady state, semicontinuous distillation is a forced periodic process, which is described next.

1.1. Semicontinuous distillation: Process

To separate a ternary zeotropic mixture of *A*, *B*, and *C* semicontinuously, one MV and one distillation column are required (Phimister and Seider, 2000a). Semicontinuous distillation entails periodic repetition of the three modes of operation, namely, the Charging (*Ch*), the Separating (*Sep*) and the Discharging (*Dis*) modes (Adams and Pascall, 2012). Fig. 1 illustrates the mode transitions in a semicontinuous process. The mode transitions occur when the mole fraction of component B in the MV ($x_{MV,B}(t)$) and/or height of liquid in the MV ($h_{MV}(t)$) (system states) periodically reach some pre-defined values during operation. The times at which the modes begin (or end) is dependent on these states and is not known *a priori*.

In a representative semicontinuous cycle, the MV continuously feeds ($F(t)$) the distillation column, and a side stream ($S(t)$) from the column is continuously recycled to the MV during all modes.

Abbreviations: A, Low volatile component; *B*, Intermediate boiling component; *C*, High volatile component in ternary mixture / Intermediate boiling component in quaternary mixture; *D*, High volatile component in quaternary mixture; MV, Middle Vessel; MV1, Middle Vessel to concentrate *B* in the quaternary separation; MV2, Middle Vessel to concentrate *C* in the quaternary separation; *Ch*, Charging Mode; *Dis*, Discharging Mode; *Sep*, Separating Mode; spec, Specification; *DB*, Distillate-Bottom control configuration; P, Proportional controller; PI, Proportional Integral controller; BTX, Benzene, Toluene, and O-Xylene; DME, Dimethyl Ether; MeOH, Methanol; ISR, Ideal Side draw recovery; PV, Process Variable; SP, Setpoint.

* Corresponding author.
E-mail address: tadams@mcmaster.ca (T.A. Adams II).

https://doi.org/10.1016/j.compchemeng.2018.09.002
0098-1354/

Nomenclature

$S(t)$	Actual side stream flow rate at a given time (kmol/h)
$S_1(t)$	Actual side stream flow rate at a given time in quaternary system (kmol/h)
$S_2(t)$	Actual side stream flow rate at a given time in quaternary system (kmol/h)
$S_{ISR}(t)$	Side stream flow rate as predicted by the ISR control model (kmol/h)
$S_{ISR,1}(t)$	S_1 as predicted by the ISR control model (kmol/h)
$S_{ISR,2}(t)$	S_2 as predicted by the ISR control model (kmol/h)
$S_{MISR}(t)$	Side stream flow rate as predicted by the Modified-ISR control model (kmol/h)
$S_{MISR,1}(t)$	S_1 as predicted by the Modified-ISR control model (kmol/h)
$S_{MISR,2}(t)$	S_2 as predicted by the Modified-ISR control model (kmol/h)
$S^*(t)$	Improved side stream flow rate as a function of time (kmol/h)
$F(t)$	Feed flow rate to the column as a function of time (kmol/h)
$F_1(t)$	Feed flow rate to the column from MV1(kmol/h)
$F_2(t)$	Feed flow rate to the column from MV2 (kmol/h)
$F_{Dis}(t)$	Middle vessel discharge flow rate (kmol/h)
$F_{MV}(t)$	Flow rate of feed to the middle vessel (kmol/h)
$Di(t)$	Distillate flow rate as a function of time (h)
$Bo(t)$	Bottoms flow rate as function of time (h)
$t_{f,Ch}$	Time at the end of the charging mode (h)
$t_{i,Ch}$	Time at the beginning of the charging mode (h)
$t_{f,Sep}$	Time at the end of the separating mode (h)
$t_{i,Sep}$	Time at the beginning of the separating mode (h)
$t_{f,Dis}$	Time at the end of the discharging mode (h)
$t_{i,Dis}$	Time at the beginning of the discharging mode (h)
t_f^l	Lower bound on the final time (h)
t_f^u	Upper bound on the final time (h)
h_{MV}^u	Upper bound on the height of liquid in the middle vessel (m)
h_{MV}^l	Lower bound on the height of liquid in the middle vessel (m)
$x_{MV,\,B}(t)$	Mole fraction of component B in the middle vessel at any given time (fraction)
$x_{Di,\,B}(t)$	Mole fraction of component B in the distillate stream at any given time (fraction)
$x_{Bo,\,B}(t)$	Mole fraction of component B in the bottom stream at any given time (fraction)
$x_{S,\,B}(t)$	Mole fraction of component B in the side stream at any given time (fraction)
$x_{MV,B}^{spec}$	Desired specification of component B in the middle vessel (fraction)
$x_{Di,\,A}(t)$	mole fraction of benzene in the distillate stream (fraction)
$x_{Bo,\,B}(t)$	mole fraction of benzene in the bottoms stream (fraction)
$\langle x_{Di,\,A}\rangle$	integral average mole fraction of A in the distillate stream (fraction)
$\langle x_{Bo,\,B}\rangle$	integral average mole fraction of C in the distillate stream (fraction)
$x_{MV1,\,B}(t)$	mole fraction of B in MV1 (fraction)
$x_{MV2,\,B}(t)$	mole fraction of B in MV2 (fraction)
$x_{MV1,\,C}(t)$	mole fraction of C in MV1 (fraction)
$x_{MV2,\,C}(t)$	mole fraction of C in MV2 (fraction)
$x_{S_1,B}(t)$	mole fraction of B in S_1 (fraction)
$x_{S_2,B}(t)$	mole fraction of B in S_2 (fraction)
$x_{S_1,C}(t)$	mole fraction of C in S_1 (fraction)
$x_{S_2,C}(t)$	mole fraction of C in S_2 (fraction)
T	Total cycle time (h)
SC	Separation cost ($/kmol)
$v_s(t)$	Side stream valve opening at any given time (%)
$v_{i,\,s}$	valve opening percentage at the end of the *ith* discretized element (%)
$v_{i,s}^l$	lower bound on the valve opening percentage at the end of the *ith* discretized element (%)
$v_{i,s}^u$	upper bound on the valve opening percentage at the end of the *ith* discretized element (%)
$\tilde{v}_s$	steady state side stream valve opening (%)
K_{Di}	proportional gain of the distillate stream composition controller
K_{Bo}	proportional gain of the bottoms stream composition controller
K_S	proportional gain of the side stream composition controller
K_j^l	lower bound on the proportional gain of the *jth* controller
K_j^u	upper bound on the proportional gain of the *jth* controller
τ_{Di}	integral time constant of the distillate stream composition controller (min)
τ_{Bo}	integral time constant of the bottoms stream composition controller (min)
τ_S	integral time constant of the side stream composition controller (min)
τ_j^l	lower bound on the integral time constant of the *jth* controller (min)
τ_j^u	upper bound on the integral time constant of the *jth* controller (min)
$\emptyset(t_f)$	Objective function value at the final time
C_r	cost of the refrigerant ($/GJ)
C_s	cost of low pressure saturated steam ($/GJ)
$Q_C(t)$	condenser duty as a function of time (GJ/h)
$Q_r(t)$	reboiler duty as a function of time (GJ/h)

Furthermore, light (A) and heavy (C) components are continuously recovered from the distillate (Di) and bottoms (Bo) streams of the distillation column respectively at the desired purities, although at decreasing flow rates as the cycle progresses. The MV has four material streams, two inlet streams and two outlet streams, and depending on the operating mode two or three streams are operational. The inlet streams supplying liquid to the MV are the side stream recycle $S(t)$ and the feed stream to the MV (F_{MV} (t)), and the two outlet streams drawing liquid from the MV are the column feed and the discharge stream ($F_{Dis}(t)$) (refer to Fig. 2).

In the separating mode, the MV has one functioning inlet stream, $S(t)$, and outlet stream, $F(t)$, while the other two streams are non-operational. A large fraction of the recovery of A and C components at the desired purities occurs during this mode. The side stream, which is higher in component B concentration than the contents of the MV, enriches the MV with this component as the mode advances to the end. When the mole fraction of component B in the MV ($x_{MV,B}$ (t)) reaches the desired purity ($x_{MV,\,B}^{spec}$), the separating mode ends. Immediately, the discharging mode begins with the opening of the discharge valve of the MV ($v_{MV,Dis}$ (t)) to collect component B at the desired purity. The discrete change in the input, $v_{MV,Dis}$ (t), has the following functional form:

$$v_{MV,Dis}(t, x_{MV,B}(t), h_{MV}(t)) := v_{MV,Dis}(t)$$

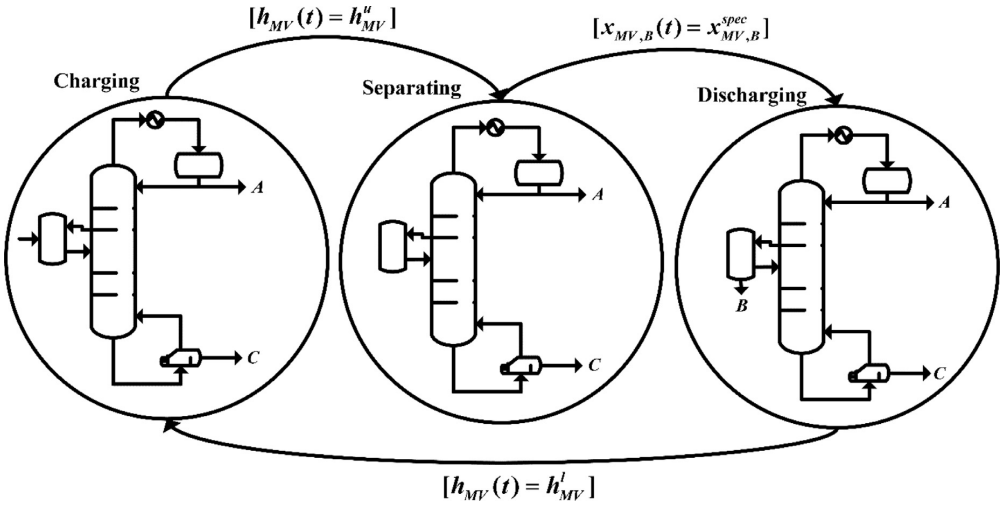

Fig. 1. State diagram illustrating modes and mode transitions during a semicontinuous distillation process.

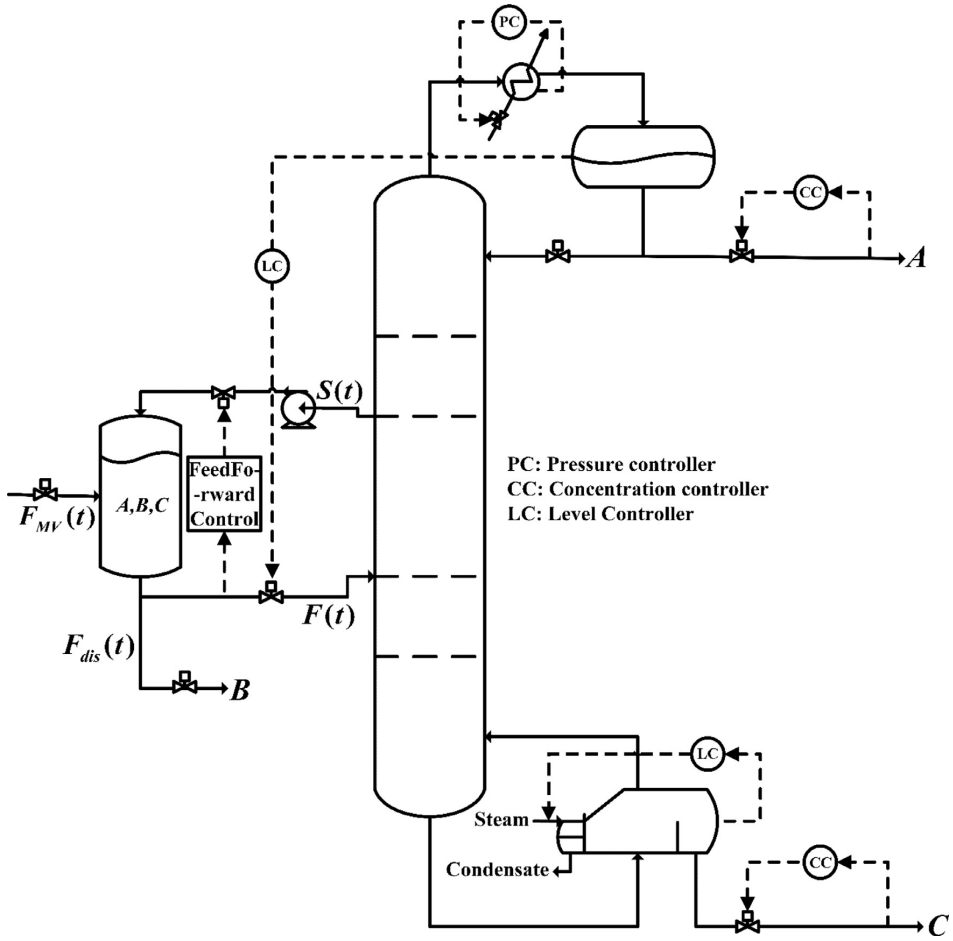

Fig. 2. Control structure as suggested by Pascall and Adams (2013). It uses DB control with reflux drum level controlled by manipulating F(t), sump level controlled by manipulating the reboiler duty ($Q_r(t)$), column pressure is controlled by manipulating condenser duty ($Q_c(t)$) and S(t) is controlled using feedforward control.

$$= \begin{cases} 0, & if\ discharging\ or\ separating\ mode \\ 1, & if\ charging\ mode \end{cases} \quad (1)$$

During the discharging mode, the MV has one functioning inlet stream, $S(t)$, and two functioning liquid streams, $F(t)$, and F_{Dis} (t). The mode ends when h_{MV} (t) falls below the pre-specified lower limit (h^l_{MV}). Instantaneously, the charging mode begins by fully opening the feed charging valve to the MV ($v_{MV,\ Ch}$ (t)) to charge the fresh feed to be separated, and simultaneously fully closing the discharge valve. The discrete input that triggers this mode transition takes the functional form:

$$v_{MV,Ch}(t,\ h_{MV}(t)) := v_{MV,Ch}(t)$$
$$= \begin{cases} 0, & if\ discharging\ or\ separating\ mode \\ 1, & if\ charging\ mode \end{cases} \quad (2)$$

Finally, a mode transition between the charging and the separating mode is triggered by fully closing the charging valve when the height of liquid in the MV (h_{MV} (t)) reaches a pre-specified upper limit (h^u_{MV}). This is the beginning of the separating mode of a new cycle. The state dependent control inputs prevent the system from ever reaching a steady-state. The control system that drives this process is described next.

1.2. Semicontinuous distillation: Control

The continuous side stream recycle introduces concentration dynamics in the MV, thus changing the column feed composition and consequently the distillate and bottoms product concentrations (mole fraction of component A in the distillate stream ($x_{Di,\ A}$ (t)) and mole fraction of component C in the bottoms stream ($x_{Bo,\ C}$ (t) respectively) with time. Therefore, to maintain these product purities near the desired values during the cycle, the Distillate-Bottoms (DB) control configuration (illustrated in Fig. 2) was proposed by Phimister and Seider (2000b). In this control configuration, the independent variables, $Di(t)$ and $Bo(t)$ are chosen for composition control from the available seven degrees of freedom, which are: (1) the distillate flow rate ($Di(t)$); (2) the bottoms flow rate ($Bo(t)$); (3) the reflux rate ($L(t)$); (4) the reboil rate ($V(t)$); (5) the feed flow rate to the column ($F(t)$); (6) the side stream flow rate ($S(t)$); (7) and the condenser duty (Q_c (t)). The DB concentration control was shown to effectively handle off-spec products in semicontinuous distillation by Phimister and Seider (2000b), because the chosen manipulated variables are independent unlike the continuous counterpart.

In the seminal work on semicontinuous distillation by Phimister and Seider (2000a), the reflux drum level (h_r (t)) and the sump level (h_s (t)) were controlled using the reflux rate ($L(t)$) and the reboil rate ($V(t)$) respectively. These manipulated variables, which change the column internal flow rates directly affect the concentration profiles of the components within the column. The column pressure ($P(t)$) was controlled using Q_c (t). However, significant details on the nature of $F(t)$ and $S(t)$ were not provided. Five degrees of freedom ($Di(t)$, $Bo(t)$, $L(t)$, $V(t)$, $Q_c(t)$) were used as manipulated variables to control the five outputs ($x_{Di,\ A}(t)$, $x_{Bo,\ C}(t)$, $h_r(t)$, $h_s(t)$, $P(t)$) near the desired values. Additionally, they also mathematically showed that the MV decouples the interactions in DB control configuration using the steady state relative gain method (Bristol, 1966).

Subsequently, an extensive control study conducted by Pascall and Adams (2013) evaluated the performance of several permutations of DB multi-loop control configurations in terms of set-point tracking and disturbance rejection. The authors concluded that the performance criteria were met successfully by controlling $h_r(t)$ using F(t), $h_s(t)$ using the reboiler duty ($Q_R(t)$), DB concentration control and side stream control. Fig. 2 illustrates this control structure, which will be referred to as the 'Pascall–Adams' control configuration in this study. The side stream, $S(t)$, is controlled using feedforward control with a control model called the Ideal Side draw Recovery (ISR) arrangement. The feedforward control was implemented via a feedback loop. One of the major limitations of the study conducted by Pascall and Adams (2013) was that the analysis did not cover the impact on the cycle time of the process when the control configuration is changed.

In an attempt to achieve better control performance for the semicontinuous distillation process, Meidanshahi et al. (2017) used cascaded subspace quality model predictive control (SQMPC). In this approach, the setpoints were given by the MPC – only during the separating mode – to all the controllers in the Pascall–Adams control configuration. The linear time invariant model for SQMPC was identified using the 'Subspace Model Identification' technique. The authors observed that the total cycle time (T) was reduced by 10% when compared with Pascall–Adams control configuration, but with $S(t)$ as a constant function. This study was the first known attempt in comparing the effect of changing the control philosophy on T and therefore on the Separating Cost (SC), which is defined as:

$$\text{SC} = \frac{\frac{\text{Capital Cost}}{3\ \text{Year Payback Period}} + \text{Annual Utility Cost}}{\text{Annual Amount of Purified Product Recovered}} \quad (3)$$

From their work, there is anecdotal evidence that $S(t)$ might have a significant impact on the SC.

In the present study, we attempt to understand how changing the control model for feedforward control of the side stream influences the cycle time and the separating cost (performance criteria). We present a new control model, referred to as the Modified-Ideal Side draw Recovery arrangement (Modified-ISR) for feedforward control, which is compared with the status quo in terms of the performance criteria. We found that the proposed control model is superior in terms of generating cycles with a lower SC compared to the state of the art. We also analyze the effects of altering the type of controller (proportional (P) or proportional integral (PI)) used in the feedback implementation of the feedforward control on the dynamic behavior of the process. Furthermore, an optimization-based procedure for finding a better side stream flow rate trajectory (during a cycle) than the one predicted by Modified-ISR control model is presented because there are no guarantees that it predicts the optimal trajectory. We found that attempts in using rigorous dynamic optimization to improve upon the control trajectories provided by the Modified-ISR framework improved neither the SC nor the cycle time relative to the Modified-ISR case. Ultimately, the key contribution is the proposed Modified-ISR control model, which according to these findings should replace the status quo ISR model for all future zeotropic semicontinuous ternary and quaternary distillation systems.

2. Side stream feedforward control

2.1. Ideal side draw recovery arrangement

The rationale for the control of the side stream flow rate was to reduce the loss of intermediate boiling component from the distillate and bottoms streams (Adams and Seider, 2008). The feedforward control model required was derived from the component B column mass balance by assuming that the column is operated at a pseudo-steady state at any given time (t), which is:

$$F(t)x_{\ MV,B}(t) = S(t)x_{S,B}(t) + Di(t)x_{Di,B}(t) + Bo(t)x_{Bo,B}(t) \quad (4)$$

where, $x_{S,\ B}(t)$ is the mole fraction of component B in the side stream, $x_{Di,\ B}(t)$ is the mole fraction of component B in the distillate stream, and $x_{Bo,\ B}(t)$ is the mole fraction of component B in the bottoms stream.

In the ideal case, there would be no loss of intermediate boiling component either through the distillate stream or the bottoms stream at any given time. In addition, none of the light or heavy species would exit through the side draw. Therefore, $x_{Di,B}(t) = x_{Bo,B}(t) = 0$, and $x_{S,B}(t) = 1$, thus resulting in the ideal side draw recovery arrangement (ISR) control model, represented by Eq (5), where $S_{ISR}(t)$ is the model-defined side stream flow rate.

$$S_{ISR}(t) := F(t)x_{MV,B}(t) \tag{5}$$

In practice however, the feedforward-side stream control is implemented through feedback control of the side stream, where $S(t)$ (output) is made to track $S_{ISR}(t)$ (setpoint), which will be henceforth referred to as "ISR feedback control". A proportional (P) controller was normally used to manipulate the side stream control valve ($v_s(t)$) to try to get the actual flow rate to track the ISR-defined flow rate setpoint (Pascall and Adams, 2013).

The ISR control model used in the Pascall–Adams control configuration has consistently shown to be effective in achieving good cycle performance and cycle stability in many studies (Ballinger and Adams, 2017; Meidanshahi et al., 2017; Meidanshahi and Adams, 2016, 2015; Pascall and Adams, 2014, 2013; Wijesekera and Adams, 2015a, 2015b). The derived control model defines an output trajectory, $S(t)$, based on the control input, F(t), the state, $x_{MV,B}(t)$, and the choice of the controller tuning parameters.

2.2. Modified-ideal side draw recovery feedforward control model

Although the ISR model for side stream control has had good demonstrable performance characteristics, simulations have shown that $x_{S,B}(t)$ is often far from unity early in the cycle and never exactly 1.0 at any time during the cycle. Consequently, we found that the ISR model yields side stream flowrate setpoints that are significantly sub-optimal by being too low (later illustrated in Sections 4.1.1 and 4.1.2 using an example). The cycle time, and as a consequence the SC can perhaps be reduced by increasing the rate of side stream recycle to the MV based on the idea that the MV can be enriched with component B faster because of the greater side stream flowrate. However, using a control policy which results in side stream flow rate setpoints that are too large could cause significant operational difficulties in the column and other performance issues. Nevertheless, the proposed feedforward control model is designed without using the assumption of a perfectly pure side draw, with Eq. (4). now reducing to the Modified Ideal Side Draw Recovery (Modified-ISR) arrangement. The new model defines, at each time instance, the amount of component B recycled to the MV through the side stream as opposed to the ISR model. In Eq. (6), $S_{MISR}(t)$ is the side stream flow rate as defined by the new model:

$$S_{MISR}(t) := \frac{F(t)x_{MV,B}(t)}{x_{S,B}(t)} \tag{6}$$

Since $x_{S,B}(t) \in [0\,1]$, comparing Eqs. (5). and (6)., $S_{MISR}(t)$ is higher in value than $S_{ISR}(t)$ at instances where there is no difference in the values of F(t) and $x_{MV,B}(t)$. The side stream will contain some amount of components A and C and thus, may be on the negative side, the approach could be essentially counter-productive by collecting too much of the heavy and light species in the side draw, thus making overall recovery times longer. An added concern with using the Modified-ISR model is the need for an additional online composition measurement of component B in the side draw. In this study, since we deal with an ideal-case analysis, the cost and measurement noise of the additional composition sensor is neglected. However, a 3-minute dead time associated with this additional composition sensor was considered.

The side stream feedforward control using the Modified-ISR control model was implemented using a feedback loop, where the setpoint of the controller in the loop was varied according to the model just like the ISR feedback control. The present study aims to understand the changes in process dynamics when using the ISR and Modified-ISR feedback control approaches and its effect on economic performance

3. Simulations using the sequential design methodology

The effect of changing the feedforward control model was studied extensively through the simulation of four semicontinuous ternary distillation systems, named, I, II, III, IV (with different feed mixture compositions and chemical components), and semicontinuous multicomponent distillation of a four-component mixture (V). These are shown in Table 1.

Systems I to III represent the separation of an almost ideal but industrially relavent ternary mixture of benzene, toluene and o-xylene (BTX), where toluene is the intermediate boiling component (B). The differences between the three systems is the concentration of toluene in the feed to the MV, with system I having the highest and system III having the lowest. System IV represents the ternary separation of dimethyl ether (DME), methanol (MeOH), and water (H_2O), which was extensively studied by Pascall and Adams (2013) because of the importance of biomass-based DME production as an alternative fuel source to diesel. These systems were specifically chosen because they were well-studied in the semicontinuous distillation literature and are illustrative of the zeotropic separations of ternary systems. System V provides a basic example of the separation of four components (alkanes-C_n, $n = 6$ to 9) used in the study by Wijesekara and Adams (2015). Quaternary semicontinuous distillation is carried out using one column and two middle vessels. Therefore, two side streams are recycled to the two MVs for separating the two intermediate boiling components. In this case, components B (heptane) and C (octane) are both intermediate boiling components, each recovered in a separate MV, while component D (nonane) is the bottoms product.

3.1. Remarks on the initial state

The design methodology adopted is the same as the one described and used by Pascall and Adams (2013) in their study, which we call the "sequential design methodology". The idea in this approach was to initially identify a "hypothetical" steady-state which is used as the initial state for dynamic simulation. At this initial state, the distillate and bottoms products are separated at the desired purities, while the side stream is not yet recycled to the MV. This state is a reasonably good approximation of the beginning of the separating mode (Wijesekera and Adams, 2015a) noting that the actual state cannot be predicted *a priori*. The steady state side stream flowrate ($\bar{S}$) can be chosen according to the ISR feedforward control model, however, this can be low enough to cause flooding in the column. Therefore, generally a slightly higher value than the ISR specified value is chosen to avoid flooding within the column at this state.

Data required for column design at the initial state, such as number of stages, feed stage location, side draw location, column pressure, pressure drop across stages (ΔP) and product composition were taken from Ling and Luyben (2009), Pascall and Adams (2013), Wijesekara and Adams (2015), and Meidanshahi and Adams (2015) (see Tables 1 and 2). The thermodynamic properties of systems I to III were calculated using the Non-random two-liquid (NRTL) activity coefficient model (Ling and Luyben, 2009). This model was validated to match well with experimental data for the isobaric state of 101.325 kPa, where the R^2 value was approximately 0.99 for each binary interaction. The experimental data were taken from Gupta and Lee (2013, 2012). The vapor liquid

Table 1
The five semicontinuous distillation systems considered in this work. Feed compositions are given in mole fraction. Stages includes the condenser and reboiler in the column and the column trays (with an assumed 75% tray efficiency), with stage 1 being the condenser. Feed stages are above stage, and side stream stages are on-stage (liquid phase). $F(t)$ at time $t=0$ (around which the column is sized) is represented as $\bar{F}$, and $S(t)$ at time $t=0$ is represented as $\bar{S}$.

System	Feed Mixture	Upstream Feed Composition				Stages	Stage Location		$\bar{F}$ (kmol/h)	$\bar{S}/\bar{F}$
		$x_{A,F}$	$x_{B,F}$	$x_{C,F}$	$x_{D,F}$		*Feed*	*Side stream*		
I	BTX	0.2	0.6	0.2	-	40	25	14	100	0.655
II	BTX	0.33	0.33	0.34	-	40	25	14	100	0.39
III	BTX	0.4	0.2	0.4	-	40	25	14	100	0.25
IV	DME, MeOH, H_2O	0.82	0.14	0.04	-	25	13	12	12.64	0.149
V	C_6, C_7, C_8, C_9	0.25	0.25	0.25	0.25	50	24, 25	15, 36	37.81	0.25, 0.25

Table 2
Column conditions at the initial state.

System	Mole Purity of Each Product Stream at the Initial State				Condenser P	Tray ΔP	Flooding
	A	B	C	D	(atm)	(atm)	*Initial State*
I	0.99	0.91	0.99	-	0.37	0.0068	No
II	0.99	0.83	0.99	-	0.37	0.0068	No
III	0.99	0.77	0.99	-	0.37	0.0068	No
IV	0.9995	0.96	0.9905	-	10	0.0068	No
V	0.95	0.95*	0.93*	0.95	1	0.0068	No

equilibrium was modeled using the Peng Robinson-Wong Sandler-UNIFAC model and the UNIQUAC-Redlich Kwong model when simulating systems IV and V respectively (Pascall and Adams II, 2013; Wijesekera and Adams II, 2015a). These models were not validated against experimental data in this study since it was already verified in the respective studies.

In systems I to III, the MV was sized to have a total molar hold-up of 200 kmol of liquid feed, and in systems IV and V, the MV was sized to have a total molar hold-up of 100 kmol of liquid feed using the design heuristics applied by Pascall and Adams (2013). The reflux drum and the sump were sized according to the design heuristics of Luyben (2006). It was verified that flooding and weeping constraints were met at the initial state (see Table 2).

The total direct costs for the systems were calculated in $US2016 using Aspen Capital Cost Estimator V10 (Aspen Technologies). The utility costs of steam and cooling water were the only operating costs that were considered in the calculation of SC because they constitute the major portion. The methodology as provided by Towler and Sinnott (2012) was used to estimate the cost of steam and cooling water based on energy market prices. A natural gas price of 2.64 $/GJ (U.S. Energy Information Administration, 2017) and electricity price of 0.097 $/kW (IESO) was used for the estimation of cooling water and steam costs.

3.2. Comments on control

The Pascall–Adams control configuration was used for the purposes of controlling the desired outputs at the chosen setpoint values. The concentration controllers maintain the distillate and bottoms product concentrations at the chosen initial state values, which are perceived as the integral average purities (during the cycle) of these products. Similarly, the level controllers maintain the reflux drum and sump levels at the respective initial state values.

PI controllers were used for concentration and level control in the simulations. The controllers are initially tuned manually such that the integral squared errors of the distillate and bottoms concentrations are minimized (Pascall and Adams, 2013). The ISR and Modified-ISR feedback control uses reverse acting P or PI controllers for setpoint tracking.

Although the Pascall–Adams control configuration was used in quaternary semicontinuous distillation, it is more intricate compared to the ternary case (see Fig. 3). In the quaternary case, there are two feed inlets to the column from the two MVs, and therefore the reflux drum level is controlled by manipulating the two feed flow rates collectively as illustrated by Wijesekera and Adams (2015a). Furthermore, in their study, both the side streams where controlled using the ISR feedforward control model as follows (Wijesekera and Adams, 2015a):

$$S_{ISR,1}(t) := F_1(t)x_{MV1,B}(t) + F_2(t)x_{MV2,B}(t) \tag{7}$$

$$S_{ISR,2}(t) := F_1(t)x_{MV1,C}(t) + F_2(t)x_{MV2,C}(t) \tag{8}$$

where $S_{ISR,i}(t)$ is the model specified setpoint of the side stream flow rate of stream i, $F_i(t)$ is the feed stream to the column from the ith MV, $x_{MVi,B}(t)$ and $x_{MVi,C}(t)$ are mole fractions of components B and C in the feed stream i to the column. The Modified-ISR control model for controlling the two side streams can be similarly defined as follows:

$$S_{MISR,1}(t) := \frac{F_1(t)x_{MV1,B}(t)}{x_{S_1,B}(t)} + \frac{F_2(t)x_{MV2,B}(t)}{x_{S_2,B}(t)} \tag{9}$$

$$S_{MISR,2}(t) := \frac{F_1(t)x_{MV1,C}(t)}{x_{S_1,C}(t)} + \frac{F_2(t)x_{MV2,C}(t)}{x_{S_2,C}(t)} \tag{10}$$

3.3. Controller tuning

The tuning parameters of the controllers are design degrees of freedom in semicontinuous distillation, whose choice will generate different control trajectories and thus different converged cycles from the same initial state. Optimal controller tuning parameters were therefore found with the objective of minimizing SC subject to constraints by using dynamic optimization. The decision variables include tuning parameters of the distillate concentration controller, bottoms concentration controller and side stream flow rate controller (represented as elements in the vector $[K_{Di}\ \tau_{Di}\ K_{Bo}\ \tau_{Bo}\ K_S\ \tau_S]^T$) with manually tuned values of these variables used as the initial guess.

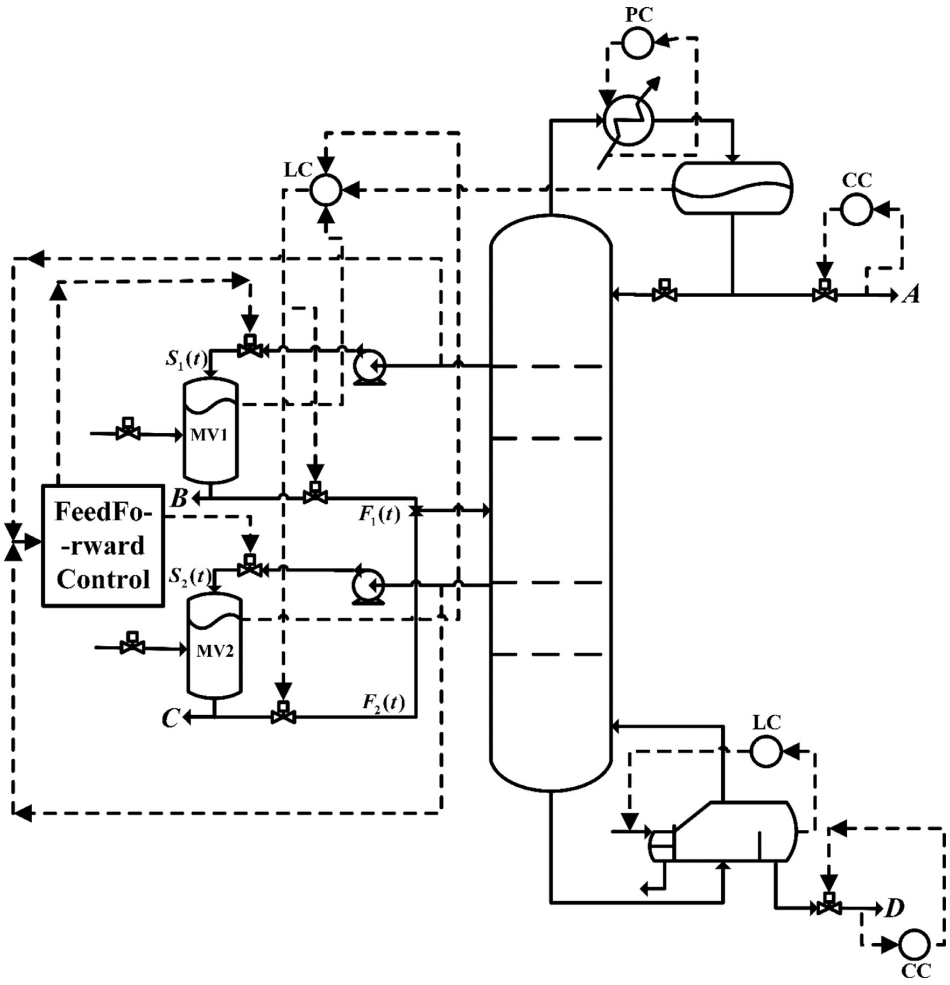

Fig. 3. Control structure as suggested by Wijesekara and Adams (2015) for quaternary semicontinuous distillation.

It should be emphasized here that the improved designs found were sub-optimal because integer decision variables such as diameter of the column, number of stages etc., were not included. Hence, for the sake of being rigorous, the design obtained through dynamic optimization is called the "improved" design and the tuning parameters are referred to as "improved" rather than "optimal". Integer design degrees of freedom were not included during optimization because of the complexity and large computational time required to find a local optimal solution (Meidanshahi and Adams, 2016). Also, since finding the optimum of each system is not the objective of the present study, a much simpler method was preferred. For details on the procedure to find an optimal semicontinuous design by including the integer design variables refer to Meidanshahi and Adams (2016).

The improved semicontinuous distillation design was found using the Aspen Dynamics dynamic optimization tool (Aspen Technologies), which uses the control vector parametrization approach. Using this tool, the controller tuning parameter values that allow the systems to converge to the best possible cycles from the respective initial states were found. Endpoint constraints were used to ensure that the average purity constraints of the distillate and bottoms streams were met. The height of liquid in the middle vessel was ensured to be close to the initial value ($|h_{MV}(t_f) - h_{MV}(t_i)| \leq \epsilon$) at the end of each cycle so that the system is periodic.

The dynamic simulation of each system is run for ten cycles from the initial state because it usually takes a few cycles for the system to converge to a stable cyclic steady state starting from the hypothetical steady state, and ten cycles is sufficiently large to obtain a cyclic steady state in all circumstances. Thus, the 10^{th} cycle is used to compute the SC of the system as a whole as follows:

$$SC = \frac{\frac{Total\ Direct\ cost}{3\ years} + \left(\frac{w}{t_f - t_i}\right) \int_{t_i}^{t_f} (C_r Q_c(t) + C_s Q_r(t))\ dt}{\left(\frac{w}{t_f - t_i}\right) \int_{t_i}^{t_f} (Di(t))dt} \tag{11}$$

where C_r is the cost of the refrigerant, C_s is the cost of low pressure saturated steam, t_i and t_f are the initial and final times of the 10th cycle in hours, and $(\frac{w}{t_f - t_i})$ is the number of cycles in a year assuming w working hours per year. The optimization problem for-

mulation is:

$$\underset{K_j,\ \tau_j,\ t_f}{\textit{minimize}} \quad \text{SC}$$

subject to

Mass Balance Constraints

Energy Balance Constraints

Momentum Balance Constraints

Equilibrium Relationships

All other model equations

$$h_{MV}^{l}(t_f) \ \le\ h_{MV}(t_f) \ \le\ h_{MV}^{u}(t_f)$$

$$x_{Di,A}{}^{l} \ \le\ \langle x_{Di,A} \rangle \le\ x_{Di,A}{}^{u}$$

$$x_{Bo,C}{}^{l} \le\ \langle x_{Bo,C} \rangle \le x_{Bo,C}{}^{u}$$

$$K_j^l \ \le\ K_j \ \le\ K_j^u$$

$$\tau_j^l \ \le\ \tau_j \ \le\ \tau_j^u$$

$$t_f^l \le\ \ t_f \ \le\ t_f^u$$

where t_f is the final cycle time, with t_f^l and t_f^u being the lower and upper bounds of final cycle time respectively. Lower and upper bounds of other variables are defined analogously. The integral average mole fraction of A in the distillate stream, $\langle x_{Di,\,A} \rangle$, is defined as:

$$\langle x_{Di,A} \rangle := \frac{\int_0^{t_f} x_{Di,A}(t) Di(t) dt}{\int_0^{t_f} Di(t) dt} \tag{12}$$

where $x_{Di,\,A}(t)$ is the mole fraction of benzene in the distillate stream at time t. The integral average mole fraction of B in the bottoms stream, $\langle x_{Bo,\,C} \rangle$, is defined analogously. Here, K_j represents the proportional gain of the j^{th} PI controller, τ_j represents integral time constant of j^{th} PI controller, where $j = (Distillate)Di$, $(Bottoms)Bo$, $(Side\ Stream)S$.

4. Simulation results and analysis

4.1. Ternary systems

The changes in the evolution of the system from the initial state when using the ISR and Modified-ISR feedback control is analyzed in detail by using system II as an example. It is later demonstrated that the analysis is consistent in all other systems under study including the quaternary system.

4.1.1. ISR feedback control of side stream flow rate

ISR feedback control was first implemented using a P controller (ISR feedback-P) in the simulation studies conducted on system II. Improved tuning parameter values were obtained from optimization of the system. From the initial state (represented as a circle in Fig. 4), the system evolved and converged to a periodic orbit (illustrated in the phase plane plot in Fig. 4). To generate the phase plane plot, the system's state variables, the molar hold up of component B on the side draw tray $M_{B,\,S}$ (t) and the molar hold up of component B on the feed tray $M_{B,\,F}$ (t) are chosen, because they are directly affected by $S(t)$ and $F(t)$ respectively. The orbit represented in Fig. 4 was traced for ten cycles by employing the improved controller tuning parameters. In the absence of any state dependent inputs that trigger a mode transition (i.e., if the system is run in separating mode without stopping), the system will be attracted to an equilibrium point (ε, the solid point). The point α is the end of the separating mode (and beginning of the discharging mode), where the concentration of toluene (component B in system II) in the MV reaches the desired purity value, in this case 0.99. α is close enough to ε that they are indistinguishable in Fig. 4. The

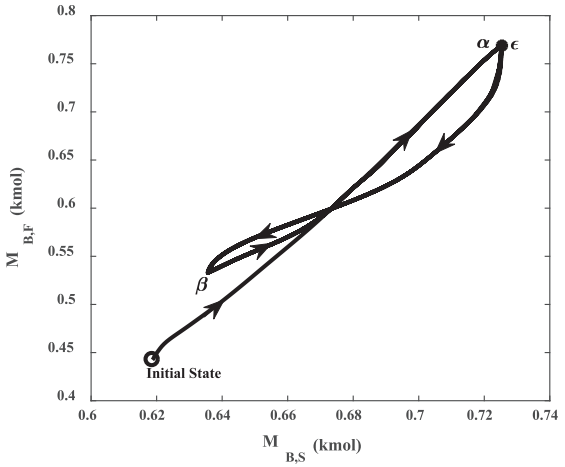

Fig. 4. Phase plane plot (includes 10 cycles) which illustrates the evolution of the system when the improved ISR feedback-P control for side stream flow rate is used. The circle indicates the initial state of the simulation.

change in the column's state during the discharging mode is not significant and hence the end of the discharging mode cannot be distinguished clearly from point α or the equilibrium point on the phase plane plot. However, during the charging mode the values of the selected variables vary substantially, moving the system from point α to point β, which signifies the end of the charging mode and the beginning of a new separating mode.

In Fig. 5, the setpoint tracking ability of the P controller using the improved tuning parameter values is presented. As illustrated for three representative cycles, by using the improved tuning parameters values the setpoint was not tracked exactly. Therefore, to understand the implications of tracking the ISR-defined setpoint as closely as possible, different controller tuning parameter values were manually chosen (called the "setpoint tracking" tuning parameter values). The cycle time and the SC were found to be greater, as expected, by tracking the setpoint closely. The cycle times were higher because the side stream valve was closed significantly during the charging mode (lower toluene concentration in the column feed) and thus having lower recycle rates during that period. Also noticeable from Fig. 5 is that the side stream flow rate trajectories are completely different in the improved and setpoint tracking cases. Therefore, by changing the tuning parameter values different control trajectories (v_s (t)) are generated.

Another approach to track the setpoint exactly is to use a PI controller (ISR feedback-PI) instead of a P controller. By changing the type of controller in the feedback loop to track the ISR-defined setpoint, it was found that the system essentially failed (Fig. 6), with the feed and side draw rates dropping to zero and the column entering total reflux mode. After close examination, it was observed that the side stream valve was fully closed because of a large integral error. The reason for this huge integral error is possibly due to the choice of the initial state. As stated previously, $\bar{S}$ is chosen to be at a slightly higher value than the ISR specified value at the initial state. Therefore, in ISR feedback loop there is a negative error ($(S_{ISR}(0) - \bar{S}) < 0$), which the controller tries to compensate by closing the valve (v_s). The integral term of the PI controller accumulated this negative error during the cycle(s) and gradually closed the side stream flow control valve fully. Simultaneously, the concentration of toluene in the distillate and bottoms streams was observed to be increasing due to the side stream valve closure, thus eventually leading to the shutting of distillate and bottoms flow control valves. At the same time, to maintain the reflux drum

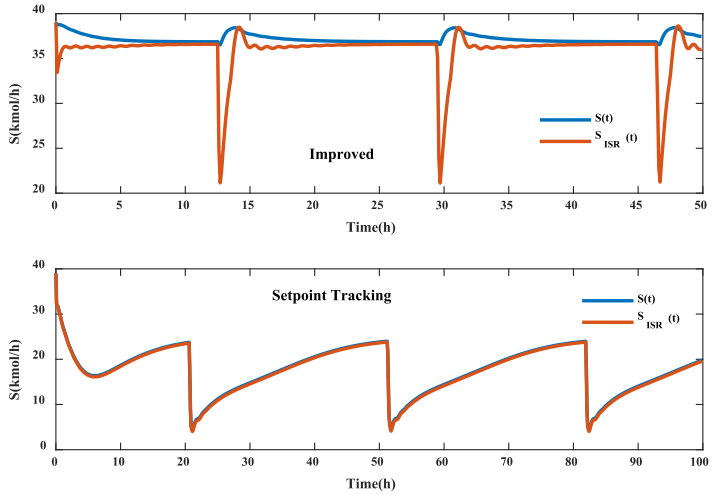

Fig. 5. Illustration of S(t) vs $S_{ISR}(t)$ when the setpoint tracking or improved tuning parameter values are used to simulate system II. The ISR feedback-P control is used.

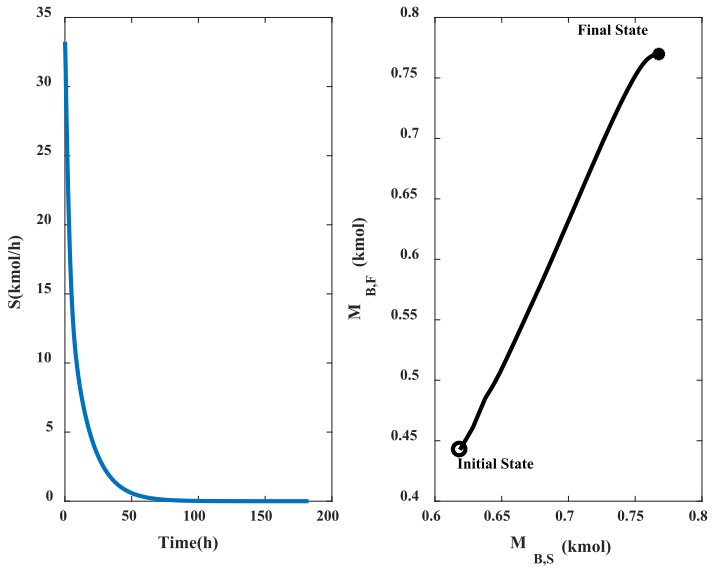

Fig. 6. The evolution of S(t), flow rate of side stream recycled to the middle vessel (kmol/h) with time and the phase plane plot illustrating the effect of using the ISR feedback-PI control for side stream flow rate. The system approaches the failure (total reflux) state.

level the feed flow control valve to the column was closed thus resulting in the total reflux state column operation. This type of dynamic behavior is undesirable for semicontinuous distillation and so the ISR feedback-P is the appropriate choice. Note that, in all prior semicontinuous studies using the ISR control model, a P controller was used instead of PI, likely for the same reason.

4.1.2. Modified-ISR feedback control of side stream flow rate

To follow the same natural progression followed in the previous section, the Modified-ISR feedback control was also first implemented with the aid of a P controller (Modified-ISR feedback-P) in the simulation studies conducted on system II. The tuning parameters were initially found manually so that the integral squared error was reduced and the Modified-ISR setpoint was tracked. The cycle time of the converged periodic orbit and the SC were then compared with improved ISR feedback-P and were found to be only marginally lower (∼0.004%). Setpoint tracking was found to be difficult in the case of Modified-ISR feedback-P because of numerical convergence issues encountered during the simulation. However, when a PI controller was used in the Modified-ISR feedback control loop (Modified-ISR feedback-PI), even before the optimization step was performed, *T* and SC were found to be significantly lower (∼12% and ∼13% respectively) than the manually tuned Modified-ISR feedback-P case, and the failure state was not reached. Thus, the optimization step was not carried out for the Modified-ISR feedback-P case. The reason for the lower *T* and SC in the Modified-ISR feedback-PI case is because of the positive error accumulated by the integral term of the PI controller, which

Table 3
The cycle time and the separating cost comparisons in system II. Cycle Time is the time taken to complete the 10th cycle.

Control	T (h)	SC($/kmol of product produced)	% decrease in SC compared to ISR feedback-P
Improved ISR feedback-P	16.97	8.25	-
Improved Modified-ISR feedback-PI	14.83	7.16	13.21
No Control ($v_s(t) = 100\%$)	14.82	7.25	12.12

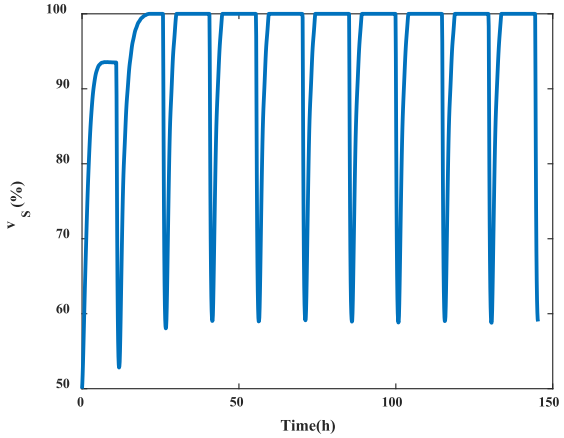

Fig. 7. Side stream valve opening as a function of time when improved Modified-ISR feedback-PI control is used in system II.

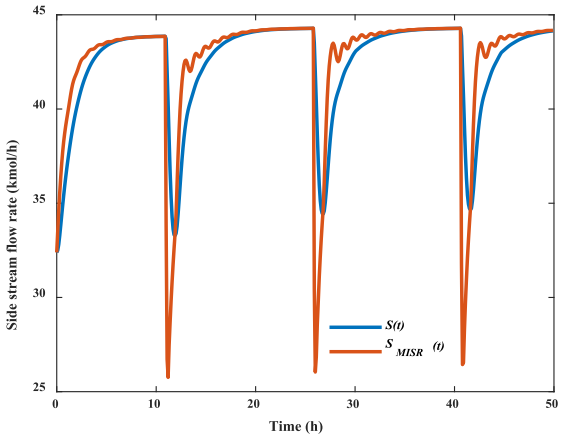

Fig. 8. Illustration of process variable not tracking the setpoint when the improved tuning parameter values are used to simulate system II. The Modified-ISR feedback control is used.

is again due to the choice of the initial state. It is well known that, $\bar{\delta} \equiv \overline{Di}\bar{x}_{Di,B} + \overline{Bo}\bar{x}_{Bo,B}$ (variables with over bar indicate steady state values) in Eq.(4), is not equal to zero in reality at steady state; unlike in the derivation of the Modified-ISR model. Thus, from Eq. (4) and Eq. (6),

$$\bar{S} = S_{MISR}(0) - \frac{\bar{\delta}}{\bar{x}_{S,B}}$$

Since $\frac{\bar{\delta}}{\bar{x}_{S,B}}$ is positive, $\bar{S}$ is less than $S_{MISR}(0)$, thus resulting in positive error ($(S_{MISR}(0) - \bar{S}) > 0$). Therefore, the side stream control valve is opened by the controller at the initial state to compensate for the error unlike the ISR case. The integral term accumulates this error to open the side stream valve fully for a certain length of time during the stable cycle (Fig. 7). Although, this occurs because of the integral windup, there is a natural anti-windup (even though it does not completely reset the integral term) process happening during the charging mode of the cycle. This is because the concentration of B is lower in the MV during this mode and thus reducing the value of the model predicted setpoint. Further, it was found that when using the improved tuning parameter values in Modified-ISR feedback-PI case, the process variable tracks the setpoint (Fig. 8) for the later portion of the cycle but does not quite track it during the earlier portion of the cycle. Thus, in general, the feed forward models in combination with side draw controller tuning parameters together act as control (v_s) trajectory generators that guide the system to reach different periodic orbits (stable cycles) in the phase space.

The improved periodic orbit to which the system converged in the Modified-ISR feedback-PI controller case is traced in (Fig. 9) and is quantitatively slightly different from the improved periodic orbit of the ISR feedback-P case (Fig. 4). This is because the set of side stream valve opening trajectories that can be generated in the former case is different from the latter. Furthermore, it is evidently

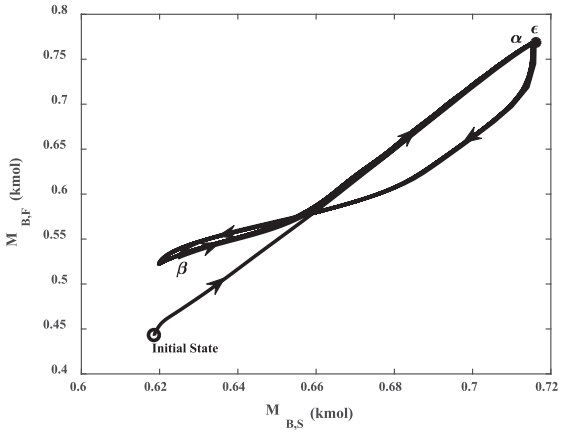

Fig. 9. Phase plane plot (includes 10 cycles) which illustrates the evolution of the system when the improved Modified-ISR feedback-PI control for side stream flow rate is used. The circle indicates the initial state of the simulation.

noticeable that it takes a few semicontinuous cycles to approach the basin of attraction of the periodic orbit unlike the ISR case.

The side stream flow rate ($S(t)$) at any given time in a stable cycle when using the Modified-ISR feedback-PI control is greater than when using the ISR feedback-P control. Consequently, the cycle time is decreased considerably in the former when compared to the latter because the middle vessel reaches the desired purity in a reduced amount of time. Thus, the frequency at which batches of feed are processed is higher simultaneously leading to reduced SC (results presented in Section 4.1.3). Furthermore, it was observed that there was no column flooding (Fig. 10) or weeping during the

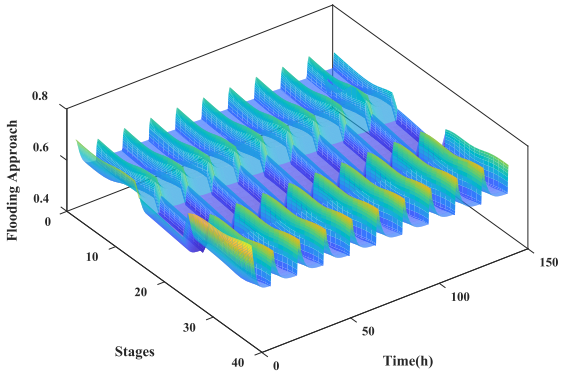

Fig. 10. Illustration of flooding approach profile in system II for 10 cycles. Modified-ISR feedback-PI control was employed.

dynamic operation and the distillate and bottoms product purities are maintained at the desired values.

4.1.3. Comparison of separating costs

The cycle time when using the Modified-ISR feedback-PI control to control the side stream flow rate in system-II is almost 12.5% lower when compared to the cycle time when using the ISR feedback-P control. Similarly, the SC when using the latter approach is substantially lower (by almost 13%) when compared to the former approach (Table 3). The Modified-ISR feedback-PI control resulted in a 13% reduction in SC for the same total direct cost, which is a remarkable improvement in SC and is even significantly bigger than the benefits of finding the improved tuning parameters. Thus, the Modified-ISR feedback control with PI controller must be fundamentally better in terms of separating the mixture faster when compared to the state of the art.

Since the Modified-ISR feedback-PI control has the lowest SC, and because the side stream valve was saturated during the cycle, perhaps the side stream control valve could be fully opened all the time instead of using either ISR or Modified ISR. This was tested and was found that the cycle time was slightly lower, but the SC was slightly worse compared to the improved Modified-ISR case (Table 3). This could be because of two reasons: (1) the loss of intermediate boiling component through the distillate and bottoms streams, and (2) higher heat duties because of higher amount of component *B* in the feed at any given time.

While the results imply that the Modified-ISR control model generates a $S(t)$ trajectory that leads to better cycles in terms of *SC* than the ISR control model, the generality of the above analysis and the relevant conclusions are presented next.

4.1.4. Comparison of ISR and Modified-ISR feedback control in other ternary systems

The analysis in the previous sections is found to be consistent even for other ternary systems, namely, I, III, and IV. The dynamic behavior of the systems changed as the tuning parameter values were altered. As an example, Fig. 11 illustrates the change in the periodic orbit when improved and setpoint tracking tuning parameters are used in ISR feedback-P control. Furthermore, in all systems that were studied, the setpoint was not tracked exactly when the improved tuning parameters were employed.

The same undesirable behavior of reaching the total reflux state was observed when the PI controller was used in ISR feedback control in all cases. Also, Modified-ISR feedback-P control with controllers manually tuned for minimizing integral squared error is only marginally better than improved ISR feedback-P control in all three simulated cases (Table 4).

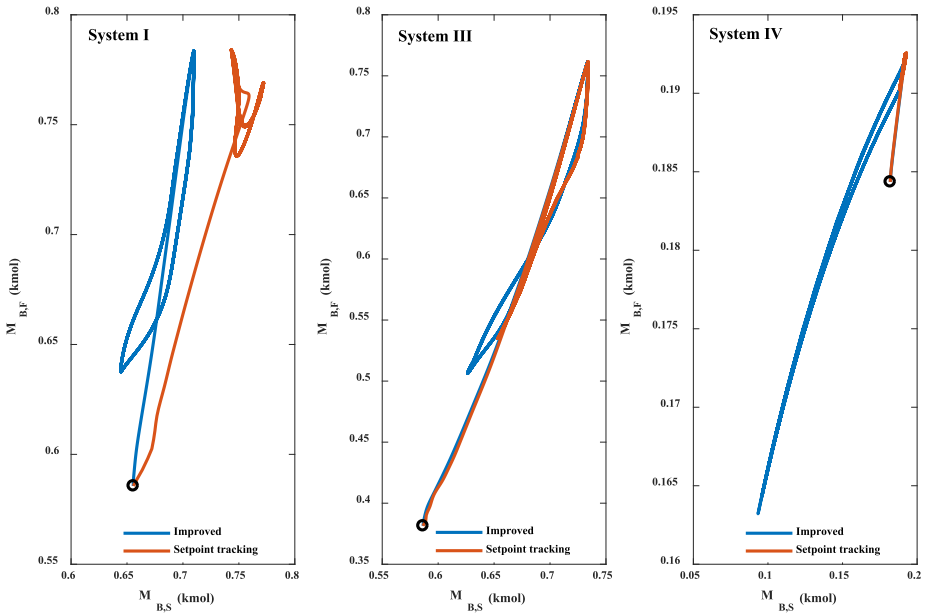

Fig. 11. Phase plane plots to illustrate the dynamic behavior because of using the ISR feedback-P control (systems I, III, IV). The open circle indicates the hypothetical steady-state (used as the initial state). "Improved" indicates that the side stream controller tuning parameters are found using optimization and "Setpoint tracking" implies that the side stream controller tuning parameters were manually selected to nearly closely track the setpoint.

Table 4
The cycle time and separating cost comparisons for the systems under study. Cycle Time is the time taken to complete the 10th cycle. * The side stream flow rate function is highly oscillatory during the cycle. § Status-quo side stream flow rate control.

	System I	System II	System III	System IV	System V
Cycle Time (T) (h)					
ISR feedback-P control - Setpoint tracking	27.52	30.81	34.44	95.28*	6.31
ISR feedback-P control - Improved§	14.36	16.97	18.87	65.19	4.60
Modified ISR feedback - P control – Manually tuned ($K_s = 0.1$ (%/%))	13.31	16.90	18.85	64.26	4.63
ISR feedback - PI control	-	-	-	-	-
Modified ISR feedback - PI control-Improved	12.79	14.83	16.36	55.62	4.08
Dynamic Optimization	12.79	14.51	16.12	55.00	-
Separating Cost (SC) (S/kmol of product produced)					
ISR feedback-P control – Setpoint tracking	24.60	15.95	14.62	21.16	29.70
ISR feedback-P control - Improved§	12.37	8.25	7.57	21.16	21.77
Modified ISR feedback - P control - Manually tuned ($K_s = 0.1$ (%/%))	11.40	8.25	7.57	20.00	21.62
ISR feedback - PI control	-	-	-	-	-
Modified ISR feedback - PI control -Improved	10.93	7.16	6.49	17.35	18.50
Dynamic Optimization	10.92	7.00	6.39	17.10	-

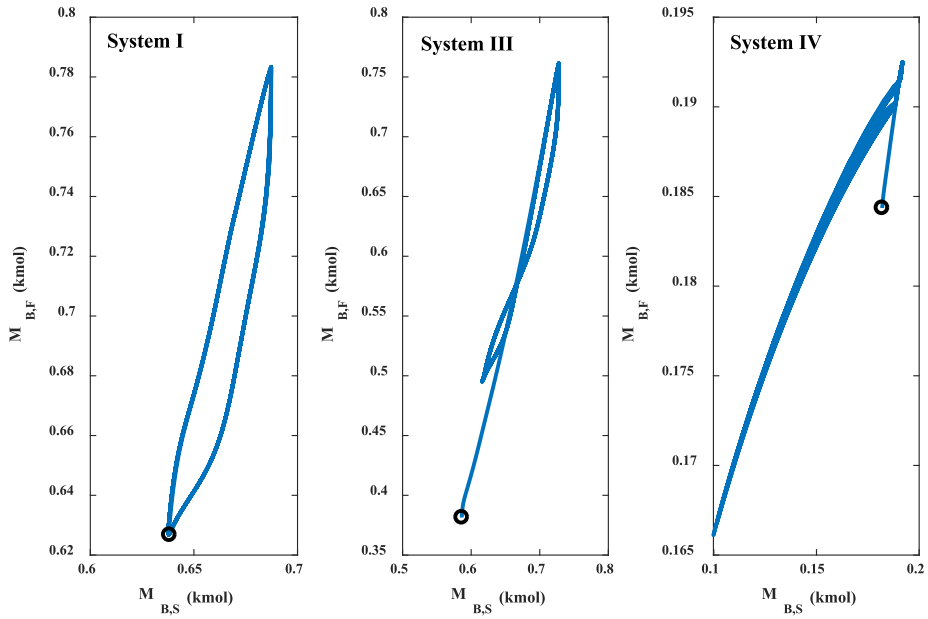

Fig. 12. Phase plane plots to illustrate the dynamic behaviour because of using the improved Modified-ISR feedback-PI control (systems I through IV). The open circle indicates the hypothetical steady-state (used as the initial state).

With improved Modified-ISR feedback-PI control, the periodic orbit (Fig. 12) traced with the improved tuning parameter values is slightly different from the periodic orbit of improved ISR feedback-P control (Fig. 11) for systems I, III and IV.

When using the improved Modified-ISR feedback-PI control to control the side stream flow rate, the cycle time was almost 10% to 15% lower when compared to the improved ISR feedback-P control. Similarly, the SC also is substantially lower by almost 10% to 19% when compared to the status quo. Therefore, from an economic perspective (Table 4), the Modified-ISR feedback-PI control is better than the state of the art in all cases. Thus, the proposed feedforward model for side stream control is better to reach periodic orbits (stable cycles) with lower SC than the ISR feedforward control model.

4.2. Quaternary systems

Interestingly, the conclusion of the analysis carried out thus far for ternary systems also holds true for the more complicated quaternary system (system V). Both the side streams when controlled using the control models as defined in Eq. (9) and Eq. (10) (Modified-ISR control model for the quaternary system) confirmed similar results. As an example, Fig. 13 demonstrates that the periodic orbits are qualitatively different when a different side stream control is applied. This illustrates the scalability in the functionality of the proposed control model for the distillation of mixtures with n-components using "*n-2*" MVs semicontinuously while resulting in lower SC cycles (see Table 4) compared to the current state of the art.

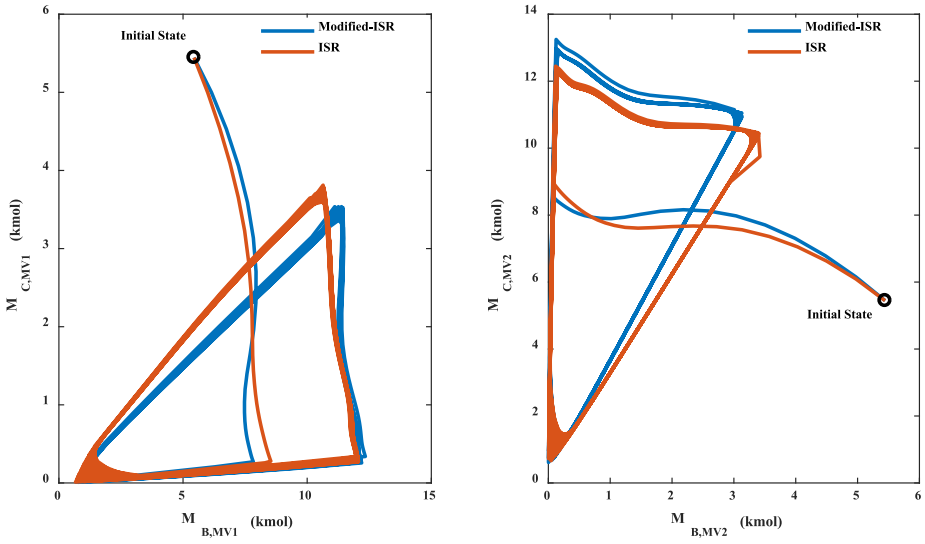

Fig. 13. Comparison of the periodic orbits in System V when using the Modified-ISR and ISR control models. MV1 and MV2 refer to the two middle vessels required for separation. $M_{B,\,MV1}$ and $M_{B,\,MV2}$ are state variables, which represent the molar holdups of component B in the two middle vessels. Similarly, $M_{c,\,MV1}$ and $M_{c,\,MV2}$ are state variables, which represent the molar holdups of component B in the two middle vessels.

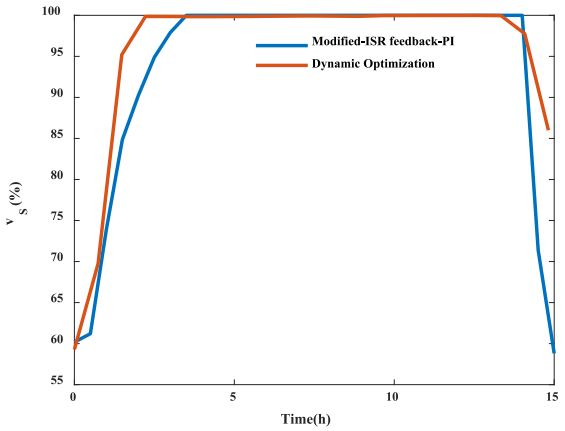

Fig. 14. Compares the side stream valve opening percentages in a stable cycle between Modified-ISR feedback-PI control and dynamic optimization (system II).

While the results imply that the Modified-ISR control model generates a $S(t)$ that is better in terms of SC when compared to the ISR control model, there is no reason to believe that it is an optimum. Thus, there is the possibility for the existence of an optimum side stream flowrate function $S^*(t)$, which might further reduce the cycle time and in turn minimize SC.

5. Dynamic optimization of semicontinuous distillation systems

Optimizing a semicontinuous distillation system is complex because of periodic processing without start-up or shutdown phases. Historically, Particle Swarm Optimization (PSO) was used to find the best tuning parameter vector, which although had been demonstrated to often find global optima, it cannot be guaranteed. The advantage of using PSO is that the system can be treated as a black-box while the SC is minimized. There is no need for periodic constraints to guarantee that the system returns to starting state of the cycle as it is taken care of by the event-driven tasks in the black-box simulation model. However, one of the disadvantages of the PSO approach is that the time required to find an improved design is large because it generally requires more function evaluations than mathematical programming methods with access to the model equations.

Therefore, to find better trajectories for the side stream flow rate, we used a dynamic optimization approach. The optimization problem was solved using the Aspen Dynamics built-in optimization tool (Aspen Technologies), which uses control vector parametrization or a direct sequential approach (Cervantes and Biegler, 2009). In this method, the control variable (side stream valve opening) is discretized over the time domain with variable element size and is approximated to be a piecewise linear function. This discretization breaks the problem into two sub-problems; the initial value problem, and the NLP program. The time invariant parameters of the piecewise linear function, element size, the final time, and the tuning parameters values of DB control, at the optimum, were decision variables, which are all determined by DMO, a Successive Quadratic Program (SQP) solver. A DAE solver in the inner loop provides objective function information and gradient information to the NLP solver that is operating in an outer loop (Aspen Technologies). This method could have convergence issues in the case of ill-conditioned systems (Biegler, 2010). Hence, tighter tolerances were chosen to accurately integrate the sensitivity equations. The method used to integrate the DAE system was backward difference formula of maximum order 5, with an absolute and relative tolerance of 0.00005. This is an adaptive step size, multi-step method that is typically used to solve DAE systems of index 1 (Ascher and Petzold, 1998). The initial step size was chosen to be 0.001 with a step reduction factor of 0.5. An initial estimate of the control function is necessary to solve the sequence of quadratic programming sub-problems in the SQP method.

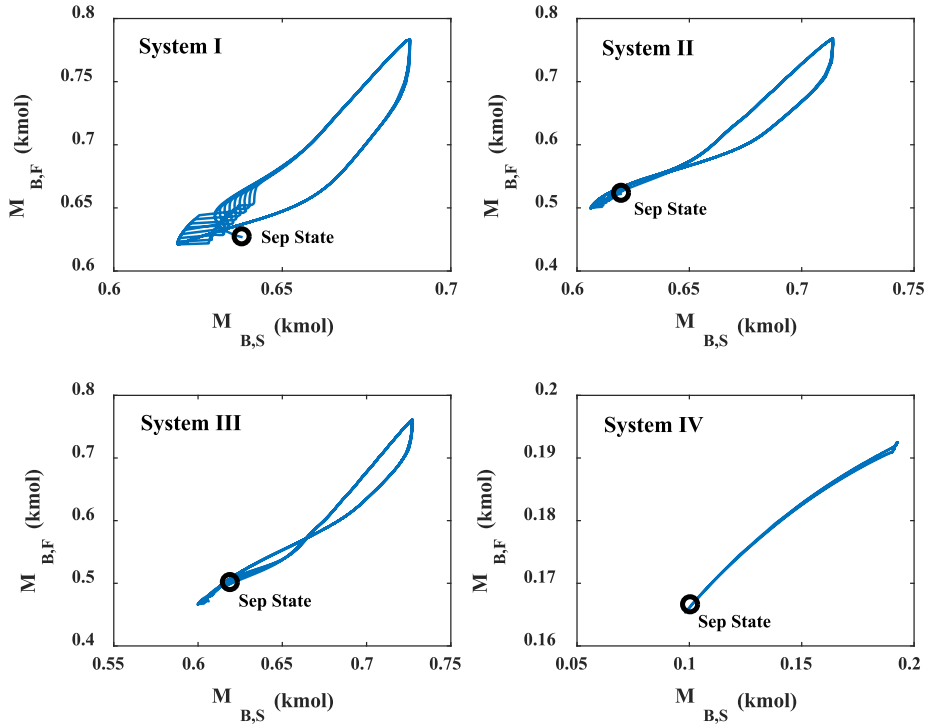

Fig. 15. Phase plane plots to illustrate the dynamic behavior when using the DO-optimized side stream valve opening (control) obtained using dynamic optimization (systems I through IV). Here, "Sep State" refers to the beginning of the Separating (*Sep*) mode of a stable cycle obtained by using the Modified-ISR feedback-PI side stream control and is also the initial state for simulation.

Before running the dynamic optimization, the system is allowed to converge to a stable periodic orbit using the Modified-ISR feedback-PI control of side stream, which is the current best known. Using dynamic optimization, the side stream flow rate trajectory that moves the system away from the Modified-ISR generated periodic orbit to a different periodic orbit with lower SC is found. The design variables that are invariant include the number of trays, the charge volume, reflux drum size, the size of the sump, feed tray location and side draw location. While the optimum is sensitive to all these fixed parameters, the objective of this study is to find an improved $S(t)$ that results in stable cycles with lower SC for a given design configuration. Endpoint constraints that ensure product purities and cycle periodicity are enforced.

The resulting "DO-optimized" side draw flow rate trajectory ($S^*(t)$)—or more appropriately, the resulting side stream valve opening schedule—is then tested by implementation to evaluate its performance and stability over many cycles. This is achieved by re-simulating 10 cycles from the beginning of the separating mode of a stable cycle using the side stream valve opening schedule exactly but allowing the cycle to terminate early when the middle vessel purity conditions have been reached. Or, if the middle vessel purity conditions have not yet been reached at the end of the valve opening schedule, the final valve opening is maintained until the purity conditions have been reached.

5.1. Optimization problem formulation

The objective function to be minimized is the separating cost, which is defined in Eq. (4),

The optimization problem formulation is,

$$
\begin{aligned}
&\underset{p_i,\ K_j,\ \tau_j,\ t_f}{\textit{minimize}} && \text{SC}\\
&\textit{subject to} && \text{Mass Balance Constraints}\\
& && \text{Energy Balance Constraints}\\
& && \text{Momentum Balance Constraints}\\
& && \text{Equilibrium Relationships}\\
& && \text{All other model equations}\\
& && v_{s,i}^{l} \le v_{s,i} \le v_{s,i}^{u}, \qquad i = 1, 2, 3, \ldots N.\\
& && h_{MV}^{l}(t_f) \le h_{MV}(t_f) \le h_{MV}^{u}(t_f)\\
& && {x_{Di,A}}^{l} \le \langle x_{Di,A} \rangle \le {x_{Di,A}}^{u}\\
& && {x_{Bo,C}}^{l} \le \langle x_{Bo,B} \rangle \le {x_{Bo,B}}^{u}\\
& && K_j^{l} \le K_j \le K_j^{u}\\
& && \tau_j^{l} \le \tau_j \le \tau_j^{u}\\
& && t_f^{l} \le t_f \le t_f^{u}
\end{aligned}
$$

where p_i represents the vector of time invariant parameters including the element size in the i^{th} interval and $v_{s,\,i}$ is the side stream valve opening at the end of the i^{th} interval. All other variables have their usual meanings.

The initial guesses for the side stream valve openings at the end points of each interval were set to corresponding valve openings

resulting from the improved Modified-ISR control model found in the previous sections.

5.2. Dynamic Optimization results

The improved valve opening function $v_s(t)$ found using dynamic optimization for the ternary systems compared to using Modified-ISR control model is shown in Fig. 14. The system using the results of the dynamic optimization reaches a 100% valve opening faster and moreover, the valve is open more for a slightly longer period during the cycle (Fig. 14). Nevertheless, the cycle times are approximately the same as the cycle times when Modified-ISR feedback-PI control was implemented, with a decrease of only 2% at most. Additionally, the convergence of the optimization problem to a solution (for ternary systems) that satisfies the periodic constraint $(h^l_{MV}(t_f) \leq h_{MV}(t_f) \leq h^u_{MV}(t_f))$ was extremely difficult because of frequent line search and QP sub-problem failures and required manual solver parameter tuning. For the quaternary system (V), the optimizer could not converge to a solution again because of similar numerical issues as stated above although the initial guess was feasible. Solver parameter tuning could not solve the problem.

New semicontinuous cycles were generated through repeated application of this "DO-optimized" control function (Fig. 15); moving away from the periodic orbit obtained from using the Modified-ISR feedback-PI control. The trajectory is dense during the end of the charging mode (or the beginning of the separating mode) because the system is not exactly periodic. This is due to the relaxation of periodicity while implementing the periodic constraint in the optimization problem formulation.

This emphasizes the need to develop an algorithm to find the optimal side stream trajectory that converges the system to a stable cycle from a chosen initial state. Although this is ideal, it is extremely difficult because of the complexity of the system. The SC computed is approximately 1 to 2% lower (see Table 4) when compared to the Modified-ISR case and almost 20% lower when compared to the ISR case. Furthermore, since SQP finds the local optimum, this result, while better than the Modified-ISR case in terms of SC, may not be the global best.

6. Conclusion and future work

The present work dealt with the effects of different choices for the side stream flowrate function $S(t)$ on SC, which was studied using simulation experiments on five different systems. The ISR control model was used in almost all prior semicontinuous studies available in the literature. The present study showed that by changing the functional structure of the control model, the periodic orbit in which the system is operated is dramatically different. The newly proposed Modified-ISR control model has not only resulted in stable periodic cycles, but also contributed to lower cycle times and correspondingly lower SC for all five case studies. A lower cycle time increases the frequency at which the feed is processed, thus leading to greater production for the same capital cost. It was found that by using the Modified-ISR feedback-PI control there was about 10 to 19% reduction in SC when compared to the status quo (ISR feedback-P control). This indicates the importance of a good side draw control for economic semicontinuous distillation design. The presence of better $S(t)$ functions in terms of reducing SC, motivated the search for optimal control functions using dynamic optimization.

Dynamic optimization with periodic constraints of a representative semicontinuous cycle (obtained by using the Modified-ISR feedback-PI control as the initial guess) to find an improved side stream trajectory, $S^*(t)$, that minimizes SC was carried out. While acknowledging that the results may be sub-optimal for other semicontinuous cycles, a trajectory that resulted lower cycle times and lower SC when compared to Modified-ISR feedback-PI control was found. For all practical purposes the improved side stream trajectory obtained through this procedure yielded an addition of one cycle per year (out of hundreds), which is a small improvement. Future work on the value of applying a model predictive control for finding the optimal $S(t)$ during a cycle when compared to Modified-ISR control model is suggested, for constant and varying feed conditions. There is also anecdotal evidence that arose during the study which suggests that the initial state might have some influence on the converged cycle trajectories and will be investigated in the future.

Acknowledgements

Support for this research is made possible through a grant from an Ontario Research Fund—Research Excellence Grant, number ORF-RE 05-072.

References

Adams II, T.A., Pascall, A., 2012. Semicontinuous thermal separation systems. Chem. Eng. Technol. 35, 1153–1170.
Adams II, T.A., Seider, W.D., 2008. Semicontinuous distillation for ethyl lactate production. AIChE J. 54, 2539–2552.
Ascher, U.M., Petzold, L.R., 1998. Computer methods for ordinary differential equations and differential-algebraic equations. Statew. Agric. Soc. Industrial Appl. Math 61.
Aspen Technologies. Aspen Plus V10.0, AspenTech. http://www.aspentech.com/products/Aspen-Plus/V10/ (accessed 7.31.17).
Ballinger, S.E., Adams, T.A., 2017. Space-constrained purification of dimethyl ether through process intensification using semicontinuous dividing wall columns. Comput. Chem. Eng. 105, 197–211.
Biegler, L.T., 2010. Nonlinear programming, society for industrial and applied mathematics. Soc. Industrial Appl. Math.
Bristol, E., 1966. On a new measure of interaction for multivariable process control. IEEE Trans. Autom. Control 11, 133–134.
Cervantes, A., Biegler, L.T., 2009. Optimization strategies for dynamic systems. Encycl. Optim. 2750–2757.
Gupta, B.S., Lee, M.J., 2013. Isobaric vapor-liquid equilibrium for binary systems of toluene+o-xylene, benzene+o-xylene, nonane+benzene and nonane+heptane at 101.3kPa. Fluid Phase Equilib. 352, 86–92.
Gupta, B.S., Lee, M.J., 2012. Isobaric vapor-liquid equilibrium for the binary mixtures of nonane with cyclohexane, toluene, m-xylene, or p-xylene at 101.3kPa. Fluid Phase Equilib. 313, 190–195.
IESO, n.d. Global Adjustment Components and Costs. http://www.ieso.ca/sector-participants/settlements/global-adjustment-components-and-costs (accessed 7.31.17).
Ling, H., Luyben, W.L., 2009. New control structure for divided-wall columns. Ind. Eng. Chem. Res. 48, 6034–6049.
Luyben, W.L., 2013. Distillation Design and Control Using ASPEN Simulation. John Wiley & Sons.
Meidanshahi, V., Adams II, T.A., 2016. Integrated design and control of semicontinuous distillation systems utilizing mixed integer dynamic optimization. Comput. Chem. Eng. 89, 172–183.
Meidanshahi, V., Adams II, T.A., 2015. Chemical engineering research and design a new process for ternary separations : semicontinuous distillation without a middle vessel. Chem. Eng. Res. Des. 93, 100–112.
Meidanshahi, V., Corbett, B., Adams II, T.A., Mhaskar, P., 2017. Subspace model identification and model predictive control based cost analysis of a semicontinuous distillation process. Computers & Chemical Engineering 103, 39–57.
Pascall, A., Adams II, T.A., 2014. Semicontinuous separation of bio-dimethyl ether from a vapor-liquid mixture. Ind. Eng. Chem. Res. 53, 5081–5102.
Pascall, A., Adams II, T.A., 2013. Semicontinuous separation of dimethyl ether (DME) produced from biomass. Can. J. Chem. Eng. 91, 1001–1021.
Phimister, J.R., Seider, W.D., 2000a. Semicontinuous, middle-vessel distillation of ternary mixtures. AIChE J. 46, 1508–1520.
Phimister, J.R., Seider, W.D., 2000b. Distillate–bottoms control of middle-vessel distillation columns. Ind. Eng. Chem. Res. 39, 1840–1849.
Towler, G., Sinnott, Ray K., 2012. Chemical engineering design - principles, practice and economics of plant and process design second edition. Elsevier.
U.S. Energy Information Administration, 2017. March 2017 Monthly Energy Review, Monthly Energy Review.
Wijesekera, K.N., Adams II, T.A., 2015a. Semicontinuous distillation of quaternary mixtures using one distillation column and two integrated middle vessels. Ind. Eng. Chem. Res. 54, 5294–5306.
Wijesekera, K.N., Adams II, T.A., 2015b. Semicontinuous distillation of quintenary and N-ary mixtures. Ind. Eng. Chem. Res. 54, 12877–12890.

Chapter 3

Improvements to the design methodology

3.1 Understanding the dynamic behaviour of semi-continuous distillation

---

The content of this section is a **published reprint** of the following peer-reviewed publication,

Madabhushi, Pranav Bhaswanth, Edgar Iván Sánchez Medina, and Thomas Alan Adams II. "Understanding the dynamic behaviour of semicontinuous distillation." In Computer Aided Chemical Engineering, vol. 43, pp. 845-850. Elsevier, 2018.

Anton Friedl, Jiří J. Klemeš, Stefan Radl, Petar S. Varbanov, Thomas Wallek (Eds.)
Proceedings of the 28th European Symposium on Computer Aided Process Engineering
June 10th to 13th, 2018, Graz, Austria.

Understanding the dynamic behaviour of semicontinuous distillation

Pranav Bhaswanth Madabhushi[a], Edgar Iván Sánchez Medina[b] and Thomas Alan Adams II [a,*]

[a]*McMaster University, Main St. W., Hamilton, Ontario L8S 4L8, Canada*
[b]*Universidad Nacional Autónoma de México, University City, Mexico City,CDMX, 04510, Mexico*
tadams@mcmaster.ca

Abstract

Semicontinuous, ternary distillation was first envisioned using a single distillation column and a middle vessel (MV) in the seminal work by Phimister and Seider. In the "sequential design methodology" introduced by Pascall and Adams for semicontinuous distillation, firstly, a steady state side-stream column that only meets the distillate and bottoms product purity specification is designed. Then by recycling the side-stream to the MV, the system is forced to move away from the steady state (initial state). Through repetitive input actions the system becomes periodic.

The objective of the current study is to understand the effect of changing the above initial state on the nature of the periodic orbit; specifically, its period. The initial state is changed by varying the values of the internal column recycle rates and also the external recycle rate. The periods of the converged periodic orbits are remarkably lower (almost 18 %) when compared to the base case design. Results revealed that the sequential design methodology is inherently sub-optimal. In conclusion, a rigorous design procedure that searches the space of initial states to reach an economically optimal periodic orbit is essential.

Keywords: Dynamic system analysis, design procedure, periodic orbits, semicontinuous process.

1. Introduction

Distillation systems are ubiquitous to chemical process industries. A significant portion of the total process industry's energy demand and therefore, a major portion of the operational costs of the plant can be attributed to these systems (Halvorsen and Skogestad, 2011). Semicontinuous distillation is aimed to be the best design for industries that are slowly transitioning from low to high production rates, which are currently being operated within intermediate production ranges (Adams and Pascall, 2012). It is an intensified process that has a forced cyclic operating policy to separate multicomponent mixtures using a single distillation column and a number of tightly integrated middle vessels (MVs). The number of MVs required are decided based on the number of intermediate boiling components in the mixture to be separated. For example, to separate an imaginary ternary mixture A, B, and C, where 'B' is the intermediate boiling component, one middle vessel and one distillation column is required. In this study, the focus is on separation of ternary mixtures. A single semicontinuous cycle is demarcated based on the concentration of intermediate boiling component ($x_{MV,B}(t)$) and the height of liquid in the MV ($h_{MV}(t)$) into three modes of operation: the separating mode, the discharging mode, and the charging mode. Discrete input actions on the flow control valves on streams associated with the MV, trigger these mode changes when the algebraic states of the system: $h_{MV}(t)$, $x_{MV,B}(t)$, reach pre-specified values.

1.1. Ternary semicontinuous distillation: Process Description

In a typical semicontinuous ternary distillation process, the feed flow to the column from the MV ($F(t)$), the distillate flow rate ($D(t)$), the bottoms flow rate ($Bo(t)$) and the side stream recycled to the MV ($S(t)$) are all continuous functions of the independent variable, time (t). The MV has two inlet streams and two outlet streams. Based on the mode of operation, the number of functional inlet streams that supply liquid material and the number of outlet streams that draw from the MV varies. In the "separating mode", the MV has only one functioning liquid inlet ($S(t)$) and one liquid outlet ($F(t)$) stream. The side stream is drawn from a location in the column that has high intermediate boiling component mole fraction when compared with the contents in the MV and therefore, the liquid in the MV gets gradually concentrated in component 'B'. Once the desired purity of component 'B' in the MV is reached, the contents of the middle vessel are discharged through a middle vessel discharge stream ($F_{dis}(t)$) by fully opening the discharge valve. This discrete input action marks the end of the separating mode and the beginning of the "discharging mode". During this mode, liquid is drawn from the middle vessel through two outlet streams: $F(t)$, $F_{dis}(t)$ and enters the MV through one inlet stream ($S(t)$). The discharge valve is fully closed when $h_{MV}(t)$ reaches a pre-specified lower limit while the charging valve is opened fully immediately, which controls the supply of liquid feed to be separated to the system ($F_{char}(t)$). Through these discrete input actions, a mode transition to the "charging mode" is signified. In this mode, the MV has two inlet streams ($S(t)$, $F_{char}(t)$) feeding liquid and one outlet stream ($F(t)$) drawing liquid from the MV. Liquid feed is fed to the MV until the liquid height in the MV reaches a pre-specified upper limit, delineating the end of the charging mode. The end of this mode also simultaneously demarcates the end of the cycle and a new cycle begins. During a cycle, because of the input actions the system is forced to move away from any steady states.

1.2. Ternary semicontinuous distillation: Control structure

Because of the concentration dynamics in the feed to the column, the process is not self-regulating, and therefore controllers are used for maintaining the distillate and bottoms purities at the desired values. The Distillate-Bottoms (DB) control configuration is used for this purpose (Figure 1). This control configuration was shown to be capable of handling off-spec products, because, in a total reflux condition, the MV prevents the preservation of liquid inventory within the column (Phimister and Seider, 2000). The control topology suggested by Pascall and Adams (2013) is typically used to regulate the reflux drum level, the sump level, and the column pressure along with the low and high volatile component concentrations in the distillate and bottoms streams. The semicontinuous ternary distillation process has seven degrees of freedom out of which five are used as control inputs in the suggested multi-loop control structure. They also recommended the use of a model-based control of the side stream flow rate to address the issue reducing the loss of intermediate boiling component

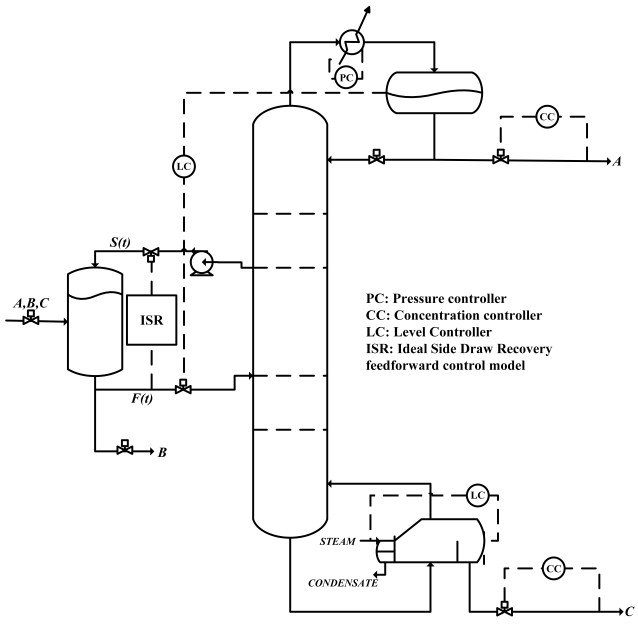

Figure 1: Semicontinuous Ternary Distillation Process

through the distillate and the bottoms streams. The model used was first derived by Adams and Seider (2008) by assuming that the column is operated at pseudo steady state and that the side stream is a 100 % pure in component 'B'. The model:

$$S(t) := F(t)x_{MV,B}(t) \tag{1}$$

was nomenclated as the "ideal side draw recovery" control law (ISR). The remaining degree of freedom, which is the reflux rate ($L(t)$) is fixed at the initial steady state value ($\bar{L}$) throughout the process.

1.3. Ternary semicontinuous distillation: The initial state

In simulation studies that ensued the seminal work on semicontinuous ternary distillation, the initial state was chosen to be a "hypothetical" steady state of a continuous side stream column, where the distillate and bottoms products are separated to the desired purity continuously. The steady state reflux rate ($\bar{L}$) and the steady state reboil rate ($\bar{V}$) are varied for a chosen steady state side stream flow rate ($\bar{S}$) to achieve the desired degree of low and high volatile product separation (Pascall and Adams, 2013). Therefore, different steady states can be generated by choosing a different value of '$\bar{S}$'. This design procedure will be henceforth referred to as the "sequential design methodology". The semicontinuous system evolves from the chosen initial steady state (or initial condition) after recycling the side stream flow rate, and through repetitive state dependent input actions it converges to a periodic orbit in the n-dimensional phase space; the operating locus of the semicontinuous distillation process described in section 1.1.

Pascall and Adams (2013) briefly mentioned the effect that '$\bar{S}$' has on the cycle time (or period of the converged periodic orbit) (T) of the semicontinuous distillation operation when using the sequential design methodology. However, there is no reason stated in the literature for choosing the initial condition of the dynamical system as a steady state where the distillate and bottoms products are separated at the desired purity. From an economic point of view, a steady state must be chosen from the space of initial conditions such that the converged periodic orbit has the minimum possible separation cost (defined as the total annualized cost per kmol of feed/product processed) subject to system constraints. The focus of this study is not to solve this general optimization problem, but to analyze the effect that the initial condition has on the system dynamics and to motivate research on proposing better algorithms to find the optimal designs of semicontinuous distillation of zeotropic mixtures.

2. Methodology

The cycle time (T) is a composition of the time taken to complete each of the three operating modes. The separating mode is completed when the concentration of intermediate boiling component in the middle vessel reaches the desired purity. Therefore, to reduce the separating time, the rate at which this component is concentrated in the MV has to be increased. From the dynamic component mass balance and the total mass balance of the MV during the separating mode:

$$\frac{dx_{MV,B}(t)}{dt} = \frac{S(t)}{M(t)}(x_{S,B}(t) - x_{MV,B}(t)) \tag{2}$$

where, $M(t)$ is the total molar holdup of liquid in the middle vessel, and $x_{s,B}(t)$ is the mole fraction of component B in the side stream recycled to the MV; in the time period close to the initial time ($t = 0$), it can be inferred that for the left hand side of Eq.(2). to be large for a given non-zero value of $M(t) \approx \bar{M}$ and $x_{MV,B}(t) \approx \bar{x}_{MV,B}$, both the values of $S(t)$ and $(x_{S,B}(t) - \bar{x}_{MV,B})$ have to be large. However, $S(t)$ is controlled using the ISR control law, and because $F(t)$ is the manipulated variable for controlling the reflux drum level, the reflux rate ($L(t) \equiv \bar{L}$) should also have an effect on the

rate at which the intermediate boiling component is concentrated in the middle vessel although they are spatially separate. Thus, the chosen steady state value of reflux rate has an effect on cycle time. However, since the mathematical analysis of the differential equation (Eq.(2).) for all time is not straightforward, numerical simulation experiments were conducted in this study. Similar dynamical equations can be written for the discharging and charging modes of a cycle.

The high purity (99 mol%) semicontinuous separation of a near-equimolar mixture (33-33-34 mol%) of benzene, toluene, and o-xylene (B-T-X) was chosen as the simulation example since it is an industrially significant and an almost ideal ternary mixture (Ling and Luyben, 2009). The design data required to simulate the steady state initial point were taken from Ling and Luyben (2009), and Meidanshahi and Adams (2015). The column was designed to have 40 stages with the feed stream location "above stage 25" and the side stream location "on stage 14". The column diameter was chosen to be 1.3716 m so that flooding within the column can be avoided at all points during the cycle. In the present study, the sequential design methodology was adopted for simulating the BTX semicontinuous separation system. The thermodynamic properties are computed using the Non-random Two-Liquid (NRTL) activity coefficient model (Ling and Luyben, 2009), which was shown to match well with experimental data for the isobaric state of 101.325 kPa (R^2 value of approximately 0.99 for each binary interaction); experimental data was obtained from Gupta and Lee (2012, 2013).

A condenser pressure of 0.37 atm with a stage pressure drop of 0.0068 atm was chosen by Ling and Luyben (2009) such that cooling water and low pressure steam can be used as condenser and reboiler utilities respectively. Since a very similar configuration was adopted by Meidanshahi and Adams (2015) to simulate a steady state continuous side stream column, and because a rigorous procedure was applied to obtain the location of the feed stream, side stream and the number of stages, the design data from this study was used. The MV, which is an essential part of semicontinuous separation was sized using the heuristics that were used in the case studies from Pascall and Adams (2013), to have total molar hold-up of 200 kmol of liquid feed, by using a length to diameter ratio of three and 90 % of its volume filled with liquid at the end of each charging mode.

All valves were sized to accommodate a 3 atm pressure drop except the distillate and the bottoms flow control valve, which were sized to have a 0.1 atm pressure drop keeping the operating pressure of the column in mind. The reflux drum and the sump were sized according to the design heuristics of Luyben (2013). The control configuration using the ISR feedforward control model for side stream molar flow control was used. A proportional controller (P) was used for reflux drum level, sump level, and side stream flow rate control and a proportional-integral (PI) controller was used to control the remaining outputs similar to the study by Meidanshahi and Adams (2015).

3. Results and Discussion

The base case was chosen as the case where $\bar{L}$, $\bar{V}$ were found such that the desired degree of benzene and o-xylene separation was achieved. The value of $\bar{S}$ for the base case can be chosen to be $\bar{F}\bar{x}_{MV,B}$ according to the ISR control law. However, at this value of the side stream flow rate, the steady state column used as initial state was found to operate beyond the flooding limit. Therefore, a slightly higher value was chosen to avoid flooding in the column. Two sets of experiments were performed: constant internal column recycle rates ($\bar{L}$, $\bar{V}$), and constant external recycle rate ($\bar{S}$).

In the first set of experiments, the ratio of side stream molar flowrate to the feed molar flow rate to the column was varied from the base case value in increments of 0.05 until a value of 0.65 in one set of numerical simulation experiments. Beyond the value of 0.65, the magnitude of bottoms flow rate was found to be small enough that it is impractical to control the bottoms product concentration by manipulating it using a controller. The reflux rate and the boilup rate were not changed from the base case value, and therefore the distillate and bottoms product purities were not maintained at the desired values. The results are presented in Table 1:

Table 1: Results of constant reflux and reboil rates experiments ($\bar{F}$ = 100 kmol/h)

	Base Case	Case 1	Case 2	Case 3	Case 4	Case 5
Steady State: Specified						
$\frac{\bar{L}}{\bar{F}}$	0.106	0.106	0.106	0.106	0.106	0.106
$\frac{\bar{V}}{\bar{F}}$	0.117	0.117	0.117	0.117	0.117	0.117
$\frac{\bar{S}}{\bar{F}}$	0.396	0.45	0.5	0.55	0.6	0.65
Steady State: Calculated						
$\bar{x}_{D,B}$	0.99	0.976	0.954	0.932	0.911	0.892
$\bar{x}_{Bo,B}$	0.99	0.999	0.999	0.999	0.999	0.999
$\bar{x}_{S,B}$	0.82	0.72	0.634	0.565	0.507	0.459
Column flooding	No	No	No	No	No	No
Periodic Orbit: Calculated						
T (h)	16.60	14.96	13.64	12.65	12.03	12.40
Column flooding	No	No	No	No	No	No

Consider for example "Case 2", the $\frac{\bar{S}}{\bar{F}}$ ratio of the steady state point used as the initial state was changed from the base case value by 25 %. At this steady state, the distillate mole fraction is less than the desired purity by 3.6 %. When the base case was used to simulate the dynamic behaviour, the cycle time was observed to be around 16.6 h. By choosing the $\frac{\bar{S}}{\bar{F}}$ ratio to be 0.5 and using the sequential design methodology ($\bar{x}_{D,B}$ = 0.99 and $\bar{x}_{Bo,B}$ = 0.99 are specified at steady state) resulted in a periodic orbit of cycle time of approximately 16.47 h (result not presented in the table). However, when the steady state presented in the table was used as the initial condition for dynamic simulation, the cycle time dropped to 13.64 h; an approximate 18 % drop. Furthermore, from the table we can infer that "Case 4" has the lowest possible cycle time when compared to the rest of the cases in the first set of experiments. The reason for the observed differences in cycle time can be attributed to the contrasts in the behaviour of the individual controllers after the side stream is recycled to the MV because of the differences in initial state. Similar results were observed (although not of the same magnitude) when one of the internal column recycle rates - reflux rate ($\bar{L}$) is maintained constant and the $\frac{\bar{S}}{\bar{F}}$ ratio is varied. For the sake of brevity these results are not presented in this article.

Since reflux rate is a degree of freedom that is maintained at a constant value $\bar{L}$ during the semicontinuous distillation operation, its effect on cycle time was also studied. This investigation resulted in the next set of experiments using a constant external recycle rate ($\bar{S}$); results are presented in Table 2. The reflux rate was increased from the base case value of 106.34 kmol/h to 140 kmol/h. Increasing this value further resulted in column flooding at steady state. In these set of experiments, the bottoms concentration was not changed from the desired value at steady state. Although reflux rate has an influence on cycle time, its effect is not as significant when compared to the previous set of experiments. In practice, ideally the optimal values of $\bar{L}$, $\bar{V}$, and $\bar{S}$ (or the optimal initial condition) has to be found, which results in the optimum separating cost.

4. Conclusion

The sequential design methodology that was historically used to converge to a periodic orbit can result in sub-optimal periodic orbits as demonstrated using the simulation experiments. The space of initial conditions from which the system can reach a stable periodic orbit has expanded to include more steady states than previously imagined. From the numerical simulation experiments, for the equimolar separation of BTX, a case was found where an approximate 18 % decrease

Table 2: Results of constant side draw flow rate experiments ($\bar{F}$ = 100 kmol/h)

	Base Case	Case 1	Case 2	Case 3
Steady State: Specified				
$\bar{x}_{Bo,B}$	0.99	0.99	0.99	0.99
$\frac{\bar{L}}{\bar{F}}$	0.106	0.12	0.13	0.14
$\frac{\bar{S}}{\bar{F}}$	0.396	0.396	0.396	0.396
Steady State: Calculated				
$\bar{x}_{D,B}$	0.99	0.994	0.995	0.996
$\frac{\bar{V}}{\bar{F}}$	0.117	0.129	0.137	0.146
$\bar{x}_{S,B}$	0.82	0.821	0.821	0.822
Column flooding	No	No	No	Close
Periodic Orbit: Calculated				
T (h)	16.60	16.35	16.18	16.03
Column flooding	No	No	No	Yes

in cycle time was observed while operating without violating the column hydraulic constraints. Although this initial state is "hypothetical", a start-up procedure for semicontinuous zeotropic separation can be devised where this steady state is first reached before allowing the system to converge to a periodic orbit. An alternate optimization based design methodology is thus required to search through the space of steady states and choose the optimal steady state. This methodology should also incorporate the other decision variables, like for example, the controller tuning parameters, to ensure that the control inputs are optimal. A dynamic optimization based procedure that considers all the above requirements would be ideal. Research in this area is currently in progress.

5. Acknowledgements

Support for this research is made possible through funding from the McMaster Advanced Control Consortium (MACC) and MITACS Globalink Program.

References

T. A. Adams II, A. Pascall, 2012, Semicontinuous thermal separation systems, Chemical Engineering & Technology 35, 1153-1170.

T. A. Adams II, W. D. Seider, 2008, Semicontinuous distillation for ethyl lactate production, AIChE journal 54, 2539-2552.

B. S. Gupta, M. Lee, 2012, Isobaric vaporliquid equilibrium for the binary mixtures of nonane with cyclohexane, toluene, m-xylene, or p-xylene at 101.3 kpa, Fluid Phase Equilibria 313, 190-195.

B. S. Gupta, M. Lee, 2013, Isobaric vapor-liquid equilibrium for binary systems of toluene+o-xylene, benzene+o-xylene, nonane+benzene and nonane+heptane at 101.3kpa, Fluid Phase Equilibria 352, 86-92.

I. J. Halvorsen, S. Skogestad, 2011, Energy efficient distillation, Journal of Natural Gas Science and Engineering 3, 571-580.

H. Ling, W. L. Luyben, 2009, New control structure for divided-wall columns, Industrial & Engineering Chemistry Research 48, 6034-6049.

W. L. Luyben, 2013, Distillation design and control using Aspen simulation, John Wiley & Sons.

V. Meidanshahi, T. A. Adams II, 2015, A new process for ternary separations: Semicontinuous distillation without a middle vessel, Chemical Engineering Research and Design 93, 100-112.

A. Pascall, T. A. Adams II, 2013, Semicontinuous separation of dimethyl ether (DME) produced from biomass, The Canadian Journal of Chemical Engineering 91, 1001-1021.

J. R. Phimister, W. D. Seider, 2000, Semicontinuous, middle-vessel distillation of ternary mixtures, AIChE journal 46, 1508-1520.

3.2 Back-stepping design methodology

The content of this section is a **published reprint** of the following peer-reviewed publication,

Madabhushi, Pranav Bhaswanth, and Thomas Alan Adams. "Finding Better Limit Cycles of Semicontinuous Distillation. 1. Back Stepping Design Methodology." Industrial & Engineering Chemistry Research 58, no. 36 (2019): 16654-16666.

I&EC research
Industrial & Engineering Chemistry Research

Article

Cite This: *Ind. Eng. Chem. Res.* 2019, 58, 16654−16666

pubs.acs.org/IECR

Finding Better Limit Cycles of Semicontinuous Distillation. 1. Back Stepping Design Methodology

Pranav Bhaswanth Madabhushi and Thomas Alan Adams, II*

Department of Chemical Engineering, McMaster University, Main Sreet West, Hamilton, Ontario L8S 4L8, Canada

ABSTRACT: Semicontinuous ternary zeotropic distillation is a periodic process that is carried out in a single distillation column and a tightly integrated external middle vessel. In the state-of-the-art design procedure of this process, a continuous distillation process that separates the top and bottom products to the desired purity is used to generate an arbitrary initial state for simulating the dynamics of the semicontinuous distillation process. Although this method is useful in estimating the limit cycle, it was later found that the operation of the process in this limit cycle was economically suboptimal. In this study, a new algorithmic design procedure, called the back-stepping design methodology, is proposed to find better limit cycles for zeotropic ternary semicontinuous distillation using the aspenONE Engineering suite. The proposed methodology was applied to two different case studies using feed mixtures with different chemical components. A comparison with the current design procedure for the two case studies indicates that the new method outperforms the state-of-the-art by finding limit cycles that were 4−16% lower in separating cost, which was the chosen measure of cycle performance.

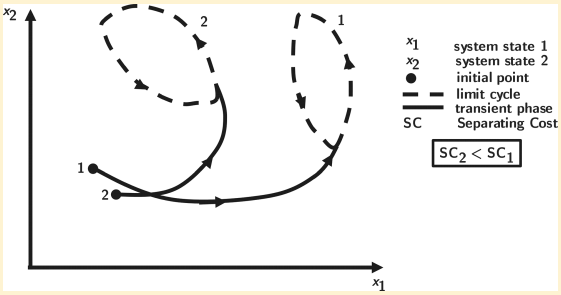

INTRODUCTION

The concept of semicontinuous distillation is intended for multicomponent separations, which are carried out in the intermediate production range. This intensified process has desirable features like higher flexibility, and lower capital investment than equivalent continuous distillation processes.[1] Indeed, the basis for process intensification was on its traditional viewpoint[2] rather than the newly developed concept of dynamic intensification by Yan et al.,[3] who focused on operational regime changes. In their work, dynamic intensification in process plants was illustrated by using the properties of output multiplicity to devise a new periodic operating mode for binary distillation.

Industries undergoing a production scale-up from the batch mode, and separations in distributed biofuel production plants are ideal cases to implement the semicontinuous distillation process.[4,5] A semicontinuous configuration was illustrated to be beneficial in terms of cost and energy utilization in heterogeneous azeotropic distillation by Tabari and Ahmad[6] using dehydration of acetic acid as a case study. In this article, however, the focus is on the semicontinuous distillation of zeotropic ternary mixtures, which requires two pieces of equipment for separations of ternary mixtures: a distillation column and a process vessel called the middle vessel, and a control system which drives the process.[4] The batches of feed to be distilled are fed periodically to the middle vessel, which in turn continually feeds the distillation column. Simultaneously, a side stream from the distillation column is continually recycled to the middle vessel. The low and high volatile components in the ternary mixture are continually removed from the top and bottom of the distillation column, while the intermediate boiling component is periodically discharged from the middle vessel. This process is, therefore, different from cyclic distillation, which is a cyclic operating mode for the operation of distillation columns. The cyclic operation comprises of a vapor flow period when liquid is stagnant and a liquid flow period when vapor flow is stopped to improve energy use, increased throughput, and separation performance.[7]

Semicontinuous distillation is an example of an autonomous hybrid limit-cycle oscillator,[8] which was defined mathematically by Khan et al. State-dependent discrete input actions, such as the periodic feed charges and product discharges, are responsible for changes in the system dynamics at discrete instants in continuous time, making it a hybrid system. Unlike continuous distillation, this process operates in a limit cycle (Γ), which is the periodic solution of the equations describing the semicontinuous distillation process. The design of the process involves finding the time-invariant parameter vector, $\mathbf{p}$, to operate the process in a desirable limit cycle. Typically, the metric that is used to evaluate the performance of a design is the separating cost, defined as the total annualized cost-per-production rate of a product.

In order to estimate the limit cycle of a semicontinuous distillation system for a particular value of $\mathbf{p}$, all previous studies[1,5,9−14] had relied on the 'brute force method'[15]. In this method, a dynamical system is numerically integrated to

Received: May 13, 2019
Revised: June 27, 2019
Accepted: July 8, 2019
Published: July 8, 2019

DOI: 10.1021/acs.iecr.9b02639
Ind. Eng. Chem. Res. 2019, 58, 16654−16666

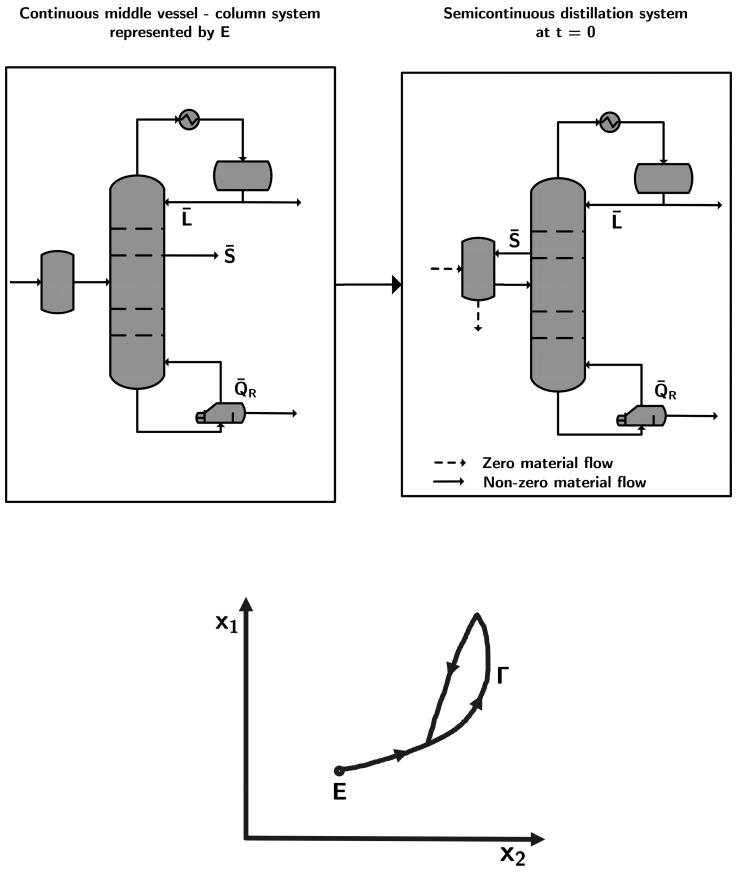

Figure 1. Top left: A schematic of the hypothetical continuous middle vessel-column system used for equipment design and to determine an arbitrary initial state for the semicontinuous system. Top right: A schematic of the semicontinuous distillation system at $t = 0$ on which the brute force method is applied. Bottom: An illustration of the evolution of the system trajectory in state space when applying the sequential design methodology.

estimate the steady state (in this case, a limit cycle) by starting from an arbitrary initial state, provided this initial state is within the basin of attraction.[15] Although it is a reliable method, it suffers from limitations, such as linear convergence,[16] and difficulty in steady-state identification. Despite these limitations, in this study, the brute force approach was chosen because it offers a practical way to approach a cycle (startup), and it features a simple computational method.

All previous studies[5,10−12,17,18] that used the brute force method determined the arbitrary initial state by designing a continuous distillation process (referred to as continuous middle vessel-column system in this study) which comprises of a distillation column with a side draw (Figure 1, top left). The continuous distillation process is designed to meet the top and bottoms product purities that is desired in the semicontinuous distillation process. However, the side draw does not satisfy the necessary purity requirements of the intermediate product. The state of this process (represented by E) only roughly approximates the semicontinuous system's true state in a semicontinuous cycle (Figure 1, top right, and Figure 1, bottom). This approach was an effective way of obtaining a consistent initial condition that satisfied the dynamic model equations of the semicontinuous distillation system. From this state, the brute force method is applied to estimate the limit cycle, Γ (Figure 1, bottom). Furthermore, the continuous distillation process was used to estimate equipment sizes such as column diameter, side stream pump capacity, and valve sizes to be used in semicontinuous distillation. A stochastic optimizer was typically used to find a better semicontinuous distillation design by using the separating cost as the objective function and the controller tuning parameters as design decision variables.

The above-described design methodology was known as the sequential design methodology and was first used by Pascall and Adams.[5] Later, Meidanshahi and Adams[11] included integer design decision variables in the optimization formulation along with the controller tuning parameters to find cost-effective designs.

Subsequently, Madabhushi and Adams[13] demonstrated the importance of the side stream flow rate function on process economics. The study directly leads to the hypothesis that the upper bound of the side stream flow rate (S^u), which is related to the side stream pump and valve design, is an important parameter in the search for finding cost-effective designs. The hypothesis was tested in the study by Madabhushi et al.,[14] where the combined effect of changing S^u and the point E (in particular, the state of the distillation column) was demonstrated to have an impact on the cycle time (period T). This effect was also briefly demonstrated by Pascall and Adams.[5] Note here that varying S^u

DOI: 10.1021/acs.iecr.9b02639
Ind. Eng. Chem. Res. 2019, 58, 16654−16666

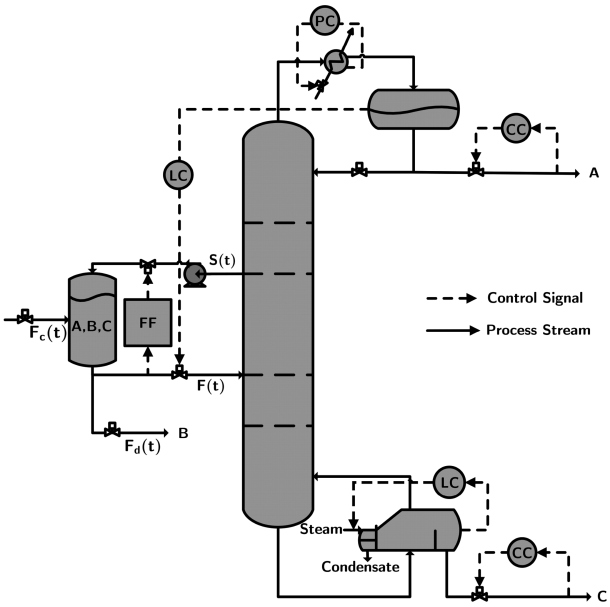

Figure 2. A schematic of the semicontinuous distillation system. Reprinted from Pranav Bhaswanth Madabhushi; Thomas A. Adams, II. Side stream control in semicontinuous distillation. *Computers & Chemical Engineering*, 2018, *119*, 450−464, with permission from Elsevier.

and the point E indirectly corresponds to changing the semicontinuous distillation system's time-invariant parameters and therefore affects the limit cycle wherein the system operates. Although these studies have shown that higher side stream recycle rates to the middle vessel could be advantageous, care should be taken to ensure that the design is hydraulically feasible throughout the operation in the limit cycle to guarantee efficient separation.

The sequential design methodology does not prescribe a procedure to change the arbitrary initial state (E) once it is determined. However, varying this state is possible by changing the side stream flow rate $(\bar{S})$, the reflux rate $(\bar{L})$, and the reboiler duty $(\bar{Q}_R)$, that is, altering the design of the continuous middle vessel-column system. Variables are affixed with an overbar to indicate that they correspond to the point, E. Therefore, this paper builds upon the results reported by Madabhushi et al.[14] and presents a new algorithmic design procedure for semicontinuous distillation design, referred to as the 'Back-stepping design methodology'. The application of this design procedure for semicontinuous distillation design in the aspenONE simulation environment is demonstrated using two different case studies. Most semicontinuous distillation studies have used Aspen Plus and Aspen Plus Dynamics software to simulate the semicontinuous distillation process, primarily due to the availability of rigorous process and physical property models. The scope of the new procedure is limited to finding the point E and S^u, which can lead to better feasible Γ in terms of cost than the state-of-the-art methodology. The next two sections focus on the detailed process description and a brief mathematical description of the process.

DETAILED PROCESS DESCRIPTION

The semicontinuous distillation system is comprised of three subsystems (Figure2): the middle vessel, the distillation column, and the control system. The middle vessel subsystem has four material streams—two inlet streams and two outlet streams. However, the number of streams in use at any given time (i.e., nonzero flow rates) will always be less than the total number of available material streams. At the beginning of the cycle, the middle vessel contains the feed to be separated at a prespecified upper limit in liquid height (h_v^u). The liquid mixture in the middle vessel is separated into its constituents in the distillation column by drawing the most volatile component (A) from the distillate, the least volatile component (C) from the bottoms, and gradually concentrating the middle vessel with an intermediate volatility component (B) by recycling the side stream. Once product B has reached the desired level of purity in the middle vessel $(x_{B,v}^{desired})$, the contents of the middle vessel are discharged. Liquid is drawn from the middle vessel through the discharge stream $(F_d(t))$ while it continues to feed the distillation column. Once the height of liquid in the middle vessel $(h_v(t))$ reaches a prespecified lower limit (h_v^l), the liquid discharge is stopped and fresh feed is charged $(F_c(t))$ to the middle vessel. The mixture to be separated is fed to the middle vessel while also still being fed into the distillation column. When the liquid height, $h_v(t)$, reaches a prespecified upper limit (h_v^u) it signifies the end of the cycle. These switches in the operation are based on the state of the middle vessel subsystem. These states of the middle vessel can be classified into three modes of system operation, which are separating mode, discharging mode, and charging mode.[4]

During all the three modes, the concentration of feed components changes continuously with time. Since the process is not self-regulating, a control subsystem is used to maintain the control outputs at the desired values. The most frequently used control subsystem in semicontinuous distillation studies was designed by Pascall and Adams.[5] In a subsequent study, Madabhushi and Adams[13] demonstrated that modifying the

DOI: 10.1021/acs.iecr.9b02639
Ind. Eng. Chem. Res. 2019, 58, 16654−16666

control configuration—specifically the side streamflow rate control—produced significant economic benefits. Madabhushi and Adams[13] controlled the side streamflow rate using the modified-ideal side draw recovery feedback control implemented using a PI controller. The set point of the controller is varied according to eq 1,

$$S_{\mathrm{MISR}}(t) := \frac{F(t)x_{B,\mathrm{v}}(t)}{x_{B,\mathrm{S}}(t)} \tag{1}$$

where $x_{B,\mathrm{v}}(t)$ is the mole fraction of B in the middle vessel, and $x_{B,\mathrm{S}}(t)$ is the mole fraction of B in the side stream.

MATHEMATICAL DESCRIPTION

The mathematical model of the semicontinuous distillation process falls under the category of hybrid (discrete/continuous) limit-cycle oscillators, which allow for the presence of both discrete and continuous state trajectories that are closed, isolated, and time-periodic.[8] The continuous-time dynamics of this process varies in different "discrete states" as a result of the changes to the mass and energy balance equations of the middle vessel subsystem. Changes to these equations are because of instantaneous events like the feed charges and product discharges, which alter the number of input streams to, and output streams from the middle vessel. A discrete state is the active mode of the process,[19] which are separating mode (mode 1), discharging mode (mode 2), and charging mode (mode 3). The mode trajectory (order of the modes visited by the system's discrete state) in a semicontinuous distillation cycle is as follows: {1, 2, 3, 1}. The mode-specific material balance, fugacity relations, summation equations, enthalpy balance, and hydraulic flow equations are represented compactly as

$$\mathbf{f}^{(k)}(\dot{\mathbf{z}}^{(k)}, \mathbf{z}^{(k)}, \mathbf{y}^{(k)}, \mathbf{u}^{(k)}, \mathbf{p}) = \mathbf{0},\ k = 1, 2, 3 \tag{2}$$

where $\mathbf{z}$ represents the differential states, $\mathbf{y}$ represents the algebraic states, $\mathbf{u}$ represents the vector of the control variables, $\mathbf{p}$ represents the vector of time-invariant parameters such as equipment design variables and the tuning parameters of the controllers in the modified Pascall-Adams multiloop control configuration. The index that designates the discrete state is represented by k. As an example, the middle vessel subsystem's component mass balance in the three modes would be,

$$\text{mode1: } \left\{ \frac{\mathrm{d}M_{\alpha}^{(1)}(t)}{\mathrm{d}t} = S^{(1)}(t)x_{\alpha,\mathrm{S}}^{(1)}(t) - F^{(1)}(t)x_{\alpha,\mathrm{v}}^{(1)}(t),\ \alpha = A, B, C \right. \tag{3}$$

$$\text{mode2: } \left\{ \frac{\mathrm{d}M_{\alpha}^{(2)}(t)}{\mathrm{d}t} = S^{(2)}(t)x_{\alpha,\mathrm{S}}^{(2)}(t) - F^{(2)}(t)x_{\alpha,\mathrm{v}}^{(2)}(t) - F_{\mathrm{d}}^{(2)}(t)x_{\alpha,\mathrm{v}}^{(2)}(t),\ \alpha = A, B, C \right. \tag{4}$$

$$\text{mode3: } \left\{ \frac{\mathrm{d}M_{\alpha}^{(3)}(t)}{\mathrm{d}t} = F_{\mathrm{c}}^{(3)}(t)x_{\alpha}^{(3)}(t) + S^{(3)}(t)x_{\alpha,\mathrm{S}}^{(3)}(t) - F^{(3)}(t)x_{\alpha,\mathrm{v}}^{(3)}(t),\ \alpha = A, B, C \right. \tag{5}$$

where, α designates the components A, B, and C, respectively, and $M_{\alpha}(t)$ is the liquid molar holdup of the component, α, in the middle vessel.

The transition from one mode to another (discrete dynamics) is based on a transition condition $(L_j^{(k)})$, where j is the next mode in the sequence.[20] Ternary semicontinuous distillation has three simple transition conditions, which are

$$L_2^{(1)}: x_{B,\mathrm{v}}^{(1)} \geq x_{B,\mathrm{v}}^{\mathrm{desired}} \tag{6}$$

$$L_3^{(2)}: h_{\mathrm{v}}^{(2)} \leq h_{\mathrm{v}}^{l} \tag{7}$$

$$L_1^{(3)}: h_{\mathrm{v}}^{(3)} \geq h_{\mathrm{v}}^{u} \tag{8}$$

with the superscripts l and u representing the predefined lower and upper limits, respectively. Since these are state dependent transitions, the event time is implicitly defined by these conditions. Specifically, these transitions are triggered by discrete control signals computed based on the system's state. Thus, the closed-loop hybrid system is an autonomous-switch hybrid limit-cycle oscillator.[21] Given that commercial process-simulation software can simulate such systems, the aspenONE Engineering suite was used in this study because of its rigorous phenomenological and control models available in the process model library, which makes it easier to model the semicontinuous distillation subsystems. The discrete dynamics were modeled using the "Tasks" functionality in Aspen Plus Dynamics V10.[22] In this study, the focus is on designing the system using the aspenONE Engineering suite by varying the side stream pump and valve capacities (via $\overline{S}$), the controller tuning parameters, and the reflux rate $(\overline{L})$, which are time-invariant parameters in the semicontinuous distillation model.

DESIGN: OPTIMIZATION PROBLEM FORMULATION

The point E, which refers to the steady-state solution of the continuous middle vessel-column system in the sequential design methodology does not represent any of the three modes of semicontinuous distillation. This state is used as the arbitrary initial state (E) for applying the brute force method on the semicontinuous distillation model. In the sequential design methodology, identifying a specific separation to be carried out in the continuous middle vessel-column system, for example, separating the top and bottoms products to the desired purity, locks the value of the reflux rate (a time-invariant parameter) in the semicontinuous distillation model to $\overline{L}$. Additionally, the side stream flow rate $(\overline{S})$, a degree of freedom of the continuous middle vessel-column system, is used to determine the capacities of the semicontinuous distillation system's side stream pump and valve, which are also fixed parameters in the semicontinuous distillation model. Therefore, to change the limit cycle in which the semicontinuous distillation process operates, the continuous middle vessel-column design should be altered by varying its degrees of freedom $(\overline{S}, \overline{L}$, and $\overline{Q}_R)$. Although $\overline{Q}_R$ is not a time-invariant parameter of the semicontinuous distillation system, it

DOI: 10.1021/acs.iecr.9b02639
Ind. Eng. Chem. Res. 2019, 58, 16654−16666

is included here because its choice could affect the selection of the modified Pascall-Adams controller tuning parameters.

A set (Θ) can be defined to contain all possible continuous middle vessel-column steady-states that can be generated by varying the values of $\overline{S}$, $\overline{L}$, $\overline{Q}_R$.

$$\Theta = \{(\overline{\mathbf{z}}, \overline{\mathbf{y}}): \mathbf{f}^{(E)}(\mathbf{z}, \mathbf{y}, \overline{S}, \overline{L}, \overline{Q}_R) = \mathbf{0}\} \quad (9)$$

where $\mathbf{f}^{(E)}$ is a system of nonlinear algebraic equations that describes the continuous middle vessel-column system. The optimization problem ($\mathbf{P}$) to be solved to find the best semicontinuous distillation design in the space of the design variables considered, which includes selecting E from Θ is shown below, where,

$$\underset{\overline{S}, \overline{L}, \overline{Q}_R, \mathbf{p}'}{\text{minimize}} \quad SC^{(\Gamma)}$$

$$\text{subject to} \quad \mathbf{f}^{(k)}\left(\dot{\mathbf{z}}^{(k)}, \mathbf{z}^{(k)}, \mathbf{y}^{(k)}, \mathbf{u}^{(k)}, \mathbf{p}\right) = \mathbf{0}, \; k = 1, 2, 3$$

$$\text{mode 1}\left\{\begin{array}{l}\text{separating mode}\end{array}\right\}: \begin{cases} L_1^{(3)}: h_v^{(3)} \geq h_v^u \\ F_c(t) = 0 \\ F_d(t) = 0 \end{cases}$$

$$\text{mode 2}\left\{\begin{array}{l}\text{dscharging mode}\end{array}\right\}: \begin{cases} L_2^{(1)}: x_{B,v}^{(1)} \geq x_{B,v}^{desired} \\ F_c(t) = 0 \\ F_d(t) = F_d \end{cases}$$

$$\text{mode 3}\left\{\begin{array}{l}\text{charging mode}\end{array}\right\}: \begin{cases} L_3^{(2)}: h_v^{(2)} \leq h_v^l \\ F_c(t) = F_c \\ F_d(t) = 0 \end{cases}$$

$$\text{hydraulic constraints}^{(\Gamma)}$$

$$\text{quality constraints}^{(\Gamma)}$$

$$\text{variable bounds}$$

$$\mathbf{f}^{(E)}\left(\mathbf{z}, \mathbf{y}, \overline{S}, \overline{L}, \overline{Q}_R\right) = \mathbf{0}$$

$\mathbf{p}'$ represents the controller tuning parameters and is a subset of $\mathbf{p}$. In this study, Aspen Plus V10 was used to design the continuous middle vessel-column system. The arbitrary initial state (E) that was generated in Aspen Plus V10[23] by solving the nonlinear system, $\mathbf{f}^{(E)}$, was used to start the numerical integration of the differential-algebraic equations (DAEs) describing the semicontinuous distillation process, which was carried out in Aspen Plus Dynamics V10.[22] The objective function was evaluated only after converging to the limit cycle (Γ) because it is a metric that is defined for the limit cycle and not elsewhere. Similarly, the hydraulic constraints (flooding, weeping, and weir loading), which are inequality-path constraints with an implicit dependence on state variables, should be satisfied during column operation in the limit cycle. The quality constraints are mass-average purities of the top and bottoms products (end-point constraints), which have to be satisfied at the end of Γ. In practice, however, different blending/mixing tanks are used (column downstream) to collect and blend the top and bottoms products separately over the time period of the cycle so as to ensure on-spec product quality.

Simulation of the Embedded System in P. Simulating the embedded hybrid system in the optimization problem, $\mathbf{P}$, using the aspenONE Engineering suite is a two-step process as briefly described above. An initial condition for the dynamic simulation of semicontinuous distillation process was obtained by first solving the continuous middle vessel-column equations in the Aspen Plus steady-state simulation software.[23] All equipment sizes, including the side stream pump and valve, were determined at this stage using the steady-state flow rates. The simulation was then exported to the Aspen Plus Dynamics software to simulate the dynamic behavior. Once the equipment sizes were fixed, solving $\mathbf{f}^{(E)}$ within the Aspen Plus Dynamics V10[22] environment to generate a new E with a different side stream pump and valve size proved to be challenging because of numerical convergence issues. Therefore, to overcome this practical issue, the idea of using a control system to move from one steady state to another for a fixed side stream pump and valve size was implemented in Aspen Plus Dynamics V10. Nevertheless, the new design methodology also includes a procedure to change the side stream pump and valve capacities (thus affecting S^u) and is discussed in the subsequent section.

Modifications were made to the continuous middle vessel-column model in Aspen Plus V10 to implement the idea mentioned above, and thus, the semicontinuous distillation model in Aspen Plus Dynamics V10. The continuous middle vessel-column model was modified in Aspen Plus V10 to include two side streams: S_1, recycled to the middle vessel with zero liquid flow rate, and S_2, wherein there was liquid flow, but was not recycled to the middle vessel. A new control system, called the continuous control configuration, was added to this modified continuous middle vessel-column superstructure in Aspen Plus Dynamics V10 to transition from one steady state to another. This control system was in addition to the modified Pascall-Adams control configuration used in semicontinuous distillation. The continuous control configuration includes two flow rate controllers: one for feed flow, and one for column side

DOI: 10.1021/acs.iecr.9b02639
Ind. Eng. Chem. Res. 2019, 58, 16654−16666

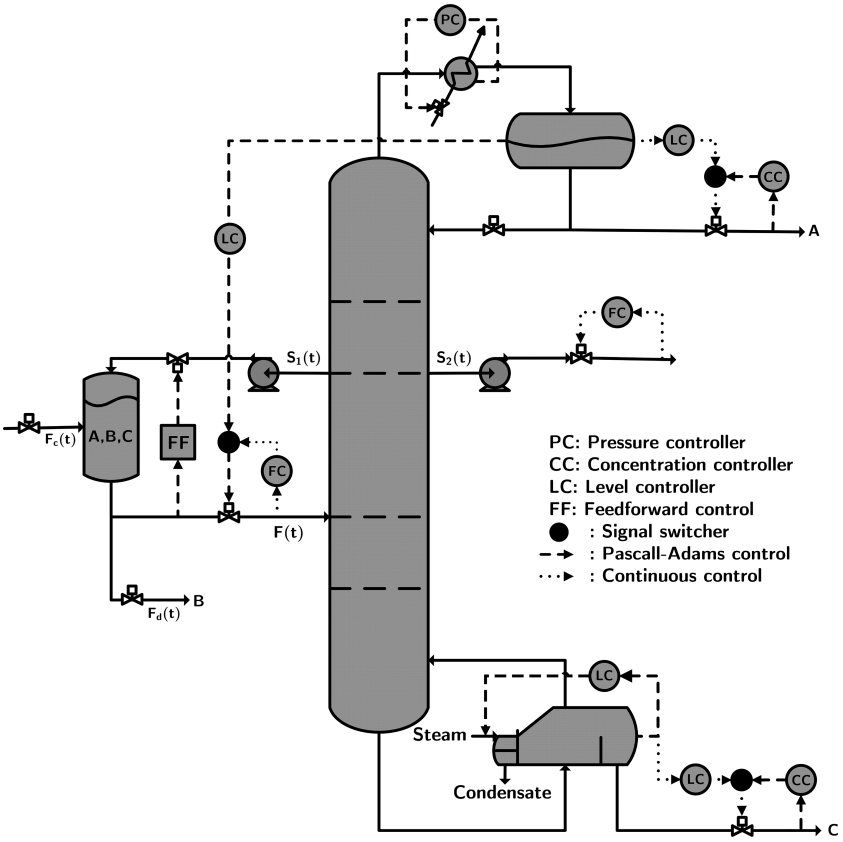

Figure 3. A schematic of the modified continuous middle vessel-column superstructure.

streamflow (S_2). It further includes two level controllers, which maintain the reflux drum and sump levels by varying the distillate and bottoms flow rates, respectively. The modified continuous middle vessel-column state was moved from one E to another by introducing a step change in the set point of the S_2 flow rate controller, the reflux rate ($\overline{L}$), and the reboiler duty $\overline{Q}_R$, while maintaining the feed flow rate. This process results in the addition of a new mode called continuous mode or mode 0. This mode precedes modes, 1, 2, and 3 in the hybrid system description of the semicontinuous process. Figure 3 illustrates the superstructure that was used to enable the mode transition from the continuous regime to the semicontinuous operating regime.

The recycle stream to the middle vessel (S_1) is operational only during semicontinuous operation (modes 1, 2, and 3), and the column side stream (S_2) is operational in the continuous mode (mode 0) only. Once a new steady state in mode 0 is reached, the semicontinuous operation begins; this transition is modeled as a time event. At this mode transition, the control system is changed from the continuous to the modified Pascall-Adams control configuration by using a switching block, and flow is introduced in S_1 while shutting down S_2. The mode trajectory in the beginning is {0, 1, 2, 3, 1}, and once the semicontinuous operation begins, the mode trajectory is {1, 2, 3, 1}. Since discrete control signals were used to switch from continuous operation to semicontinuous operation at a specific time, the hybrid model no longer has pure autonomous switches; rather, it has a combination of both controlled and autonomous switches. The events that govern the mode transitions, which are modeled using the "Tasks" functionality,[22] are shown below,

$$L_1^{(0)}: t^{(0)} = t \tag{10}$$

$$L_2^{(1)}: x_{B,v}^{(1)} \geq x_{B,v}^{\text{desired}} \tag{11}$$

$$L_3^{(2)}: h_v^{(2)} \leq h_v^{l} \tag{12}$$

$$L_1^{(3)}: h_v^{(3)} \geq h_v^{u} \tag{13}$$

Since waiting for the limit cycle is not a practical option, any cycle after the initial transient phase can be chosen to represent the limit cycle for evaluating the SC and enforcing the constraints. The cycle number is the index that is used to identify this cycle, and Γ is replaced by this representative limit cycle, that is,

DOI: 10.1021/acs.iecr.9b02639
Ind. Eng. Chem. Res. 2019, 58, 16654−16666

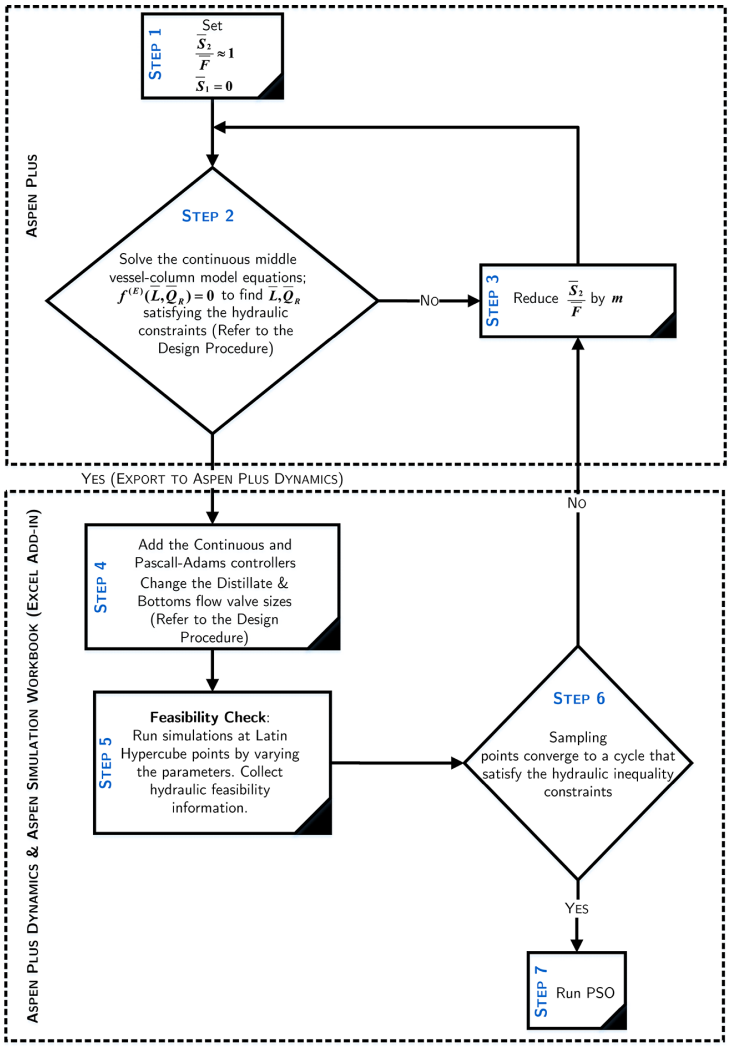

Figure 4. Flowchart illustrating the back-stepping design methodology.

$$\mathrm{SC}^{(\Gamma')} = \begin{cases} \dfrac{\text{total direct cost/payback period} + \text{annual operating cost}}{\text{annual ammount of product processed}} & \text{cycle number} = \Gamma' \\ 0 & \text{otherwise} \end{cases} \tag{14}$$

Side Stream Flow Rate: Pump and Valve Design. In the optimization problem formulation **P**, all bounds on the decision variables can be chosen independently except for the upper bound on the variable $\bar{S}_2$ (or $\bar{S}_1$), which is a function of the side stream pump and valve design in the aspenONE Engineering suite. The design of the side stream pump and the valve happens during the process of exporting the simulation from Aspen Plus to Aspen Plus Dynamics based on steady-state flow rates. Specifically, the design procedure uses the value of $\bar{S}_2$, which is a degree of freedom in the design of the continuous middle vessel-column system. The exported simulation in Aspen Plus Dynamics V10 has fixed equipment design variables, which are difficult to change.

Madabhushi et al.[14] demonstrated that a high $\frac{\bar{S}_2}{\bar{F}}$ ratio is preferable for good cycle performance in terms of cycle time, which indicates that pump and valve designs with maximum possible operational flexibility—the range of flow rates that can be accommodated by equipment of a known capacity—are necessary. Additionally, after extensively studying several simulation cases, it was observed that cycles generated from an arbitrary initial state that violates the flooding constraint, or close to the flooding constraint are infeasible hydraulically. Hydraulically infeasible means that the hydraulic path constraints are not satisfied at some/all points in the limit cycle. This infeasibility was a result of drawing more than

DOI: 10.1021/acs.iecr.9b02639
Ind. Eng. Chem. Res. 2019, 58, 16654−16666

acceptable liquid content from the column during the cycle. Obviously, the operational flexibility of the side stream pump and valve should be selected such that the semicontinuous operation is feasible. However, to vary the operational flexibility by changing the values of the equipment design variables (specifically, the pump), a different steady state has to be resimulated in Aspen Plus and then exported again to Aspen Plus Dynamics to avoid any model inconsistencies. Therefore, the new design procedure includes iteratively back-stepping from $\frac{\overline{S}_2}{\overline{F}} \approx 1$ in order to design a side stream pump and valve with enough operational flexibility to maintain hydraulic constraint feasibility. Three to four iterations were required to find a suitable $\frac{\overline{S}_2}{\overline{F}}$ ratio based on the different case studies carried out. Note that although the side stream pump and valve design was fixed even before solving the optimization problem, **P**, $\overline{S}_2$ was still used as a decision variable as it may affect the choice of the modified Pascall-Adams controller tuning parameters and the reflux rate.

Proposed Algorithmic Design Procedure: Back-Stepping Design Methodology. Based on the information provided in the above three sections, the following new algorithmic design procedure is proposed to find a better limit cycle (in terms of SC) of the semicontinuous distillation process than the state-of-the-art. This design procedure consists of the steps listed below (Figure 4).

- **Step 1**: Select a value of $\frac{\overline{S}_2}{\overline{F}} \approx 1$. The value of $\overline{S}_1$ is fixed at zero.
- **Step 2**: Solve $\mathbf{f}^{(E)}(\mathbf{z}, \mathbf{y}, \overline{L}, \overline{Q}_R; \overline{S}_1, \overline{S}_2) = \mathbf{0}$ by varying $\overline{L}$ and $\overline{Q}_R$ such that the flooding, weeping, and weir loading constraints are satisfied. If a solution is found, jump to Step 4; if no solution is found, continue on to Step 3.
- **Step 3**: Lower the ratio of $\frac{\overline{S}_2}{\overline{F}}$ by a factor of m $(0 < m < 1)$ and return to Step 2. Repeat Step 3 until a solution is found and then jump to Step 4.
- **Step 4**: Export the simulation from Step 2 to Aspen Plus Dynamics and add the controllers required for continuous state transition and semicontinuous operation with the help of the signal-selector block. Add tasks to switch between different modes. Additionally, the distillate and bottoms flow-valve sizes are adjusted to allow for greater operational flexibility.
- **Step 5**: Run simulations at Latin hypercube points by varying the decision variable values and collect information about the type of steady-state and hydraulic inequality path constraint feasibility at these points.
- **Step 6**: Check if the hydraulic path constraints are satisfied for at least some sampling points in the domain of interest to ensure cycle feasibility. If there is no feasible point, repeat Steps 3 to 5.
- **Step 7**: Use the sequential direct approach (see "Optimization Problem Solution" section below) to solve the optimization problem **P** in the domain of interest. If optimizer finds a solution near/along the edge of the, then relax the domain and repeat Step 7.

Optimization Problem Solution. In the past, researchers have made several attempts to solve optimization problems with embedded models of processes with periodic forcing using the variational approach.[24,25] The most recent review of dynamic optimization of forced-periodic systems was by Guardabassi et al.[26] Most of these studies were entirely theoretical based on mathematical analyses of simple systems having not more than three differential states. But, rigorous models of semicontinuous distillation have more than 50 differential states, and thus direct methods of dynamic optimization are more appropriate.

The optimization problem **P** falls under the category of multistage dynamic optimization because of the hybrid limit-cycle oscillator's fixed mode sequence. The sequential direct method is a reliable, practical method for solving multistage dynamic optimization problems like **P**, as a nonlinear program (NLP).[19] In this method, the problem is divided into two subproblems: (1) the initial value subproblem (IVP), and (2) the nonlinear program (NLP) master problem. A gradient-based method or a derivative-free method can be used to solve the master NLP problem depending on the case. A gradient-based method could be used to solve parametric autonomous hybrid system optimization problems when the sequence of events in the parametric domain of interest is unchanged, and when the sensitivities do not jump at the event time because in these cases the Master NLP is smooth.[27]

On the contrary, if the sequence of events varies from region to region in the parametric space, a derivative-free algorithm is the preferred choice, as this behavior suggests that the Master NLP may be nonsmooth.[20] In this study, the solution of the sensitivity equations of the embedded hybrid system in **P** can vary a lot because the system can have very different limiting behavior for arbitrarily close initial conditions as a result of the sequence of events changing in the parametric space. Furthermore, gradient-based local solvers embedded within Aspen Plus Dynamics were found to be ineffective[13] for the current case. Because of these two reasons, the derivative-free alternative (a stochastic NLP solver) was used in this study.

The particle swarm optimization (PSO) algorithm has repeatedly yielded good results in semicontinuous distillation studies.[5,11] In this stochastic search method, many particles are spread across the search space in a Latin hypercube grid. Each particle has personal objective and constraint function values. The particles' movement to new points in the decision variable space for subsequent iterations is computed based on their social interactions. Termination of the algorithm happens when all of the particles gather in some arbitrarily small neighborhood, or after reaching the maximum number of iterations.[28]

In this method, the embedded hybrid dynamic model is treated as a black box. A predefined stopping criterion should be satisfied for terminating the dynamic simulation. In this study, the stopping criterion is ten complete cycles with the transition condition from mode 3 to mode 1 as the end point. PSO is time-consuming because a large number of dynamic simulations of the system have to be run for many values of the decision variables, which are the particle positions in the decision variable space. Furthermore, these simulations must be run iteratively, further increasing the computational time. Also, solution optimality, including local optimality, cannot be guaranteed due to the heuristic termination criteria. Therefore, PSO is intended only to produce a solution that is an improvement on the best-known solutions.

In this study, all constraints were handled using the penalty method wherein the objective function is penalized appropriately for violating any constraints.[29] The end-point and inequality path constraints were handled within the master NLP using a penalty function (max{} function), where the function value is zero if the constraint is not violated and large if it is violated. In the case of inequality path constraints, the maximum constraint violation along the path was used as a

DOI: 10.1021/acs.iecr.9b02639
Ind. Eng. Chem. Res. 2019, 58, 16654−16666

Table 1. Continuous Middle Vessel-Column Design Data for the Two Case Studies[a]

		upstream feed mole fraction				stage location				
case	feed mixture	x_A	x_B	x_C	stages	F	S	P (atm)	ΔP (atm)	$\bar{F}$ (kmol/h)
1	HHO	0.33	0.33	0.34	40	25	14	1	0.0068	39.66
2	BTX	0.33	0.33	0.34	40	25	14	0.37	0.0068	100

[a]Murphee stage efficiency = 75%. Stage 1 is the condenser, and the last stage is the reboiler. $\bar{F}$ is the feed flow rate to the middle vessel and thus the column. P is the top stage pressure, ΔP is the stage pressure drop.

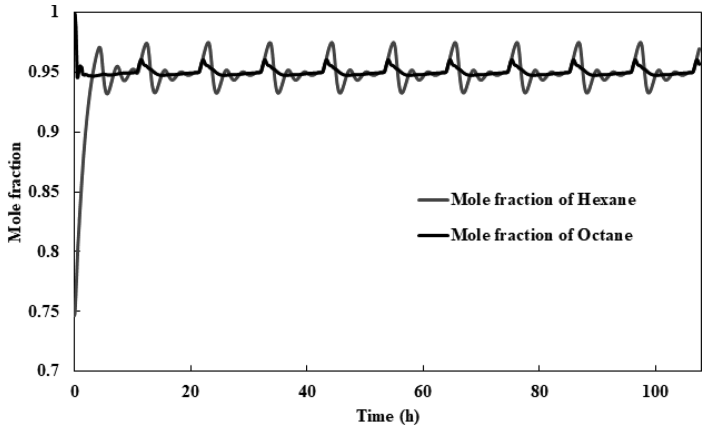

Figure 5. Mole fraction trajectory of the top and bottoms products in Case 1. The last cycle is the representative cycle ($\Gamma' = 10$). The desired values of mole fraction of the top and bottoms products are 0.95 and 0.95, respectively.

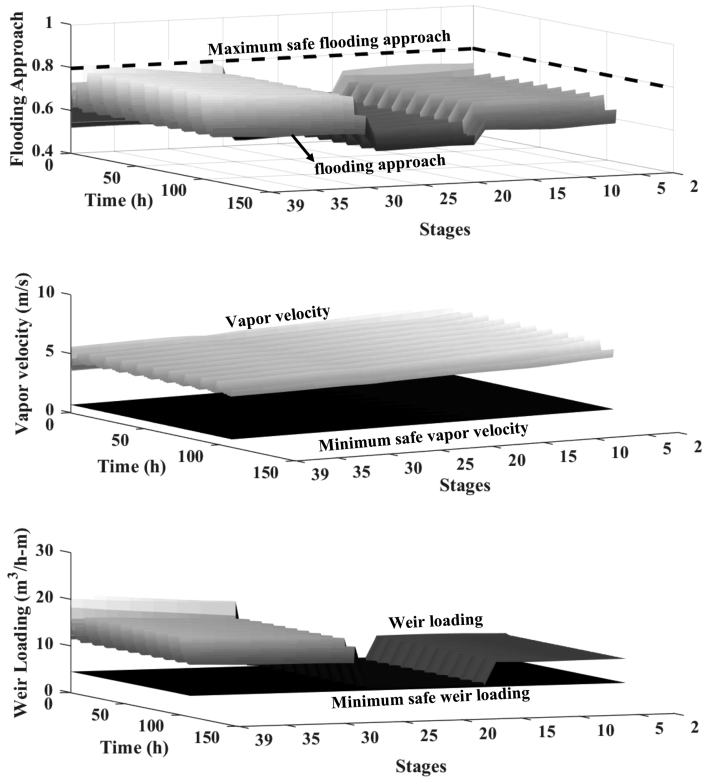

Figure 6. Plot illustrating the hydraulic feasibility of the representative cycle ($\Gamma' = 10$) found using the back-stepping design procedure for Case 1.

DOI: 10.1021/acs.iecr.9b02639
Ind. Eng. Chem. Res. 2019, 58, 16654−16666

measure to quantify the amount of constraint violation. The constraint violation was measured as a linear function of the distance from the boundary of the constraint. Also, the penalty parameter associated with the penalty function was a constant value during the PSO iterations and was chosen based on the scale of the objective function value.

CASE STUDIES

The proposed design algorithm was applied to two different case studies involving increasingly difficult separations of two different zeotropic mixtures. The first case study (Case 1) is the semicontinuous separation of a near equimolar mixture comprised of three alkanes: hexane, heptane, and octane (HHO). The continuous middle vessel-column design data for this case study were taken from the Wijesekera and Adams[17] seminal study on the separation of quaternary mixtures and were adapted appropriately for ternary mixture separation. The products were separated to minimum purities of 95 mol %, 96 mol %, and 95 mol % of hexane, heptane, and octane, respectively. The selected column pressure was 1.013 bar with a stage pressure drop of 0.0068 bar. The column was designed to have a diameter of 3 ft with an active tray area of 80%. The second case study (Case 2) is the semicontinuous separation of a near equimolar mixture of benzene, toluene, and o-xylene (BTX). All three products were separated to 99 mol % purity. The data to design the continuous middle vessel-column for this case study were directly taken from Madabhushi and Adams[13] without any modifications. A summary of some of the required design data is presented in Table 1.

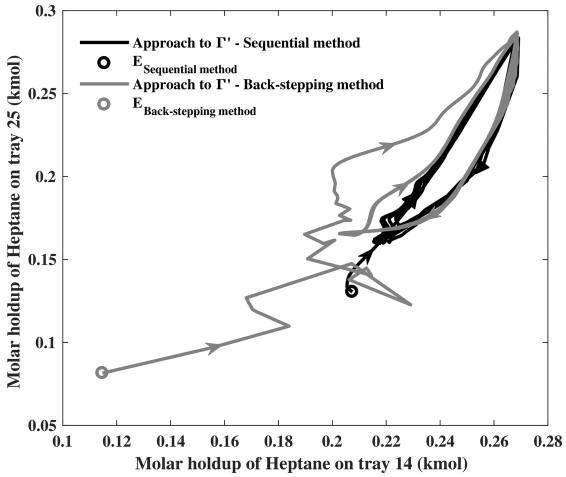

Figure 7. Phase plot illustrating different limit cycles found using the two design procedures in Case 1.

The middle vessel was designed to hold 100 kmol of feed in Case 1,[17] and 200 kmol of feed in Case 2.[13] Since property methods were validated before they were used in the respective studies, they were directly used here without any validation. The present analysis also considered the variations in total direct costs (does not include the cost of controllers) because of changes to equipment capacities as a result of continuous middle vessel-column design changes when iterating between, either Step 3 to Step 2 or Step 6 to Step 2. The capital costs were estimated using the Aspen Capital Cost Estimator V10 program.[30] As with all prior semicontinuous distillation studies, the operating cost only factored in the duties of the reboiler and the condenser. The utility prices used in these case studies were taken from Madabhushi and Adams.[13] The dynamic simulation in Aspen Plus Dynamics V10 is pressure-driven.

The implementation of the PSO algorithm for semicontinuous design optimization was done in Microsoft Excel VBA. The direct sequential method of dynamic optimization was carried out by linking Microsoft Excel to Aspen Plus Dynamics V10 using the Aspen Simulation Workbook V10-Excel add-in. The PSO parameters used in this study were taken from Adams and Seider.[29] The hydraulic feasibility constraints of operation during the PSO iterations was selected as follows:

- the flooding approach had to be less than 0.8,
- weir loading had to be greater than the minimum of 4.47 m^3/h-m (default value in Aspen Plus V10[23]),
- the vapor velocity should be greater than the weeping velocity.

Note that these constraints are path constraints. Since there were no noticeable changes after the third or fourth cycle usually, the 10th cycle was chosen to be the representative cycle (Γ′) to calculate the SC for the two case studies.

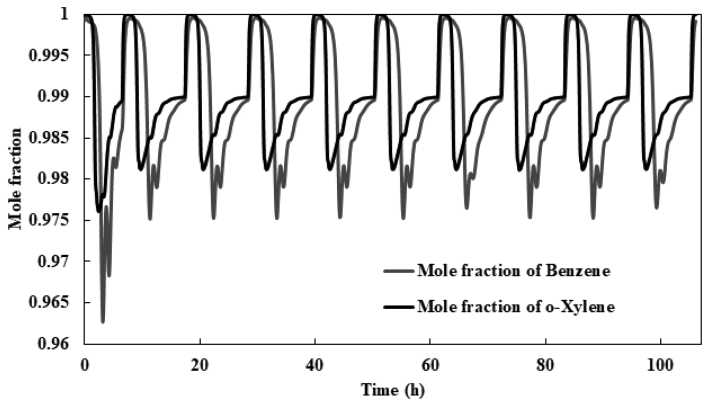

Figure 8. Mole fraction trajectory of the top and bottoms products in Case 2. The last cycle is the representative cycle (Γ′ = 10). The desired values of mole fraction of the top and bottoms products are 0.99, and 0.99, respectively.

DOI: 10.1021/acs.iecr.9b02639
Ind. Eng. Chem. Res. 2019, 58, 16654−16666

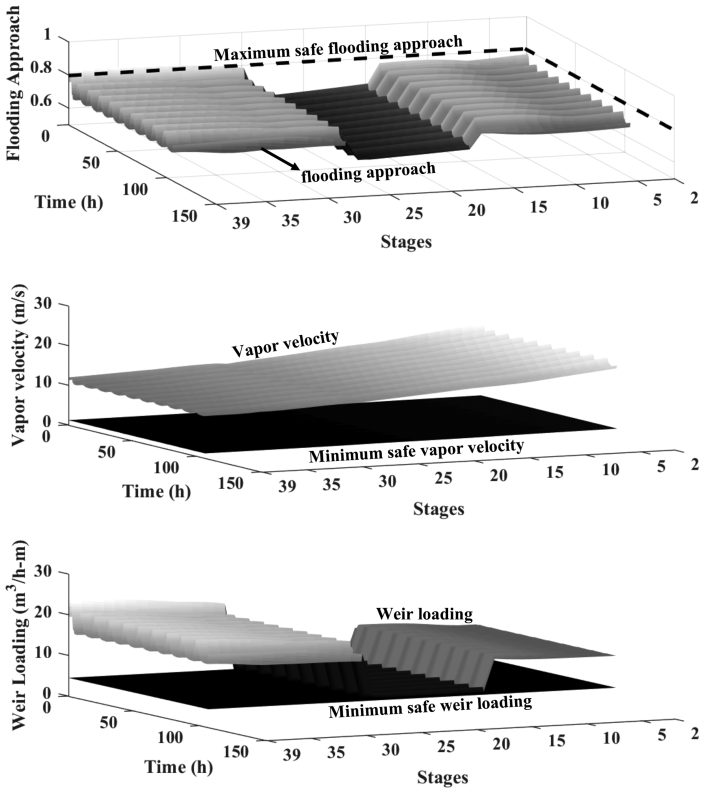

Figure 9. Plot illustrating the hydraulic feasibility of the representative cycle ($\Gamma' = 10$) found using the back-stepping design procedure for Case 2.

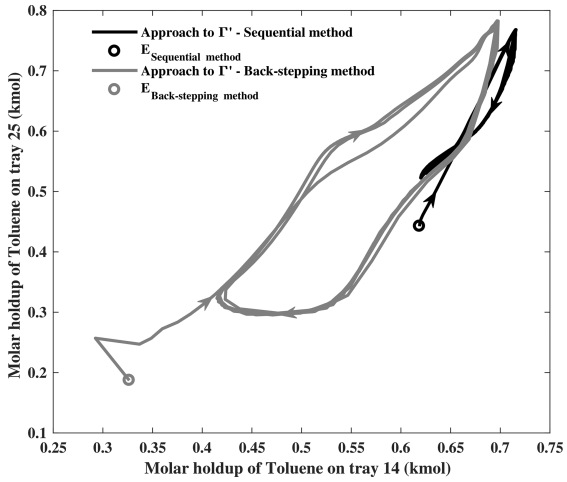

Figure 10. Phase plot illustrating different limit cycles found using the two design procedures in Case 2.

Case 1: Results. Three iterations of Steps 3−5 of the back-stepping design methodology were required to find a desirable continuous middle vessel-column design. The values of the design degrees of freedom of this continuous system, $\overline{S}_2$, $\overline{L}$, and $\overline{Q}_R$ were identified to be 20.43 kmol/h, 54.56 kmol/h, and 1.67 GJ/h, respectively. The capacities of the side stream pump and the valve were determined using the above-obtained value of $\overline{S}_2$.

Table 2. Results of the Case Studies

	system	
	HHO (Case-1)	BTX (Case-2)
	Best-Known Using Sequential Method	
$\overline{L}$ (kmol)	42.72	116.7
$\overline{S}$ (kmol)	15.86	39.0
SC ($/kmol)	8.18	7.16
wall-clock simulation time (min)	1.68	1.38
	New Best-Known Using Back-Stepping Method	
$\overline{L}$ (kmol)	45.53	132.44
$\overline{S}$ (kmol)	22.08	69.54
SC ($/kmol)	7.83	6.02
% decrease in SC	4.28%	16%
wall-clock simulation time (min)	2.06	1.8

The decision variable value that yielded the best SC during the hypercube sampling in Step 5 was used to initialize a particle in the PSO routine. The best-known point resulting from the sequential design methodology was not used to initialize any PSO particle in the back-stepping design methodology. The optimizer returned an improved decision variable vector after 20 iterations with 30 particles (600 simulation runs). The resultant limit cycle from the proposed design procedure has a cycle time that is approximately 9.28% lower, and an SC of almost 4.25% lower compared to the best-known design obtained by using the

DOI: 10.1021/acs.iecr.9b02639
Ind. Eng. Chem. Res. 2019, 58, 16654−16666

sequential design methodology. The SC includes the total direct cost changes due to variations in equipment size as a result of using the back-stepping design methodology. The mass-averaged product purity at the end of the reference cycle, and the hydraulic constraints during the reference cycle ($\Gamma' = 10$) were met. Good control of the top and bottoms products purities with the help of the distillate and bottoms concentration PI controllers (Figure 5) helped in meeting the mass-averaged product purities by the end of a cycle.

Figure 6 demonstrates the hydraulic feasibility of operating in this reference cycle. Note that the weir loading constraint becomes active on some of the column stages. Active weir loading constraint indicates withdrawal of a large quantity of liquid from the column.

The reason why the design obtained using the new methodology has a lower cycle time than the previously best-known design is because the former design has a larger side stream pump and valve capacity than the latter. Thus, the side stream controller in the new design can take control actions where the recycle rate to the middle vessel is larger than the maximum possible recycle rate in the old design. The rate at which the middle vessel vessel becomes pure in the intermediate boiling component is dependent on the recycle rate, thus affecting the cycle time and, in turn, the separating cost.

In Figure 7, the approach to a limit cycle from the arbitrary initial state is illustrated. The initial points are attracted to different limit cycles since the designs (time-invariant parameters) obtained by following the design procedures are different.

Case 2: Results. Application of the back-stepping design methodology to Case 2 resulted in a continuous middle vessel-column design that was desirable after two iterations of Steps 2 and 3. Upon close observation of this continuous middle vessel-column design, the weir loading constraint was found to be violated, although the dynamic simulation of the semi-continuous distillation resulted in hydraulically feasible cycles. In other words, the best known feasible semicontinuous design was found using an infeasible initial state. The continuous middle vessel-column design degrees of freedom variable values were as follows: $\overline{S}_2 = 75$ kmol/h, $\overline{L} = 102.04$ kmol/h, and $\overline{Q}_R = 3.69$ GJ/h. As in Case 1, an analysis of the information obtained from the 100 latin hypercube points sampled in Step 5 revealed that the selected decision variable values from the domain of interest only converged to limit cycles.

Initialization of a particle before running PSO with the best-known decision variable values from Step-5 as in Case-1, and the total number of simulation runs for PSO was set the same as in Case-1. The resultant design from the new methodology operates in a limit cycle that has 26% lower cycle time, and a 16% lower SC than the best-known design obtained using the sequential design methodology. As opposed to Case 1, the previously best-known design had significantly lower side stream recycle rate and was not close to any of the hydraulic feasibility constraints. This distance from the constraints gave the back-stepping design algorithm enough wiggle room to find better designs by increasing the side stream recycle rate. The SC improvement again includes the total direct cost changes as in Case-1. The mass-averaged product purity at the end of the reference cycle ($\Gamma' = 10$) was satisfied and the hydraulic constraints were met throughout the cycle. The top and bottoms product purities were well-controlled in the reference cycle by the distillate and bottoms PI controllers (Figure 8), thus meeting the mass-average product purities by the end of the cycle.

The hydraulic feasibility plot (Figure 9), again as in Case 1, illustrates that a substantial quantity of liquid was withdrawn through the side stream and thus, the weir loading constraint becomes active on some stages. The flooding and weeping constraints were however satisfied.

Figure 10 shows the approach to a limit cycle from an arbitrary initial state. From the plot, it can be observed that there is a large variation in the liquid molar holdup of toluene in the distillation column in the cycle from the new design compared to the cycle from the previous state-of-the-art methodology. This deviation was observed because a larger capacity side stream pump and valve design was specified through the new methodology, and thus withdrawal of more liquid content from the side stream stage is possible whenever required by the side stream controller.

A summary of the results, which includes the values of SC, and decision variables $\overline{L}$ and $\overline{S}$, of the two case studies are presented in Table 2.

CONCLUSIONS

This paper detailed a new semicontinuous distillation design procedure, known as the back-stepping design methodology. This new procedure is capable of yielding excellent results in relation to its ability to find more cost-effective designs for zeotropic ternary semicontinuous distillation. Indeed, the application of this algorithmic design procedure on the two case studies confirms that the limit cycles found were 4−16% lower than the limit cycles found using the status quo design methodology. Although this method is intended to find a limit cycle for known column and middle vessel sizes, it can also be extended to include integer variables. Furthermore, despite being computationally intensive, this procedure is an easy to implement approach of finding a limit cycle in the absence of prior system knowledge. Further research is required to assess the applicability of this method to other distillation processes like pressure swing distillation, azeotropic distillation, etc., which can be operated semicontinuously.[4] In part-2 of the paper, the back-stepping design procedure is extended to restrict the domain of search during optimization to a parametric space where the semicontinuous distillation dynamics asymptotically converge to a limit cycle.

All simulation files are available on LAPSE: http://psecommunity.org/LAPSE:2019.0423

AUTHOR INFORMATION

Corresponding Author

*E-mail: tadams@mcmaster.ca.

ORCID

Thomas Alan Adams, II: 0000-0002-9871-9851

Notes

The authors declare no competing financial interest.

ACKNOWLEDGMENTS

This work was supported by the McMaster Advanced Control Consortium (MACC). We are grateful to Dr. Farhang Jalali Farahani (McMaster University), for having the conversations which helped in improving the manuscript.

NOMENCLATURE

Abbreviations

DAEs = differential algebraic equations
IVPs = initial value problems
NLP = nonlinear program

DOI: 10.1021/acs.iecr.9b02639
Ind. Eng. Chem. Res. 2019, 58, 16654−16666

PSO = particle swarm optimization
SC = separating cost

Greek Letters

α = designates components, $\alpha = A, B, C$
Γ = limit cycle (periodic steady-state)
Γ' = representative limit cycle
Θ = set containing all possible continuous middle vessel-column steady-states

Other Symbols

$\overline{F}$ = feed flow rate to the column at $t = 0$
$\overline{L}$ = reflux rate at E - a time-invariant parameter in semicontinuous distillation
$\overline{Q}_R$ = reboiler duty at $t = 0$
$\overline{S}$ = side stream flow rate at $t = 0$
A = most volatile component
B = intermediate volatility component
C = least volatile component
P = optimization problem
$\mathbf{f}^{(E)}$ = system of nonlinear algebraic equations that describes the continuous middle vessel-column system
$\mathbf{f}^{(k)}$ = a system of differential-algebraic equations describing the semicontinuous distillation dynamics in mode k
$\mathbf{p}'$ = controller tuning parameter vector and is a subset of $\mathbf{p}$
$\mathbf{p}$ = time-invariant parameter vector
$\mathbf{u}$ = represents the vector of control variables
$\mathbf{y}$ = represents algebraic states
$\mathbf{z}$ = represents differential states
E = continuous middle vessel-column state (or) initial state of the semicontinuous distillation system
$F_c(t)$ = liquid flow rate of the middle vessel charging stream
$F_d(t)$ = liquid flow rate of the middle vessel discharge stream
$h_v(t)$ = height of liquid in the middle vessel
h_v^l = lower bound of height of liquid in the middle vessel
h_v^u = upper bound of liquid height in the middle vessel
j = index that describes the next mode in the sequence
k = index designating the discrete state, $k = 1,2,3$
$L_j^{(k)}$ = transition condition for transition from one mode to another
$M_\alpha(t)$ = liquid molar holdup of the component α in the middle vessel
S_1 = side stream recycled to the middle vessel in the modified continuous middle vessel-column system
S_2 = side stream not recycled to the middle vessel in the modified continuous middle vessel-column system
T = cycle time
t = time
$x_{B,S}(t)$ = molefraction of B in the side stream
$x_{B,v}(t)$ = molefraction of B in the middle vessel
$x_{B,v}^{desired}$ = desired purity of intermediate volatility component in the middle vessel

REFERENCES

(1) Phimister, J. R.; Seider, W. D. Semicontinuous, middle-vessel distillation of ternary mixtures. *AIChE J.* **2000**, *46*, 1508−1520.
(2) Bielenberg, J.; Bryner, M. Realize the potential of process intensification. *Chemical Engineering Progress* **2018**, *114*, 41−45.
(3) Yan, L.; Edgar, T. F.; Baldea, M. Dynamic process intensification of binary distillation based on output multiplicity. *AIChE J.* **2019**, *65*, 1162−1172.
(4) Adams, T. A., II; Pascall, A. Semicontinuous thermal separation systems. *Chem. Eng. Technol.* **2012**, *35*, 1153−1170.
(5) Pascall, A.; Adams, T. A., II Semicontinuous separation of dimethyl ether (DME) produced from biomass. *Can. J. Chem. Eng.* **2013**, *91*, 1001−1021.
(6) Tabari, A.; Ahmad, A. A semicontinuous approach for heterogeneous azeotropic distillation processes. *Comput. Chem. Eng.* **2015**, *73*, 183−190.
(7) Pătruţ, C.; Bîldea, C. S.; Liţă, I.; Kiss, A. A. Cyclic distillation−Design, control and applications. *Sep. Purif. Technol.* **2014**, *125*, 326−336.
(8) Khan, K. A.; Saxena, V. P.; Barton, P. I. Sensitivity analysis of limit-cycle oscillating hybrid systems. *SIAM Journal on Scientific Computing* **2011**, *33*, 1475−1504.
(9) Adams, T. A., II; Seider, W. D. Semicontinuous distillation for ethyl lactate production. *AIChE J.* **2008**, *54*, 2539−2552.
(10) Meidanshahi, V.; Adams, T. A., II A new process for ternary separations: Semicontinuous distillation without a middle vessel. *Chem. Eng. Res. Des.* **2015**, *93*, 100−112.
(11) Meidanshahi, V.; Adams, T. A., II Integrated design and control of semicontinuous distillation systems utilizing mixed integer dynamic optimization. *Comput. Chem. Eng.* **2016**, *89*, 172−183.
(12) Meidanshahi, V.; Corbett, B.; Adams, T. A., II; Mhaskar, P. Subspace model identification and model predictive control based cost analysis of a semicontinuous distillation process. *Comput. Chem. Eng.* **2017**, *103*, 39−57.
(13) Madabhushi, P. B.; Adams, T. A., II Side stream control in semicontinuous distillation. *Comput. Chem. Eng.* **2018**, *119*, 450−464.
(14) Madabhushi, P. B.; Medina, E. I. S.; Adams, T. A., II Understanding the dynamic behaviour of semicontinuous distillation. *Comput.-Aided Chem. Eng.* **2018**, *43*, 845−850.
(15) Parker, T. S.; Chua, L. *Practical Numerical Algorithms for Chaotic Systems*; Springer Science & Business Media, 2012.
(16) Houben, S. H. M. J.; Maubach, J. M. Periodic steady-state analysis of free-running oscillators. *Lect. Notes Comput. Sci. Eng.* **2001**, *18*, 217−224.
(17) Wijesekera, K. N.; Adams, T. A., II Semicontinuous distillation of quaternary mixtures using one distillation column and two integrated middle vessels. *Ind. Eng. Chem. Res.* **2015**, *54*, 5294−5306.
(18) Wijesekera, K. N.; Adams, T. A., II Semicontinuous distillation of quintenary and N-ary mixtures. *Ind. Eng. Chem. Res.* **2015**, *54*, 12877−12890.
(19) Barton, P. I.; Lee, C. K.; Yunt, M. Optimization of hybrid systems. *Comput. Chem. Eng.* **2006**, *30*, 1576−1589.
(20) Galán, S.; Feehery, W. F.; Barton, P. I. Parametric sensitivity functions for hybrid discrete/continuous systems. *Applied Numerical Mathematics* **1999**, *31*, 17−47.
(21) Branicky, M. S. *Studies in hybrid systems: Modeling, analysis, and control*; 1995.
(22) Aspentech, Aspen Plus Dynamics V10, 2018. https://www.aspentech.com/en/products/engineering/Aspen-Plus-dynamics (accessed 2018−07−23).
(23) Aspentech, Aspen Plus V10, 2018. https://www.aspentech.com/en/products/engineering/Aspen-Plus (accessed 2018−07−23).
(24) Horn, F.; Lin, R. Periodic processes: a variational approach. *Ind. Eng. Chem. Process Des. Dev.* **1967**, *6*, 21−30.
(25) Speyer, J.; Evans, R. A second variational theory for optimal periodic processes. *IEEE Trans. Autom. Control* **1984**, *29*, 138−148.
(26) Guardabassi, G.; Locatelli, A.; Rinaldi, S. Status of periodic optimization of dynamical systems. *Journal of Optimization Theory and Applications* **1974**, *14*, 1−20.
(27) Feehery, W. F. Dynamic optimization with path constraints. Ph.D. thesis, Massachusetts Institute of Technology, 1998.
(28) Kennedy, J. Particle swarm optimization. *Encyclopedia of Machine Learning* **2010**, 760−766.
(29) Adams, T. A., II; Seider, W. D. Practical optimization of complex chemical processes with tight constraints. *Comput. Chem. Eng.* **2008**, *32*, 2099−2112.
(30) Aspentech, Aspen Capital Cost Estimator V10, 2018. https://www.aspentech.com/en/products/engineering/aspen-capital-cost-estimator (accessed 2018−07−23).

DOI: 10.1021/acs.iecr.9b02639
Ind. Eng. Chem. Res. 2019, 58, 16654−16666

3.3 Extended back-stepping design methodology

The content of this section is a **published reprint** of the following peer-reviewed publication,

Madabhushi, Pranav Bhaswanth, and Thomas A. Adams. "Finding Better Limit Cycles in Semicontinuous Distillation. 2. Extended Back-Stepping Design Methodology." Industrial & Engineering Chemistry Research 58, no. 36 (2019): 16667-16675.

I&EC research
Industrial & Engineering Chemistry Research

Article

Cite This: *Ind. Eng. Chem. Res.* 2019, 58, 16667−16675

pubs.acs.org/IECR

Finding Better Limit Cycles in Semicontinuous Distillation. 2. Extended Back-Stepping Design Methodology

Pranav Bhaswanth Madabhushi and Thomas A. Adams, II*

Department of Chemical Engineering, McMaster University, 1280 Main Street West, Hamilton, Ontario L8S 4L8, Canada

ABSTRACT: In Part 1 [Madabhushi and Adams *Ind. Eng. Chem. Res.* **2019**, 10.1021/acs.iecr.9b02639] of this work, we introduced a new design procedure, called the back-stepping design methodology, for the design of zeotropic ternary semicontinuous distillation systems using the aspenONE Engineering suite. The objective of this paper (Part 2) is to present an extended back-stepping design methodology for certain cases whose design space contains a large number of designs that result in an undesirable steady-state behavior compared to a relatively small number of desirable periodic steady states. The extended methodology uses the principal component analysis technique to identify and constrain the domain of the design space to a much smaller region. This domain restriction helps in optimization by greatly reducing that amount of time spent exploring undesirable regions and is particularly useful for high dimensional spaces. The extended design methodology was applied to design the semicontinuous distillation of dimethyl ether, methanol, and water, as a case study. Results indicate that the new design procedure outperforms the status quo by finding a limit cycle that is 57% lower in separating cost.

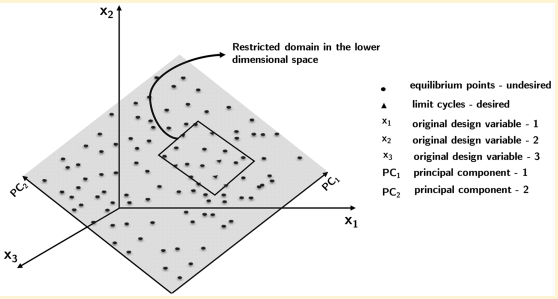

INTRODUCTION

The first paper[4] in this series introduces a new design methodology for semicontinuous distillation called the back-stepping design methodology. This design methodology is an iterative design procedure with an optimization step for finding the best hydraulically feasible (meets flooding, weeping, and weir loading constraints) semicontinuous distillation design for a given zeotropic ternary mixture separation. The design obtained from this method will have the maximum feasible flow rate to recycle to the middle vessel through the column's side stream.[4] This feature of the design procedure is particularly favorable because our prior work[2,3] demonstrated (through simulations) that increasing the side stream flow rate has a positive effect in lowering cycle time and ultimately, lowering the separating cost (SC). The new design methodology was applied to two case studies in the first paper.[4] In both cases, we obtained feasible designs with lower SC compared to the sequential design methodology[1] that was used in all previous studies.

In this paper, we propose an extension for the back-stepping design methodology for certain cases where the steady-state behavior of the semicontinuous distillation dynamics is different at different points in the design space. In the context of this paper, design space refers to the space defined by both the design parameters of the semicontinuous distillation system (e.g., reflux rate, controller tuning parameters, etc.) and the degrees of freedom that define the initial state (E) of the system. In the case of ternary semicontinuous distillation, depending on the chosen design, the steady-state behavior is either an undesired fixed point (a distillation system that operates in classic steady-state mode but does not achieve the desired purities) or a desired limit cycle (a periodic steady state that achieves the desired mass-averaged product purities). This extension to the design procedure is necessary because *a priori* knowledge of the systems' steady-state behavior for a given set of design parameters does not exist.

In our experience, we have found that in most semicontinuous case studies fixed points are rare or nonexistent across the space of possible design parameters, and so the design methodology presented in Part 1 (10.1021/acs.iecr.9b02639) is quite effective. However, in one case, we have found that a large majority of design parameters within the design space results in semicontinuous systems with undesired fixed points, and only a small subset of that design space contains design parameters which result in desirable limit cycles. In this case, the method presented in Part 1 (10.1021/acs.iecr.9b02639) is inefficient because in the optimization step the algorithm used was observed to spend much time searching in undesired regions of the design space needlessly. Furthermore, the high dimensionality of the design space and lack of *a priori* knowledge makes it difficult to manually restrict the design space to the region which contains only the desired limit cycles. Therefore, in this paper, we present an extension of the back-stepping design methodology for these special cases which incorporates principle component analysis

Received: July 1, 2019
Revised: August 8, 2019
Accepted: August 12, 2019
Published: August 12, 2019

DOI: 10.1021/acs.iecr.9b03519
Ind. Eng. Chem. Res. 2019, 58, 16667−16675

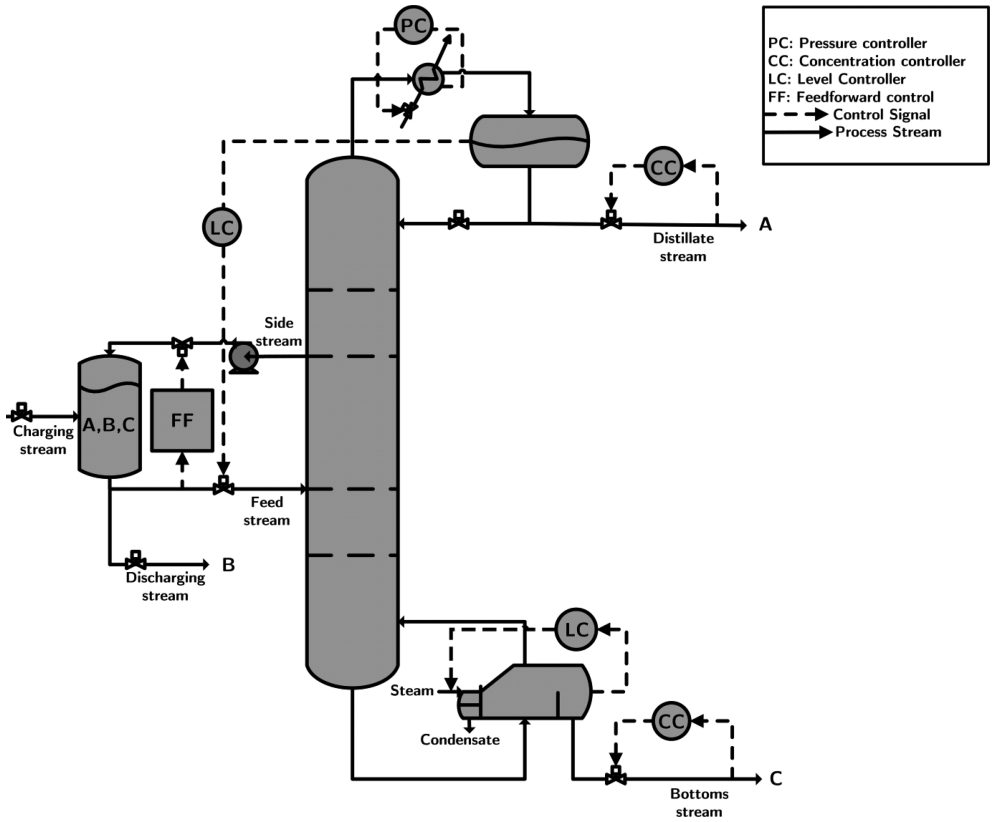

Figure 1. Schematic of a semicontinuous distillation system. Reprinted with permission from ref 3. Copyright 2018 Elsevier.

(PCA) to identify, define, and restrict the design space to a much smaller region. This allows the optimization algorithm to avoid large portions of the design space containing only undesired fixed points.

The organization of this paper is in four broad sections. The first section has a brief introduction of the semicontinuous distillation process and its dynamic behavior. The reader should refer to Part 1[4] for a more in-depth overview of the process and its mathematical description. The second section introduces the case of separating the nonideal ternary mixture of dimethyl ether (DME), methanol (MeOH), and water (H_2O) using semicontinuous distillation and a discussion on the steady-state behavior in the design space. The third section presents the extension to the back-stepping design procedure using principal component analysis for restricting the optimizer's decision variable space to a region with the desired semicontinuous distillation steady-state behavior. The last section summarizes the results obtained by using this extended design methodology for designing the semicontinuous distillation of DME, MeOH, and H_2O. Note that the back-stepping design methodology and its extension have been presented in the context of the aspenONE Engineering suite. Based on the software environment chosen, the specifics may change slightly, but the overall strategy remains the same.

SEMICONTINUOUS DISTILLATION OF TERNARY MIXTURES

Semicontinuous distillation technology used for the thermal separation of ternary mixtures requires a distillation column and a process vessel, which is called the middle vessel. Apart from the process equipment, to carry out the separation, a control system is necessary to maintain the desired top and bottoms product purity, reflux drum and sump levels, and column pressure. A side stream from the distillation column is continually recycled to the middle vessel to make it rich in the intermediate volatility component (B). A feedforward control law, called the modified ideal side-draw recovery (MISR) arrangement, is used to control the flow rate of material in the side stream.

Upon reaching the desired purity of component B in the middle vessel ($x_{B,v}^{desired}$), an on−off controller fully opens the control valve to allow the material to flow into the discharge stream (Figure 1). The controller stops the flow of material through the discharge stream when the liquid level in the middle vessel reaches the desired lower limit (h_v^l). Simultaneously, a different on−off controller now allows the flow of the feed mixture, yet to be separated, into the middle vessel. The controller stops this flow to the middle vessel when the liquid level is at the desired upper limit (h_v^u). Therefore, the on−off controllers discretely change the flow through the discharging and charging streams when the system reaches a specific state. After the controller stops the flow, the above-

DOI: 10.1021/acs.iecr.9b03519
Ind. Eng. Chem. Res. 2019, 58, 16667−16675

described process is repeated again, thus making the system periodic.

SEMICONTINUOUS DISTILLATION DYNAMICS

Semicontinuous distillation operation described above is typically viewed to have three different operating modes[1] based on the primary function of the middle vessel. These modes are as follows:

(1) Separating mode[1] (Mode 1): The middle vessel supplies liquid material only to the distillation column at varying flow rates for thermal separation in this mode. It does not receive any feed from the upstream units.
(2) Discharging mode[1] (Mode 2): In this mode, the middle vessel supplies liquid material to the column and also discharges the liquid to a downstream unit. It does not receive any feed from the upstream units.
(3) Charging Mode[1] (Mode 3): The upstream units feed the middle vessel with the feed mixture to be separated, while the middle vessel supplies liquid material to the distillation column.

From a mathematical point of view, these discrete changes in material flow change the functional form of the differential-algebraic equations describing the dynamics of the middle vessel.[4] The system evolves in time based on the dynamics until it reaches the state dependent transition condition, such as meeting the desired purity of component B. In semicontinuous distillation (which is a hybrid (discrete/continuous) system[5]), the continuous and discrete state trajectories are time-periodic, closed, and isolated (limit cycle). Therefore, the mode trajectory followed is {Mode 1, Mode 2, Mode 3, Mode 1}.[4]

In the modes, the trajectories of the state variables are dependent on the system's design variables (or time-invariant parameters), which are the independent variables. Therefore, care should be taken to ensure that proper values of the design variables are selected such that the system evolves and follows the above-defined mode trajectory.

USING THE ASPENONE ENGINEERING SUITE FOR SEMICONTINUOUS DISTILLATION DESIGN

The fundamental idea behind the back-stepping design methodology is that for different values of the design parameters (or time-invariant parameters ($\boldsymbol{p}$)), the distillation dynamics are simulated starting from an arbitrary initial state (E). Each design is evaluated based on SC, and the best design is chosen from among them. The arbitrary initial state (E) was chosen to be the state of a hypothetical continuous distillation system that carries out the separation of the ternary mixture to some arbitrary degree. This system is also used to determine the integer design parameters such as feed stage location, side stream stage location, the number of stages, and equipment sizes for simulating the semicontinuous distillation process. The degrees of freedom of the continuous system are the initial side stream flow rate ($\bar{S}$), the reflux rate ($\bar{L}$), and the reboiler duty ($\bar{Q}_R$), which can be used to change the state (E). Aspen Plus V10,[6] Aspen Plus Dynamics V10,[7] and Aspen Simulation Workbook V10[8] available in the aspenONE Engineering suite were used to model and design the semicontinuous distillation system using the back-stepping design methodology.

When using this simulation environment, however, the design of the continuous distillation system (carried out in Aspen Plus V10[6]) was found to be intricately coupled to the semicontinuous distillation design (carried out in Aspen Plus Dynamics V10[7]).[2] For example, the maximum allowable side stream flow rate (S^u) during a semicontinuous cycle, which depends on the side stream pump and valve capacity (an integer time-invariant parameter) and the controller tuning parameters (a continuous time-invariant parameter), is also implicitly a function of the initial side stream flow rate ($\bar{S}$).[2] Therefore, the back-stepping design procedure uses a theoretical distillation configuration called the modified middle vessel-column system as described in the first paper.[4]

Briefly, the modified middle vessel column consists of a distillation column with two side streams and a middle vessel. This distillation system configuration has both continuous mode and semicontinuous mode of operation. One of the side streams (S_1) is recycled to the middle vessel and has no material flow in the continuous mode of operation. The second side stream (S_2) has no material flow in the semicontinuous mode of operation and is not recycled.

The modified middle vessel column is first designed in Aspen Plus V10[6] to find the equipment sizes and a guess for the initial state (E). The equipment sizes specified in the "dynamic mode" of Aspen Plus V10 include reflux drum, sump, column, and the middle vessel, which are sized based on flows recorded in the continuous operation of the modified middle vessel column. The values of the inlet stream flow rates to the side stream pump and valve are respectively used by the software to estimate their capacity. Acceptable sizing of the side stream pump, side stream valve, and the distillation column for semicontinuous operation may not be possible through the above procedure. At this point, a redesign of the modified continuous middle vessel-column system is necessary. The back-stepping design methodology includes these "issue identification" and "redesign" steps.[4]

The steady-state model (nonlinear algebraic equations) from Aspen Plus V10[6] is then exported to Aspen Plus Dynamics V10 as a pressure-driven dynamic model. Modification of the dynamic model is then carried out by adding the controllers and signal switchers that allow the user to set the system to operate in both continuous and semicontinuous modes of operation. The "Tasks" functionality in Aspen Plus Dynamics[7] is used to model the discrete state transitions.

To find a better semicontinuous distillation design in terms of cost the decision variables considered are the set point of the side stream flow rate S_2, $\bar{L}$, $\bar{Q}_R$, and the controller tuning parameters. A particle swarm optimizer written in Microsoft Visual Basic for Applications calls the Aspen Plus Dynamics V10[7] model through the Aspen Simulation Workbook V10[8] excel add-in. Apart from optimizing the system, this interface is also used for running dynamic simulations at different Latin hypercube sampling points in the domain of interest and then collecting information about the system for "issue identification" and system "redesign". In the next section the DME, MeOH, and H_2O case study is introduced to illustrate why the back-stepping design procedure presented in Part 1 (10.1021/acs.iecr.9b02639) does not work well for this particular case.

SEMICONTINUOUS SEPARATION OF DIMETHYL ETHER, METHANOL, AND WATER

Dimethyl ether (DME) has been receiving widespread attention because of its desirable properties,[11,12] which makes it have the potential for use as a fuel additive or substitute while being environmentally benign.[1] The production of DME can either be from a fossil fuel-based source or a

DOI: 10.1021/acs.iecr.9b03519
Ind. Eng. Chem. Res. 2019, 58, 16667−16675

biomass-based source.[1] Studies in the literature suggest that biomass to DME production can be economical with the integration of a direct synthesis (methanol synthesis and dehydration over a catalyst) step with process intensification strategies.[13]

This case study considers the switchgrass-to-DME gasification-based process synthesized by Larson et al.[14] In this process, gasified switchgrass is cleaned and sent to a DME synthesis reactor. The reaction product mixture is flashed in a flash drum to remove unreacted syngas (H_2 and CO). The liquid product from this drum is sent to a distillation column in which CO_2 is removed in the distillate. The bottoms product from the column contains DME, MeOH, H_2O, and small amounts of CO_2. In this ternary mixture, DME is the high volatile component, H_2O is the low volatile component, and MeOH has volatility in between DME and water. In the Larson et al. process,[14] the bottoms product is further separated into DME, MeOH, and H_2O streams using continuous distillation in a sequence of two distillation columns. Intensified distillation systems like dividing wall distillation and semicontinuous distillation (including semicontinuous dividing wall distillation) were proposed in the literature for separating this ternary mixture as an alternative to conventional distillation technology because they use less energy and are smaller in size.[19] In this paper, the concentration is on semicontinuous distillation (with middle vessel) proposed by Pascall and Adams[1] as a potential process intensification approach for the separation of DME, MeOH, and H_2O, replacing the two continuous columns in the Larson et al.[14] The Pascall and Adams simulation-based study demonstrated that semicontinuous distillation has a lower total annualized cost for production rates lower than 5700 tonne/year compared to the continuous counterpart.[1] However, the authors used the sequential design methodology[1] to design the semicontinuous distillation system, which as shown in Part 1 (10.1021/acs.iecr.9b02639) of this work, generally results in more expensive systems than if designed by using the newly proposed back-stepping design methodology.

In this study, we consider the same feed mixture for designing a semicontinuous distillation process using the back-stepping design methodology. The feed mixture contains DME at 81.57 mol %,[1] MeOH at 14.43 mol %,[1] water 3.98 mol %,[1] and minute amounts of CO_2 (0.02 mol %[1]). We consider a feed flow rate of ∼8 MMkg/year to design the modified continuous middle vessel-column system. The feed temperature is at 328.54 K,[1] and the pressure of feed entering the distillation column is ∼10 atm.[1] These thermodynamic conditions are consistent with the studies by Larson et al.[14] and Pascall and Adams.[1] The weight-averaged product purities considered were according to the study by Pascall and Adams.[1] Recovery of DME product was at 99.95 mol %,[1] MeOH product recovery was at 96 mol %[1] purity, and finally, water purity was at 99.05 mol %.[1]

Vapor−liquid equilibrium was predicted using the Peng−Robinson equation state with the Wong Sandler mixing rule and the UNIFAC model for Helmholtz excess energy calculation (called the PRWS model in Aspen Plus V10[6]). This property model accurately predicts the vapor−liquid equilibrium of binary and ternary systems in the feed mixture when compared with the experimental data.

The distillation column was modeled using the Radfrac equilibrium-based model. The operating conditions of the column are 10 atm top-stage pressure[1] with a pressure drop of 0.0068 atm.[1] The vapor from the top is condensed using a total condenser to subcooled temperatures. The liquid in the sump is partially vaporized using a kettle reboiler. The column diameter of 1.5 ft. from the study of Pascall and Adams[1] was considered to be the starting point. However, when the semicontinuous separation was simulated using the previous design that was determined using the sequential design methodology,[1] the weir loading constraint was found to be violated on the trays near the bottoms stream. The hydraulic infeasibility may have occurred because Pascall and Adams,[1] in their study, did not consider the weir loading constraint during the design. Therefore, the column was redesigned to have two different diameters, a rectifying section of 3 ft. and a stripping section of 2 ft. This change ensured that the semicontinuous distillation system operation was in a hydraulically feasible limit cycle when using the sequential design methodology to have a fair base-case for comparison. The total number of stages for separation was 25,[1] which includes the condenser and the reboiler. The feed stage location was stage 13 (above-stage), and the side stream stage location was 12.

The middle vessel was designed to hold 100 kmol[1] of feed. This study considers the variation in total direct cost (does not include the cost of controllers) as a result of iterations in the back-stepping design procedure. The capital costs were estimated using Aspen Capital Cost Estimator V10.[9] The operating cost only includes the cost incurred for providing the required condenser duty and the reboiler duty during the cycle. The utility prices from the study of Madabhushi and Adams[3] were used in the estimation of the operating costs.

The hydraulic feasibility constraints imposed during the semicontinuous operation were as follows:

1) Flooding approach <0.8
2) Weir loading >4.47 $\frac{m^3}{h-m}$
3) Vapor velocity > weeping velocity.

The 10th cycle was chosen to the representative limit cycle (Γ') to calculate the separating cost (SC).

APPLICATION OF THE BACK-STEPPING DESIGN METHODOLOGY

In the first two steps of the design methodology, a modified middle vessel column is designed in Aspen Plus V10[6] by starting with the ratio of $\frac{\bar{S}_2}{\bar{F}}$ approximately 1. The value of the ratio is then lowered by a predefined factor until the hydraulic constraints are satisfied in the continuous mode of operation. After adding the controllers and signal switchers to the modified middle vessel column in Aspen Plus Dynamics V10,[7] dynamic simulations were run at Latin hypercube points, which were sampled by varying the set point of the side stream flow rate S_2, $\bar{L}$, $\bar{Q}_R$, and the controller tuning parameters in the domain of interest, to check if the semicontinuous operation is hydraulically feasible at least at some points.

However, an analysis of the dynamic simulations at the sampling points revealed that some of the points did not converge to a limit cycle in the domain of interest. All points that did not converge to a limit cycle converged to an undesirable fixed point (continuous steady state). The first cycle after the transition from the continuous mode to the semicontinuous mode had the desirable mode trajectory of {Mode 1, Mode 2, Mode 3, Mode 1}. However, in Mode 1 of the subsequent cycle, the distillate and bottoms concentration controllers slowly shut down the distillate and bottoms

DOI: 10.1021/acs.iecr.9b03519
Ind. Eng. Chem. Res. 2019, 58, 16667−16675

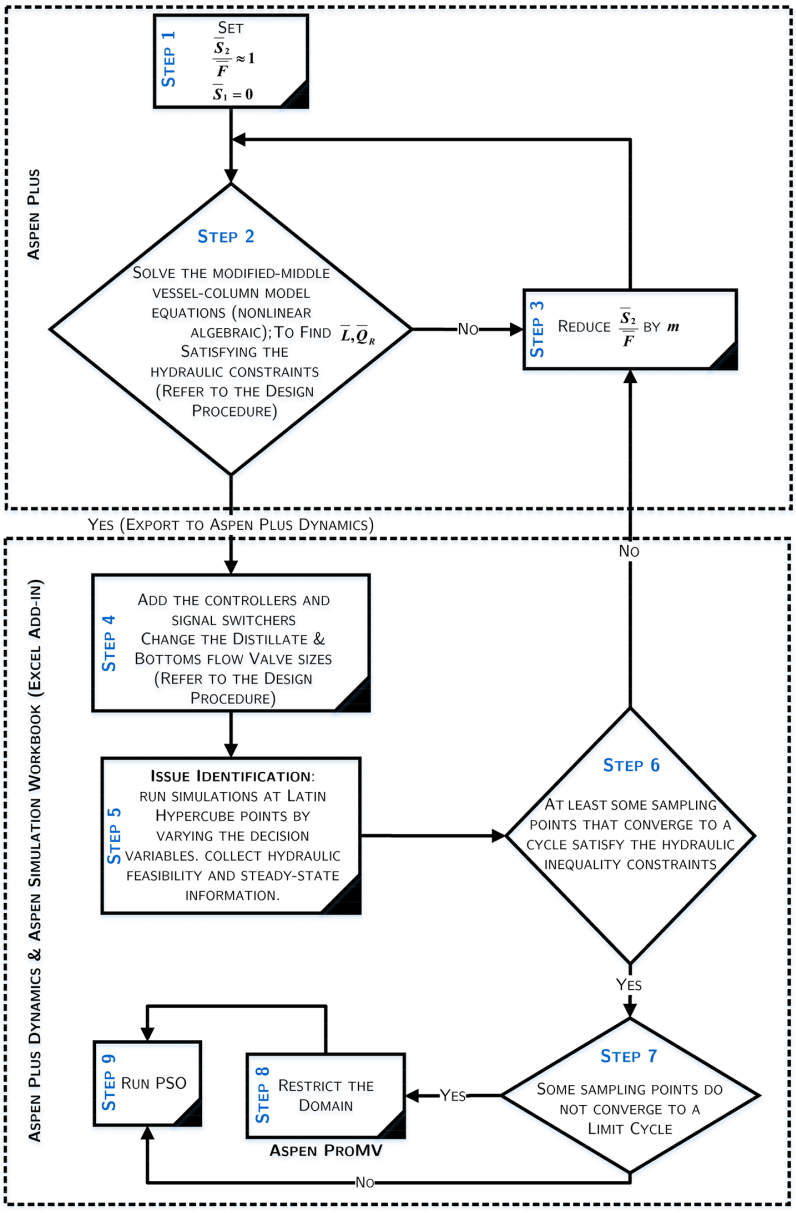

Figure 2. Schematic of the flowchart of the extended back-stepping design methodology.

streamflow, respectively, while the feed flow rate to the column matched the side stream recycle flow rate. This steady-state behavior could have been caused perhaps because of the choice of the initial state (E), the controller tuning parameters, or a combination of both. Furthermore, in this case, only 15% of the points found had the desired steady-state behavior.

Because of the nature of the process, in semicontinuous distillation, only limit cycle behavior is sought after for separating components in a ternary mixture. Therefore, characterization of the design space can be useful, especially to save computational time in the optimization phase of the back-stepping design methodology.

PRINCIPAL COMPONENT ANALYSIS FOR DOMAIN REDUCTION

The decision variable space is nine-dimensional, which makes visualization of the space impossible. Although visualization of two-dimensional plots of combinations of decision variables is possible, the total number of combinations is 36 out of which some are, of course, redundant. Generation and analyses of the plots are possible for delineating the desirable region, but it is cumbersome.

Therefore, this paper explores the use of dimensionality reduction techniques for domain restriction. In dimensionality reduction, high dimensional data is transformed into a lower

DOI: 10.1021/acs.iecr.9b03519
Ind. Eng. Chem. Res. 2019, 58, 16667−16675

dimensional space either by using linear transformation or nonlinear transformation by retaining the geometry of the original data set as much as possible.[16] van der Maaten presented a systematic survey of all the available linear and nonlinear dimensionality reduction techniques.[16] Although the geometry of the steady-state behavior of dynamical systems is known to be nonlinear in the parametric space, in this study, the focus is on dimensionality reduction techniques that rely on the linear transformation of the data. Linear dimensionality reduction techniques are perhaps the oldest and simplest to use techniques.[16] Linear discriminant analysis for dimensionality reduction was applied to the data, but this yielded a transformation matrix with complex eigenvalues, indicating that the problem is too nonlinear for this method to be applicable. Instead, this study uses the principal component analysis primarily because it is the simplest of the dimensionality reduction techniques without relying on any specific assumptions on the data. In this study, Aspen ProMV[10] was used to apply this technique on the data in the design space.

Principal Component Analysis (PCA) projects the data in the higher dimensional space onto a lower dimensional subspace by finding the linear basis that maximizes the variance in the data.[15] The linear basis consists of principal eigenvectors, which are called principal components, of the mean-centered covariance matrix of the data. In this study, PCA is used to project the points in the nine-dimensional design space onto a lower dimensional subspace, which is either two-dimensional or three-dimensional. Once the points are projected onto this subspace, a simple convex hull is constructed around the region containing the feasible points, i.e., lower and upper bounds in the two-dimensional space were identified forming a rectangle. This convex hull is then linearly transformed (inverse) into the original space, which geometrically looks like a hyperparallelepiped. Note that the convex hull constructed by using the above-described procedure is neither guaranteed to contain strictly desirable designs nor is it guaranteed to enclose all desirable designs but will only lower the chances of encountering an undesirable design.

EXTENSION TO THE BACK-STEPPING DESIGN METHODOLOGY

The back-stepping design methodology proposed for semicontinuous distillation design in Part 1[4] has seven steps. The design procedure is extended in this paper to have an optional step called "domain space restriction" based on the discussion in the previous two sections.

The design procedure outlined below is appropriately modified to include the optional step and summarized in Figure 2. The first four steps of the back-stepping design procedure need no modification but are repeated here exactly as described in Part 1 for convenience.[4]

Step 1. Select a value of $\frac{\bar{S}_2}{\bar{F}} \approx 1$.

Step 2. Solve the system of nonlinear algebraic equations describing the modified middle vessel column by varying $\bar{L}$ and $\bar{Q}_R$ such that the flooding, weeping, and weir loading constraints are satisfied. If a solution is found, jump to Step 4; if no solution is found, continue to Step 3.

Step 3. Lower the ratio of $\frac{\bar{S}_2}{\bar{F}}$ by a factor of m $(0 < m < 1)$ and return to Step 2. Repeat Step 3 until a solution is found and then jump to Step 4. Exit if no solution is found.

Step 4. Export the simulation from Step 2 to Aspen Plus Dynamics and add the controllers required for continuous transition and semicontinuous operation with the help of the signal-selector block. Add tasks to switch between different modes. Additionally, the distillate and bottoms flow-valve sizes are adjusted to allow for greater operational flexibility.

Step 5. Run simulations at Latin hypercube points by varying the decision variable values and collect information about the type of steady-state and hydraulic inequality path constraint feasibility at these points.

Step 6. Check if the hydraulic path feasibility constraints are satisfied for at least some sampling points in the domain of interest to ensure cycle feasibility. If there are no feasible points, repeat Steps 3−5.

Step 7. If at least one feasible point was found in Step 6, check the steady-state information and classify the domain. If the domain has points that only converge to limit cycles, then jump to Step 9.

Step 8. Project the domain onto a lower dimensional space and identify a convex hull of the points that mostly converge to a limit cycle. This domain restriction technique helps save computational time during optimization.

Step 9. Use the sequential direct approach to solve the optimization problem **P** in the domain identified in Step 7 or Step 8. If the optimizer finds a solution near/along the edge of the restricted domain, then relax the domain and repeat Step 9.

APPLICATION OF THE EXTENDED DESIGN METHODOLOGY TO THE DME, MEOH, AND H_2O SEMICONTINUOUS DISTILLATION DESIGN

The DME, MeOH, and H_2O semicontinuous separation, as illustrated, exhibits different kinds of steady-state behavior

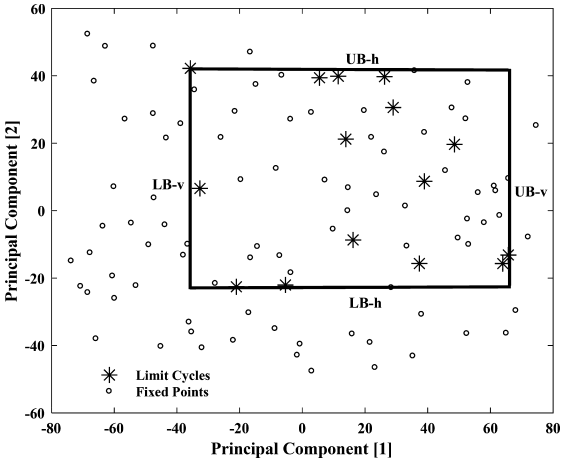

Figure 3. Plot illustrating the convex hull constructed in the lower dimensional subspace found using Principal Component Analysis.

(limit cycle or fixed point) in the design space. Therefore, according to the extended design procedure, simulation results from Step 5 were labeled as a limit cycle or fixed point based on the steady-state behavior. After ensuring that at least some

DOI: 10.1021/acs.iecr.9b03519
Ind. Eng. Chem. Res. 2019, 58, 16667−16675

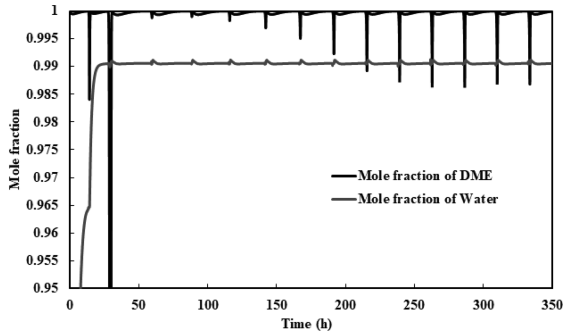

Figure 4. Mole fraction trajectory of the top and bottoms products. The representative cycle is $\Gamma' = 10$. More than 10 cycles are shown in the figure to illustrate convergence to a limit cycle. The desired values of mole fraction of the top and bottoms products are 0.9995 and 0.9905, respectively.

points have hydraulic feasibility, principal component analysis was carried out on this labeled data using Aspen ProMV.[10] The data was mean centered by the program before projecting them onto the lower dimensional subspace. The linear basis of the lower dimensional space consists of two principal components. Since prediction is not the primary goal of principal component analysis in this study, various statistics about the model's predictive performance are not necessary for the analysis.

A convex hull was then identified in this lower dimensional subspace as illustrated in Figure 3. The vertical line, LB-v (Figure 3), was constructed by identifying the extreme left most desirable point, which is the lower bound of the convex hull in the horizontal direction. Similarly, a vertical line UB-v (Figure 3) was constructed by identifying the extreme right most desirable point, which is the upper bound of the convex hull in the horizontal direction. Likewise, lower and upper bounds of the convex hull in the vertical direction were constructed by identifying the bottom-most and topmost desirable points (LB-h and UB-h in Figure 3). Of course, the convex hull constructed by this means is not the tightest in terms of encompassing all desirable points, but the geometrical procedure to build it is simple.

These simple inequality constraints that describe the closed region of the convex hull were mapped back into the original dimension. These equations of hyperplanes in the original dimension were implemented as constraints in the particle swarm optimization (PSO) with particles randomly initialized in and confined to the restricted domain. However, one PSO particle was initialized with the decision variable vector with the best SC sampled in Step 5 of the design procedure. None of the particles were initialized with the best-known design obtained from using the sequential design methodology to ensure a fair comparison. Typically, in the particle swarm optimization, the particle velocity was calculated using a heuristic.[18] However, when the calculated particle velocity is beyond a certain threshold, it is reduced to the threshold value.[17]

Nevertheless, in this study, during PSO iterations, the calculated particle velocity was iteratively reduced to confine the particles to the restricted domain. The optimizer returned an improved decision variable vector after 20 iterations with 30 particles (600 simulation runs). The wall clock simulation time

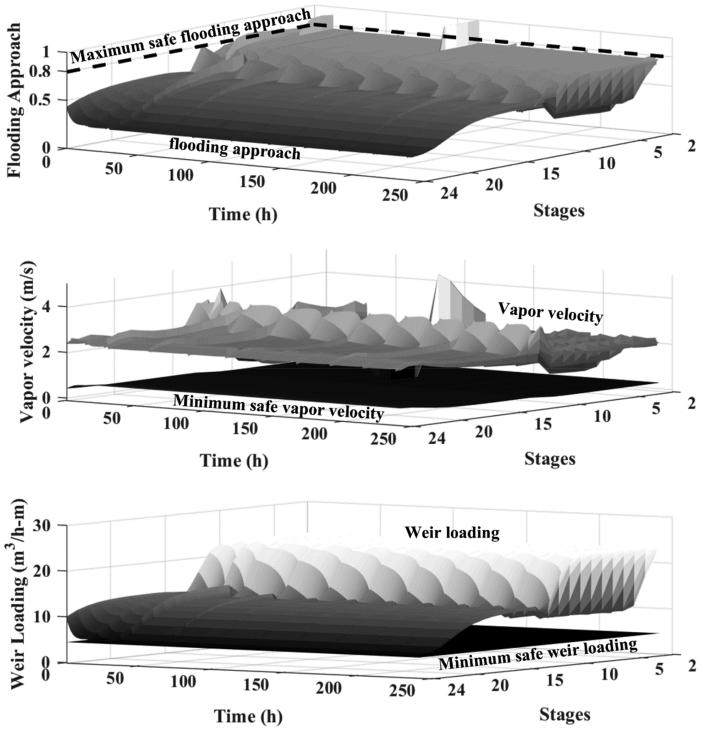

Figure 5. Plot illustrating the hydraulic feasibility of the limit cycle found using the back-stepping design procedure.

DOI: 10.1021/acs.iecr.9b03519
Ind. Eng. Chem. Res. 2019, 58, 16667−16675

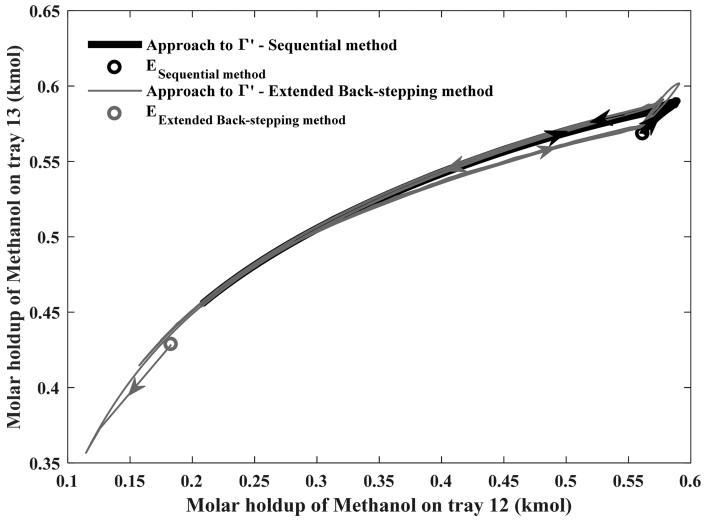

Figure 6. Phase plot illustrating the different limit cycles found using the two design procedures.

of each simulation is approximately 10 min, and thus, the total time spent in the optimization routine is approximately 4 days.

The resultant design from the optimizer has a decreased cycle time of approximately 50% and a decreased separating cost of almost 57% when compared with the cycle obtained using the design variable values returned by the sequential design methodology. Figure 4 demonstrates good control of mole fractions of top and bottoms products by the distillate and bottoms proportional-integral controllers in order to meet the mass-averaged purities by the end of the cycle. Notice that although the control performance of the distillate controller in the first few cycles was not qualitatively acceptable, it was able to recover and deliver consistently in the later cycles.

Figure 5 illustrates the hydraulic feasibility of operating in the reference cycle ($\Gamma' = 10$). In the hydraulic feasibility plot (Figure 5), because of the withdrawal of substantial liquid content from the column during operation, the weir loading constraint is active on some stages.

In Figure 6, the approach to a limit cycle from the arbitrary initial state is illustrated. Again, as in the cases demonstrated in the first paper[4], from the phase plot, it is clear that there is a significant variation in the liquid molar holdup of methanol in the distillation column (especially in the stages between the side stream stage and the feed stage) compared to the design from the state of the art methodology. This variation is due to the larger capacity side stream pump and valve capacity that was obtained using the new methodology, which causes the withdrawal of more liquid content from the side stream stage whenever the side stream controller demands.

CONCLUSION

This paper extends the back-stepping design methodology to cases that exhibit different types of steady-state behavior. The extended back-stepping design methodology applied to the case of semicontinuously distilling DME, MeOH, and H_2O returned a cost-effective design (57% lower in separating cost) compared to the sequential design methodology. Although being computationally intensive, the design procedure is easy to implement using the aspenONE Engineering and Asset performance management suites. Overall, we have found it to be the best approach in terms of finding limit cycles with lower separating cost than the status quo design procedure in the absence of prior system knowledge. A more rigorous design procedure that relies on some underlying system knowledge will perhaps be useful to design the semicontinuous distillation system better, which will be the focus of future work.

AUTHOR INFORMATION

Corresponding Author

*E-mail: tadams@mcmaster.ca.

ORCID

Thomas A. Adams, II: 0000-0002-9871-9851

Notes

The authors declare no competing financial interest.

The simulation files in this study are available and may be accessed on LAPSE at http://psecommunity.org/LAPSE:2019.0423.

ACKNOWLEDGMENTS

This work was supported by the McMaster Advanced Control Consortium (MACC). The authors are grateful to Dr. Farhang Farahani Jalali (McMaster University) and the reviewers for helping to improve the manuscript.

NOMENCLATURE

Abbreviations

A = more volatile component
B = intermediate volatility component
C = less volatile component
DME = dimethyl ether
MeOH = methanol
H_2O = water
CO_2 = carbon dioxide
PCA = principal component analysis
PSO = particle swarm optimization

Mathematical notation

SC = separating cost
$x_{B,v}^{desired}$ = desired purity of component B in the middle vessel
h_v^l = desired lower limit of liquid height in the middle vessel

DOI: 10.1021/acs.iecr.9b03519
Ind. Eng. Chem. Res. 2019, 58, 16667−16675

h_v^u = desired upper limit of liquid height in the middle vessel
$\boldsymbol{p}$ = time-invariant parameter vector
E = arbitrary initial state
$\overline{S}$ = initial side stream flow rate
$\overline{L}$ = reflux rate
$\overline{Q}_R$ = initial reboil duty
S^u = maximum allowable side stream flow rate
S_1 = side stream recycled to the middle vessel (modified middle vessel column configuration)
S_2 = side stream not recycled to the middle vessel (modified middle vessel column configuration)
Γ' = representative limit cycle
$\overline{F}$ = feed flow rate to the column at $t = 0$
m = factor by which the $\frac{\overline{S}_2}{\overline{F}}$ ratio is decreased

REFERENCES

(1) Pascall, A.; Adams, T. A., II Semicontinuous separation of dimethyl ether (DME) produced from biomass. *Can. J. Chem. Eng.* **2013**, *91*, 1001−1021.
(2) Madabhushi, P. B.; Medina, E. I. S.; Adams, T. A., II Understanding the dynamic behaviour of semicontinuous distillation. *Comput.-Aided Chem. Eng.* **2018**, *43*, 845−850.
(3) Madabhushi, P. B.; Adams, T. A., II Side stream control in semicontinuous distillation. *Comput. Chem. Eng.* **2018**, *119*, 450−464.
(4) Madabhushi, P. B.; Adams, T. A., II *Ind. Eng. Chem. Res.* **2019**, DOI: 10.1021/acs.iecr.9b02639.
(5) Gálan, S.; Feehery, W. F.; Barton, P. I. Parametric sensitivity functions for hybrid discrete/continuous systems. *Applied Numerical Mathematics* **1999**, *31*, 17−47.
(6) Aspentech, Aspen Plus V10. https://www.aspentech.com/en/products/engineering/Aspen-Plus, 2018. Accessed 2018-07-23.
(7) Aspentech, Aspen Plus Dynamics V10. https://www.aspentech.com/en/products/engineering/Aspen-Plus-Dynamics, 2018. Accessed 2018-07-23.
(8) Aspentech, Aspen SimulationWorkbook V10. https://www.aspentech.com/en/products/engineering/aspen-simulation-workbook, 2018. Accessed 2018-07-23.
(9) Aspentech, Aspen Capital Cost Estimator V10. https://www.aspentech.com/en/products/engineering/aspen-capital-cost-estimator, 2018. Accessed: 2018-07-23.
(10) Aspentech, Aspen ProMV V10. https://www.aspentech.com/en/products/apm/aspen-promv, 2018. Accessed: 2018-07-23.
(11) Semelsberger, T. A.; Borup, H. L. Dimethyl ether (DME) as an alternative fuel. *J. Power Sources* **2006**, *156* (2), 497−511.
(12) Arcoumanis, C.; Bae, C.; Crookes, R.; Kinoshita, E. The potential of di-methyl ether (DME) as n alternative fuel for compression ignition engines: A review. *Fuel* **2008**, *87* (7), 1014−1030.
(13) Moulijn, J. A.; Stankiewicz, A.; Grievink, J.; Górak, A. Process intensification and process systems engineering: a friendly symbiosis. *Comput. Chem. Eng.* **2008**, *32* (1−2), 3−11.
(14) Larson, E. D.; Yang, H. Dimethyl ether (DME) from coal as a household cooking fuel in China. *Energy Sustainable Dev.* **2004**, *8* (3), 115−126.
(15) Lu, H.; Plataniotis, K. N.; Venetsanopoulos, A. N. MPCA: Multilinear principal component analysis of tensor objects. *IEEE transactions on Neural Networks* **2008**, *19* (1), 18−39.
(16) van der Maaten, L.; Postma, E.; van den Herik, J. Dimensionality reduction: a comparative review. *Journal of Machine Learning Research* **2009**, *10* (66−71), 13.
(17) Adams, T. A., II; Seider, W. D. Practical optimization of complex chemical processes with tight constraints. *Comput. Chem. Eng.* **2008**, *32*, 2099−2112.
(18) Kennedy, J. Particle swarm optimization. *Encyclopedia of machine learning* **2010**, 760−766.
(19) Ballinger, S. E.; Adams, T. A., II Space-constrained purification of dimethyl ether through process intensification using semi-continuous dividing wall columns. *Comput. Chem. Eng.* **2017**, *105*, 197−211.

DOI: 10.1021/acs.iecr.9b03519
Ind. Eng. Chem. Res. 2019, 58, 16667−16675

Chapter 4

Application of the single shooting method for semicontinuous distillation design

---

The content of this chapter is the **final manuscript draft** and is submitted to the journal Chemical Engineering Research and Design,

Madabhushi, Pranav Bhaswanth, and Thomas A. Adams II. "On the application of shooting method for semicontinuous distillation design." submitted.

On the application of shooting method for semicontinuous distillation design

Pranav Bhaswanth, Madabhushi, Thomas A. Adams II*

Department of Chemical Engineering, McMaster University, 1280 Main Street West, Hamilton, Ontario, L8S 4L8, Canada
Email: tadams@mcmaster.ca

Abstract

Semicontinuous distillation is a new separation technology for distilling multicomponent mixtures. This process was designed using design methodologies with heuristic components that evolved over twenty years. However, the fundamental philosophy of these design methodologies, which involves guessing, checking and then using a black-box optimization procedure to find the values of the design variables to meet some performance criteria, has not changed. Mainly, to address the problem of having a heuristic simulation termination criterion in the black-box optimization phase, the single shooting method for semicontinuous distillation design was proposed in this study. We envision that this is a first step in the transformation of the semicontinuous distillation design process for obtaining optimal designs. We demonstrate the application of this method using two case studies, which involve the separation of hexane, heptane and octane.

Keywords: Semicontinuous distillation, Hybrid dynamical system, Process Design, Shooting method

1. Introduction

Distillation is a mature technology with a plethora of possibilities for achieving cost reduction combined with energy efficiency (Kiss, 2014), thus paving the way for the development of advanced distillation technologies. Some of these advanced technologies are reactive distillation (Kiss, 2013), divided-wall column distillation (Petlyuk, 2004), cyclic distillation (Maleta et al., 2011), heat pump assisted distillation (Annakou and Mizsey, 1995), membrane distillation (Khayet, 2011). Along similar lines, Phimister and Seider, 2000, proposed the semicontinuous operation of the middle-vessel column for ternary mixture separations. This technology is an alternative to ordinary batch and continuous distillation and was called semicontinuous distillation (Adams II and Pascall, 2012). A multicomponent extension of this process was also simulated (Wijesekera and Adams, 2015a, 2015b).

In the semicontinuous distillation of multicomponent mixtures containing c components, thermal separation is performed using one distillation column and $c-2$ process vessels. These process vessels are called the 'middle-vessels' (Wijesekera and Adams, 2015a) in semicontinuous distillation literature. However, throughout this article, the focus will be on the semicontinuous distillation of ternary-zeotropic mixtures, which requires only one middle-vessel. This process vessel continuously supplies a ternary mixture of time-varying composition to the distillation column through the feed stream (Figure 1). The flowrates of the distillate and bottoms streams of the distillation column are thus manipulated to control the purities of the high volatile component

(HVC) and the low volatile component (LVC) in these streams, respectively (Phimister and Seider, 2000). The composition of the contents of the middle-vessel is time-varying because a side stream from the distillation column, which contains a sufficiently high concentration of intermediate volatile component (IVC) than the contents of the middle-vessel, is continuously recycled to it.

The semicontinuous distillation of ternary mixtures has three different operating modes, which were classified based on the state of the middle-vessel (Adams and Pascall, 2012). In the separating mode, the concentration of the IVC in the middle-vessel increases and reaches the desired value. Upon reaching the desired purity value, the separating mode ends, and the discharging mode begins. In this mode, the material in the middle-vessel is discharged through the discharge stream (Figure 1), until reaching a pre-determined lower limit of liquid height. Instantaneously, material flow through the discharge stream is shut, and fresh feed to be separated is charged to the middle-vessel through the charging stream (Figure 1). The event marks the end of the discharging mode and the beginning of the charging mode. This mode ends as soon as the liquid height in the middle-vessel reaches a pre-determined upper limit. This event indicates the start of the separating mode of a new cycle, thus, making the process operation periodic.

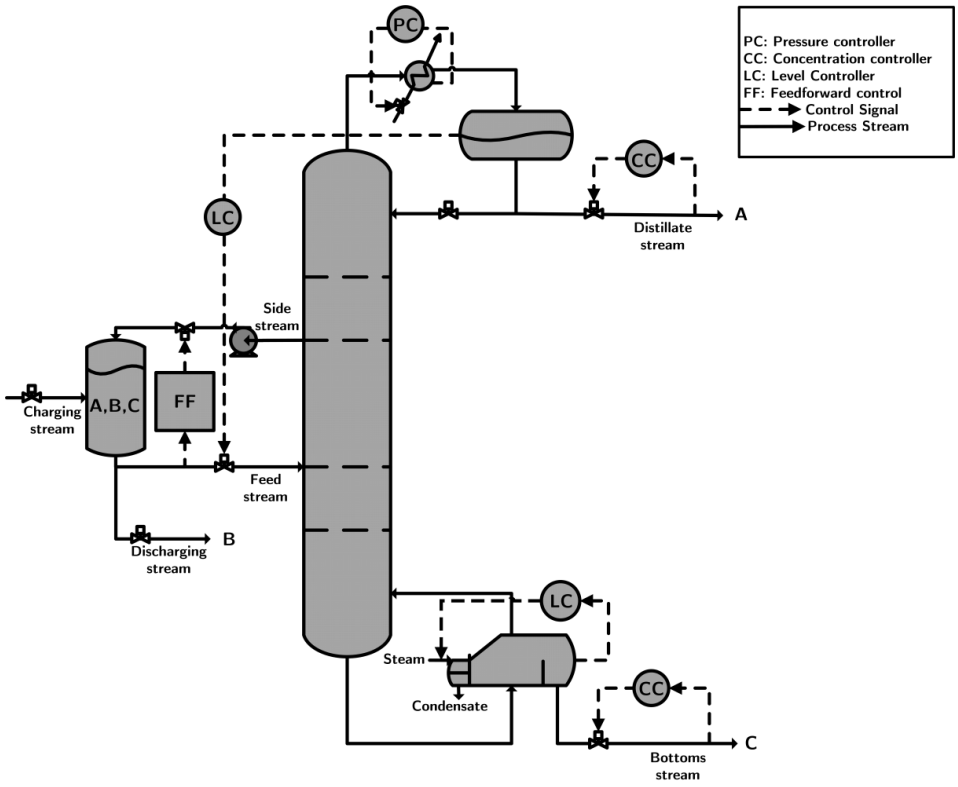

Figure 1: Schematic of the semicontinuous distillation system for separating ternary mixtures. Reprinted with permission from Madabhushi,PranavBhaswanth, and Thomas A. Adams II. "Side stream control in

semicontinuous distillation." Computers & Chemical Engineering 119 (2018): 450464. Copyright 2018 Elsevier.

The process operation within each mode is dynamic; however, the overall process operates in a steady-state called the 'limit cycle' because of its periodic behaviour (Madabhushi and Adams, 2019). A decentralized control system, which is an integral part of the process, is used to drive the column operation. This control system has multiple feedback loops to maintain the top and bottoms product purities, the reflux drum and sump levels, the column pressure and the side stream flowrate (Madabhushi and Adams, 2018).

The semicontinuous distillation process can be carried out in a traditional distillation column without any changes to the internals (Adams and Pascall, 2012), unlike cyclic distillation, which might need specially designed internals (Kiss, 2014; Toftegàrd et al., 2016). Simulation studies have shown that this process is economical at the intermediate production scale (Pascall and Adams, 2013; Wijesekera and Adams, 2015a, 2015b) while suggesting that it could be operationally flexible (Phimister and Seider, 2000).

2. Semicontinuous distillation design

In this section, we first review the evolution of the design methodologies used for the design of semicontinuous distillation of ternary mixtures. Later we expound some of the philosophical underpinnings of these design methodologies, which fundamentally differ from the proposed approach.

The seminal paper on the semicontinuous distillation of ternary mixtures introduced the first design methodology. It is a shortcut design procedure that adapted the Fenske-Underwood equations to determine the minimum reflux ratio and the number of stages (Phimister and Seider, 2000). These equations were applied, assuming that the system operates at a pseudo-steady state when the column is at, or near, the total reflux state during the dynamic operation within an operating mode (Phimister and Seider, 2000). Furthermore, using this pseudo-steady state, the trays were sized, and the column internal flowrates were determined. The internal flowrates were used to estimate the column diameter while ensuring hydraulically feasible (no flooding and weeping) column operation at this state (Phimister and Seider, 2000). The parameters of the controllers in the decentralized control system were tuned to ensure proper control performance (setpoint tracking and disturbance rejection) during the dynamic operation. Performance testing of the design is carried out by simulating the system, which entails numerical integration of the system's model equations until reaching a limit cycle. We call this the original design methodology.

Later, Pascall and Adams, 2013, proposed a completely new design methodology. They used the steady-state of a continuous distillation system that separates the low and high volatile components to the desired purity values to find the design of the semicontinuous distillation system. This state happens to closely represent the dynamic operation of the semicontinuous distillation system at the beginning of the separating mode (Pascall and Adams, 2013). The continuous distillation system was derived from the semicontinuous distillation system by merely not recycling the side stream to the middle-vessel. The values of the number of trays, feed and side stream stage locations, and the reflux and reboil rates were determined such that the continuous

distillation system operates in the desired steady-state. Based on the flowrates at this steady-state, equipment sizes for semicontinuous distillation were determined. Then using the sized equipment and the steady-state as the initial state, dynamic simulations of semicontinuous distillation were run. These simulations were carried out for different combinations of controller tuning parameter values to find a limit cycle. Then a black-box optimization procedure was used to find the tuning parameter values that minimized the total annualized cost per production rate of a product. This design procedure was called the sequential design methodology by Meidanshahi and Adams, 2016.

Subsequently, more changes were made by Madabhushi and Adams, 2019, to the way the steady-state of the continuous distillation system was chosen. Discovery that the cycle time (period of the limit cycle) is sensitive to the choice of this steady-state by Madabhushi et al., 2018, led to the development of a new design methodology. This design procedure introduced an iterative method to change the steady-state at which a slightly modified version of the previously described continuous distillation system operates (Madabhushi and Adams, 2019). In the designs obtained by using this method, the material is recycled to the middle vessel through the side stream at a maximum possible flowrate (Madabhushi and Adams, 2019). Moreover, at the same time, the column is operated in a hydraulically feasible limit cycle (Madabhushi and Adams, 2019). Equipment in the semicontinuous distillation system were again sized based on the steady-state flowrates. This design methodology was called the backstepping design methodology (Madabhushi and Adams, 2019).

As the first step of this design methodology, the ratio of side stream to feed flowrate of the modified continuous distillation system was chosen to be approximately 1.0. This ratio is a degree of freedom in the design of this system. The other degrees of freedom of this system were determined such that this system operates in a steady-state that satisfies the hydraulic feasibility constraints. As stated before, based on the flowrate values at this steady-state, the equipment sizes for semicontinuous distillation were determined. Then using the sized equipment and the steady-state as the initial state, dynamic simulations of semicontinuous distillation were run. These simulations were carried out at different latin hypercube sampling points. The points were sampled from the space formed by the controller tuning parameters, reflux rate, the initial side stream flowrate, and the initial reboil rate. Initial here refers to the values of these variables at the beginning of the semicontinuous distillation simulation. A different steady-state was chosen by lowering the ratio of side stream to feed flowrate if desirable limit cycles cannot be found at any of these sampling points. A desirable limit cycle is hydraulically feasible, where components were separated to the desired purity values. This process is repeated until at least one desired limit cycle is found at any of the sampled points. After finding desirable limit cycles, a black-box optimization procedure was used to find the design that minimized the total annualized cost per production rate of a product.

The underlying philosophy behind the original, sequential and backstepping design methodologies is that many simulations of the semicontinuous distillation system were performed first to find a feasible design. Then an optimal design is sought after using black-box optimization. In these design procedures, although better heuristic knowledge is incorporated to yield improved designs (in terms of cost benefits), the process is ultimately still a guess and check procedure. A large number of otherwise avoidable simulations might be necessary to reject parts of the design space, thus requiring a significant amount of CPU time (typically of the order of weeks) for design

optimization. Moreover, since a black-box optimization procedure was used in these design methodologies, the guarantee of reaching a global or even a local optimum did not exist.

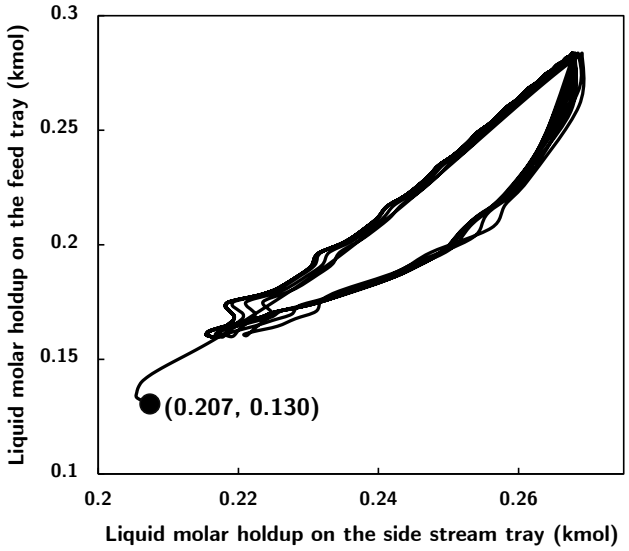

Figure 2: Phase plane (2-D) of hexane, heptane and octane semicontinuous distillation. The trajectory that settles on the limit cycle starting from the initial state at (0.207, 0.130)

In the simulation of the semicontinuous distillation process, the accurate dynamic model of the system that includes operating mode transitions is numerically integrated, starting from an initial state that does not lie on the limit cycle. Therefore the system trajectory passes through a transient phase before settling on the limit cycle (Figure 2) (Seydel, 2010). The length of this transient phase is dependent on the design and the initial state (Figure 3). Termination of the numerical integration, during simulation, is based on visual confirmation that a limit cycle is reached. However, visually tracking trajectories to ascertain that a limit cycle is attained is not possible in the black-box optimization phase, which necessitates having a heuristically chosen termination criterion. For example, we chose the 10^{th} cycle to be the limit cycle after extensively studying the systems presented in Madabhushi and Adams, 2019, for different designs.

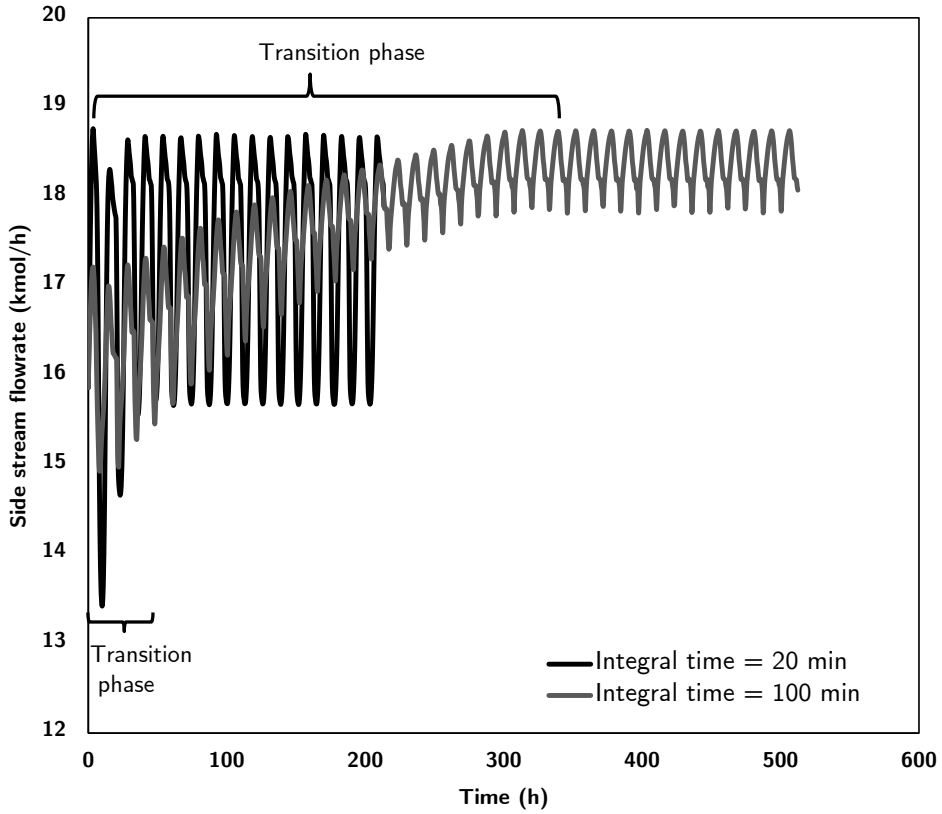

Figure 3: Different lengths of the transition phase when the controller tuning parameter of the side stream flowrate controller (Proportional-Integral) is changed in the semicontinuous distillation of hexane, heptane and octane.

In this paper, for the first time, we demonstrate the application of the shooting method to precisely locate the limit cycle of the semicontinuous distillation system. This method of simulating the process addresses the problem of using a heuristic simulation termination criterion. The shooting method is particularly suitable for use in combination with any of the gradient-based optimization methods to find the optimal semicontinuous distillation design. We envision that this systematic design method will have the potential for reducing CPU times significantly to obtain the optimal design. It also immediately opens up opportunities to find guaranteed local optimal designs with prospects in the future for finding a globally optimal design.

We present the two-point boundary value formulation of the semicontinuous distillation system with non-separable periodic boundary conditions (Ascher and Petzold, 1998). We numerically solve this boundary value problem (BVP) using the shooting method, which converts the BVP to an initial value problem (IVP). Then the zeros of the boundary conditions are calculated to find the limit cycle (Ascher and Petzold, 1998; Parker et al., 1989). The application of this method is

demonstrated using two case studies to illustrate the paradigm shift in the way the semicontinuous distillation process will be designed in the future.

3. The mathematical model of the process

The non-linear dynamic model of semicontinuous distillation is embedded with events that trigger discrete changes to the equations in this model. These types of systems can be modelled using the hybrid (discrete/continuous) systems mathematical framework (Barton and Lee, 2004). The mathematical model of the process is described subsequently using the language of this framework.

The hybrid automaton representation of the process has three distinct modes ($\{\mu_1, \mu_2, \mu_3\}$), each of which represents a process operating mode. The nonlinear dynamic model of the process within each mode includes the equation systems of the distillation column, the middle-vessel, and the control system. This dynamic model describes the continuous evolution of the system in the time interval $[t_{i-1}(\boldsymbol{p_d}, \boldsymbol{p_r}), t_i(\boldsymbol{p_d}, \boldsymbol{p_r}))$, in mode μ_i, where $\boldsymbol{p_d}$ represents the vector of design variables that take discrete values (discrete design variables), and $\boldsymbol{p_r}$ represents the vector of design variables that take real values (real design variables). A general representation of the non-linear dynamic model of the semicontinuous distillation process in mode μ_i as a system of semi-explicit differential-algebraic equations (DAEs) is given below,

$$\dot{\boldsymbol{z}}^{(\mu_i)}(t, \boldsymbol{p_d}, \boldsymbol{p_r}) = \begin{bmatrix} \boldsymbol{\Psi}_{cc}\left(\boldsymbol{z}^{(\mu_i)}, \boldsymbol{y}^{(\mu_i)}(t, \boldsymbol{p_d}, \boldsymbol{p_r}), \boldsymbol{p_d}, \boldsymbol{p_r}\right) \\ \boldsymbol{\Psi}_{mv}^{(\mu_i)}\left(\boldsymbol{z}^{(\mu_i)}, \boldsymbol{y}^{(\mu_i)}(t, \boldsymbol{p_d}, \boldsymbol{p_r}), \boldsymbol{p_d}, \boldsymbol{p_r}\right) \end{bmatrix}$$

$$\boldsymbol{0} = \begin{bmatrix} \boldsymbol{\Phi}_{cc}\left(\boldsymbol{z}^{(\mu_i)}, \boldsymbol{y}^{(\mu_i)}(t, \boldsymbol{p_d}, \boldsymbol{p_r}), \boldsymbol{p_d}, \boldsymbol{p_r}\right) \\ \boldsymbol{\Phi}_{mv}^{(\mu_i)}\left(\boldsymbol{z}^{(\mu_i)}, \boldsymbol{y}^{(\mu_i)}(t, \boldsymbol{p_d}, \boldsymbol{p_r}), \boldsymbol{p_d}, \boldsymbol{p_r}\right) \end{bmatrix} \quad i = \{1, 2, 3\} \qquad (1)$$

where $\boldsymbol{z}$ represents the vector of differential states, $\boldsymbol{y}$ represents the vector of algebraic states. In the DAE system, $\boldsymbol{\Psi}_{cc}$, and $\boldsymbol{\Phi}_{cc}$ represent the system of differential and algebraic equations, respectively, of the column and the control system together. And, $\boldsymbol{\Psi}_{mv}^{(\mu_i)}$, and $\boldsymbol{\Phi}_{mv}^{(\mu_i)}$ represent the differential and algebraic equations, respectively, of the middle vessel in mode μ_i. Note that the column and control system DAEs are not mode dependent. State-dependent events, which cause instantaneous transitions from mode, μ_i, to mode, μ_j, at the time, t_i, trigger switches in the equations describing the middle-vessel only. These state-dependent discrete events and the associated discrete control actions taken are listed below,

(1) **Separating mode ($\boldsymbol{\mu_1}$) to discharging mode ($\boldsymbol{\mu_2}$) transition**:
Event: mole fraction of the IVC in the middle-vessel ($x_{mv,IVC}^{(\mu_1)}(t, \boldsymbol{p_d}, \boldsymbol{p_r})$) is at the desired purity value ($x_{mv,IVC}^{desired}$), i.e., the event occurs when the transition condition $\Omega_{\mu_1}^{\mu_2}(t, \boldsymbol{p_d}, \boldsymbol{p_r}) = 0$ is met, where $\Omega_{\mu_1}^{\mu_2}(t, \boldsymbol{p_d}, \boldsymbol{p_r}) \coloneqq x_{mv,IVC}^{(\mu_1)}(t, \boldsymbol{p_d}, \boldsymbol{p_r}) - x_{mv,IVC}^{desired}$. Here, $\Omega_{\mu_1}^{\mu_2}$ is the condition required to transition from mode μ_1 to mode μ_2 at $t_1(\boldsymbol{p_d}, \boldsymbol{p_r})$.
Control action: Fully open the discharge stream valve (Figure 1).

(2) **Discharging mode (μ_2) to charging mode (μ_3) transition**:
Event: The height of the liquid in the middle-vessel ($h_{mv}^{(\mu_2)}(t, \boldsymbol{p_d}, \boldsymbol{p_r})$) is at the predetermined lower limit (h_v^l), i.e., the event occurs when the transition condition $\Omega_{\mu_2}^{\mu_3}(t, \boldsymbol{p_d}, \boldsymbol{p_r}) = 0$ is met, where $\Omega_{\mu_2}^{\mu_3}(t, \boldsymbol{p_d}, \boldsymbol{p_r}) \coloneqq \left(h_{mv}^{(\mu_2)}(t, \boldsymbol{p_d}, \boldsymbol{p_r}) - h_{mv}^{l}\right)$. Here, $L_{\mu_2}^{\mu_3}$ is the condition required to transition from mode μ_2 to mode μ_3 at $t_2(\boldsymbol{p_d}, \boldsymbol{p_r})$. This condition ensures that the downstream pump, which feeds the distillation column, does not cavitate.
Control action: Fully close the discharge stream valve (Figure 1), and fully open the charging stream valve (Figure 1).

(3) **Charging mode (μ_3) to separating mode (μ_1) transition**:
Event: the height of the liquid in the middle-vessel is at the predetermined upper limit (h_{mv}^u), i.e., the event occurs when the transition condition $\Omega_{\mu_3}^{\mu_1}(t, \boldsymbol{p_d}, \boldsymbol{p_r}) = 0$ is met, where $\Omega_{\mu_3}^{\mu_1}(t, \boldsymbol{p_d}, \boldsymbol{p_r}) \coloneqq \left(h_{mv}^{(\mu_3)}(t, \boldsymbol{p_d}, \boldsymbol{p_r}) - h_{mv}^{u}\right)$. Here, $\Omega_{\mu_3}^{\mu_1}$ is the condition required to transition from mode μ_3 to mode μ_1 at $t_3(\boldsymbol{p_d}, \boldsymbol{p_r})$. This condition ensures the safety of the process operation.
Control action: Fully close the charging stream valve (Figure 1).

Note here that the transition times, $t_1(\boldsymbol{p_d}, \boldsymbol{p_r})$, $t_2(\boldsymbol{p_d}, \boldsymbol{p_r})$, and $t_3(\boldsymbol{p_d}, \boldsymbol{p_r})$ at which the transition conditions, $\Omega_{\mu_1}^{\mu_2}(t, \boldsymbol{p_d}, \boldsymbol{p_r})$, $\Omega_{\mu_2}^{\mu_3}(t, \boldsymbol{p_d}, \boldsymbol{p_r})$, and $\Omega_{\mu_3}^{\mu_1}(t, \boldsymbol{p_d}, \boldsymbol{p_r})$ are satisfied are unknown *a priori* since the events are state-dependent. As the process is periodic, it follows this particular fixed mode sequence: $\{\mu_1, \mu_2, \mu_3, \mu_1\}$, which is called the hybrid mode trajectory (T_μ) (Barton and Lee, 2004). In this paper, we consider that the operation starts at the beginning of the separating mode and again ends here.

The contiguous closed time intervals $[t_{i-1}(\boldsymbol{p_d}, \boldsymbol{p_r}), t_i(\boldsymbol{p_d}, \boldsymbol{p_r})]$ in which the modes evolve are called epochs (θ_i) (Barton and Lee, 2004) and a finite sequence of epochs ($\{E_i, i \in 1 \text{ to } n_e\}$) is known as a hybrid time trajectory (Barton and Lee, 2004). Based on the hybrid mode trajectory and starting from the beginning of μ_1, the semicontinuous distillation process has four epochs, where $\theta_1 \in [t_0(\boldsymbol{p_d}, \boldsymbol{p_r}), t_1(\boldsymbol{p_d}, \boldsymbol{p_r})]$, $\theta_2 \in [t_1(\boldsymbol{p_d}, \boldsymbol{p_r}), t_2(\boldsymbol{p_d}, \boldsymbol{p_r})]$, $\theta_3 \in [t_2(\boldsymbol{p_d}, \boldsymbol{p_r}), t_3(\boldsymbol{p_d}, \boldsymbol{p_r})]$, and $\theta_4 \in [t_3(\boldsymbol{p_d}, \boldsymbol{p_r}), t_3(\boldsymbol{p_d}, \boldsymbol{p_r})]$, and the hybrid time trajectory is $T_t = \{\theta_1, \theta_2, \theta_3, \theta_4\}$. The last epoch only ensures that the system transitions back to the beginning of mode μ_1, and thus the time elapsed in the mode is zero.

The DAE system in each mode is initialized using transition functions, which are defined to relate variables in the mode μ_i to variables in the subsequent mode μ_j (Galán et al., 1999). In the hybrid model of the semicontinuous distillation system, the transition function ensures the continuity of the differential and algebraic state variables when transitioning from one mode to another. Thus, the function initializes the DAE system of the subsequent mode after the mode transition with the values of these variables at the event time.

$$\boldsymbol{\Theta}_{\boldsymbol{z}_{\mu_i}}^{\mu_j}(t, \boldsymbol{p_d}, \boldsymbol{p_r}) \coloneqq \boldsymbol{z}^{(\mu_i)}\left(\boldsymbol{p_d}, \boldsymbol{p_r}, t_i(\boldsymbol{p_d}, \boldsymbol{p_r})\right) - \boldsymbol{z}^{(\mu_j)}\left(\boldsymbol{p_d}, \boldsymbol{p_r}, t_i(\boldsymbol{p_d}, \boldsymbol{p_r})\right) = 0 \quad (2)$$

$$\boldsymbol{\Theta}_{\boldsymbol{y}_{\mu_i}}^{\mu_j}(t, \boldsymbol{p_d}, \boldsymbol{p_r}) \coloneqq \boldsymbol{y}^{(\mu_i)}\left(\boldsymbol{p_d}, \boldsymbol{p_r}, t_i(\boldsymbol{p_d}, \boldsymbol{p_r})\right) - \boldsymbol{y}^{(\mu_j)}\left(\boldsymbol{p_d}, \boldsymbol{p_r}, t_i(\boldsymbol{p_d}, \boldsymbol{p_r})\right) = 0 \quad (3)$$

where $i \neq j$ and $i < j$, and $\boldsymbol{\Theta}_{\boldsymbol{z}_{\mu_i}}^{\mu_j}$ represents the transition functions related to the differential variables, and $\boldsymbol{\Theta}_{\boldsymbol{y}_{\mu_i}}^{\mu_j}$ represents the transition functions related to the algebraic variables.

3.1 The dynamic model of the semicontinuous distillation system

The sub-systems in the semicontinuous distillation system, which comprises of the distillation column, the middle-vessel, and the control system were modelled using the principle of mass conservation, vapour-liquid equilibrium relationship, tray hydraulics and control laws.

The distillation column dynamic model was well-studied in the literature by different authors, such as Gani et al., 1986, Flatby et al., 1994, Bansal et al., 2002, for different applications such as start-up, control, and design optimization. Different assumptions were made in each of the studies depending on the application of the model. In this study, we used several classical simplifying assumptions, since the purpose of the study is to demonstrate the application of the single shooting method to use this procedure later for finding the optimal design of the process.

The assumptions that were used are adiabatic column operation, constant top stage pressure with a constant pressure drop across a stage, negligible vapour-holdup, perfect mixing on the trays, 100% Murphee tray efficiency, and total condenser with saturated liquid outlet conditions. Also, we assume constant molar overflow, which yields from energy balance, $V_n = V_{n-1}$ (Skogestad, 1997), where n represents the stage number which is assigned from the top of the column, and V is the total vapour flowrate. The dynamic model of the column, however, considers the liquid flow dynamics by the inclusion of the Francis Weir Equation. The mass balance equations of the column were expressed as differential equations at each stage for each component, while the phase equilibrium and the hydraulic models are algebraic.

Column Material Balances

The component material balance equations of the total condenser stage, which includes the reflux drum ($n = 1$) are compactly represented below:

$$\frac{dm_{1,c}}{dt} = v_{2,c} - l_{1,c} - d_c, \ c = \{\text{HVC}, \text{IVC}, \text{LVC}\} \tag{4}$$

where,

$m_{1,c}$ is the liquid molar holdup of component c on stage 1

$l_{1,c}$ is the molar reflux rate of component c leaving stage 1

$v_{2,c}$ is the vapour molar flowrate of component c entering stage 1

d_c is the distillate molar flowrate of component c leaving stage 1.

The component material balance equations of stages $n = \{2,3,\dots,N_s - 1\}$, where N_s is the total number of stages, are compactly represented below:

$$\frac{dm_{n,c}}{dt} = l_{n-1,c} + v_{n+1,c} - l_{n,c} - v_{n,c} + \zeta f_c - \varsigma s_c, \ c = \{\text{HVC}, \text{IVC}, \text{LVC}\} \tag{5}$$

where,

$m_{n,c}$ is the liquid molar holdup of component c on stage n

$l_{n,c}$ is the liquid molar flowrate of component c leaving stage n

$v_{n,c}$ is the vapour molar flowrate of component c leaving stage n

f_c is the molar flowrate of component c in the liquid feed

s_c is the molar flowrate of component c in the liquid side stream

$$\zeta = \begin{cases} 1, & n = n_f \\ 0, & else \end{cases}$$

$$\varsigma = \begin{cases} 1, & n = n_s \\ 0, & else \end{cases}$$ (n_f is the feed stage location, n_s is the side stream stage location)

Finally, the component material balance equations of the partial reboiler stage ($n = N_s$) are compactly represented below:

$$\frac{dm_{N_s,c}}{dt} = l_{N_s-1,c} - b_c - v_{N_s,c}, \ c = \{\text{HVC}, \text{IVC}, \text{LVC}\} \quad (6)$$

where,

$m_{N_s,c}$ is the liquid molar holdup of component c on stage N_s

$l_{N_s-1,c}$ is the liquid molar flowrate of component c entering the stage N_s

$v_{N_s,c}$ is the vapour molar flowrate of component c leaving the stage N_s

b_c is the bottoms molar flowrate of component c leaving the stage N_s.

Column - Vapour Liquid Equilibrium

On each stage of the distillation column, the vapour and the liquid phases are in contact and are assumed to be at equilibrium throughout the periodic operation in this article. The phase equilibrium was modelled using Raoult's Law and the Antoine equation.

$$K_c(T_n, P_n) = \frac{y_{n,c}}{x_{n,c}} \quad (7)$$

$$K_c(T_n, P_n) = \frac{P_c^{sat}(T_n)}{P_n} \quad (8)$$

$$\ln\left(P_c^{sat}(T_n)\right) = A_c + \frac{B_c}{T_n} + C_c \log(T_n) + D_c T_n^{E_c} \quad (9)$$

where,

$K_c(T_n, P_n)$ is the phase equilibrium ratio of component c on stage n

$y_{n,c}$ is the mole fraction of component c in the vapour leaving stage n

$x_{n,c}$ is the mole fraction of component c in the liquid leaving stage n

$P_c^{sat}(T_n)$ is the vapour pressure of c on stage n

T_n is the temperature of the stage n

P_n is the pressure of the stage n

A_c, B_c, C_c, D_c, E_c are the Antoine parameters for component c.

The mole fraction of the components in the vapour streams and the liquid streams are normalized using the following set of equations, where L_n is the total flowrate of liquid leaving stage n, V_n is the total flowrate of vapour leaving stage n, and M_n is the total molar holdup of liquid on stage n.

$$\sum_c x_{n,c} = \sum_c y_{n,c} = 1 \tag{10}$$

$$l_{n,c} = x_{n,c} L_n \tag{11}$$

$$v_{n,c} = y_{n,c} V_n \tag{12}$$

$$\frac{m_{n,c}}{M_n} = \frac{l_{n,c}}{L_n} \tag{13}$$

Column - Tray Hydraulics

The Francis weir equation (Perry and Green, 2013; Prokopakis and Seider, 1983) was used to predict the total liquid flowrate over the weir based on the weir height (h_{weir}), weir length (L_{weir}), tray cross-sectional area (A_{Tray}), the density of liquid on tray n ($\rho_n^{liq}(x_{n,c}, T_n, P_n)$), and the gravitational constant (g). We assume that the weir used is a segmental weir.

$$M_n = A_{Tray} \rho_n^{liq}(x_{n,c}, T_n, P_n) \left[h_{weir} + 1.41 \left(\frac{L_n}{\rho_n^{liq}(x_{n,c}, T_n, P_n) L_{weir} \sqrt{g}} \right)^{2/3} \right] \tag{14}$$

The density of liquid on stage n is approximated using the Rackett equation (Green and Southard, 2019),

$$\ln\left(\frac{1}{\rho_{n,c}^{liq}(x_{n,c}, T_n, P_n)} \right) = \ln\left(\frac{R_{gas} T_c^{cr}}{P_c^{cr}} \right) + \left[1 + \left(1 - \frac{T_n}{T_c^{cr}} \right)^{2/7} \right] \ln\left(Z_c^{Ra} \right) \tag{15}$$

$$\rho_n^{liq}(x_{n,c}, T_n, P_n) = \sum_c x_{n,c} \rho_{n,c}^{liq}(x_{n,c}, T_n, P_n) \tag{16}$$

where,

R_{gas} is the ideal gas constant

T_c^{cr} is the critical temperature of component c

P_c^{cr} is the critical pressure of component c

Z_c^{Ra} is the Rackett compressibility factor of component c.

Control Sub-System

The semicontinuous distillation control subsystem has five different feedback control loops, which are:

(1) Distillate concentration control loop

(2) Bottoms concentration control loop

(3) Reflux drum level control loop

(4) Sump level control loop

(5) Side stream flowrate control loop

The controller used in all these feedback control loops is a proportional-integral (PI) controller. In this paper, we use the parallel form of the PI control law, which is

$$u(t) = u_{bias} \mp K_p e(t) \mp K_i \int_0^t e(\tau) d\tau \quad (17)$$

where,

$u(t)$ is the manipulated variable

u_{bias} is the controller bias

K_p is the proportional gain

K_i is the integral gain

$e(t)$ is the error (Setpoint – Process Variable value at time t).

The error is further defined as follows,

$$e(t) = SP - PV(t) \quad (18)$$

where, SP is the setpoint, and $PV(t)$ is the process variable value at time t. The negative sign in the equation comes into play when the controller is reverse-acting and not direct-acting. Instead of directly using the form of the control law presented in (13), the following differential form of the control law is used, where I is the differential state.

$$\frac{dI}{dt} = e(t) \tag{19}$$

$$u(t) = u_{bias} \mp K_p e(t) \mp K_i I \tag{20}$$

Table 1: The table shows the manipulated variables, setpoints, and the process variables in the different control loops.

	$\boldsymbol{u(t)}$	$\boldsymbol{SP}$	$\boldsymbol{PV(t)}$
Distillate concentration control loop	Distillate flowrate ($d(t)$)	Desired mole fraction of HVC on stage 1 ($x_{1,HVC}^{desired}$)	Mole fraction of HVC on stage 1 ($x_{1,HVC}(t)$)
Bottoms concentration control loop	Bottoms flowrate ($b(t)$)	Desired mole fraction of HVC on stage N_s ($x_{N_s,LVC}^{desired}$)	Mole fraction of HVC on stage N_s ($x_{N_s,LVC}(t)$)
Reflux drum level control loop	Feed flowrate to the column ($F(t)$)	Desired height of liquid in the reflux drum ($h_{reflux}^{desired}$)	Height of liquid in the reflux drum ($h_{reflux}(t)$)
Sump level control loop	Reboil rate ($V_{N_s}(t)$)	Desired height of liquid in the sump ($h_{sump}^{desired}$)	Height of liquid in the sump ($h_{sump}(t)$)
Side stream flowrate control loop	Side stream flowrate ($S(t)$)	Feed stream component IVC flowrate ($f_{n_f,IVC}(t)$)	Side stream component IVC flowrate ($s_{n_s,IVC}(t)$)

From Table 1, notice that the modified-ideal side draw recovery arrangement is used to change the setpoint of the side stream flowrate controller (Madabhushi and Adams, 2018). Also, note that it is ensured that the manipulated variables are clipped between desired lower and upper bound values.

The height of the liquid in the reflux drum (stage 1) and sump (stage N_s) are obtained using the following relationships, where A_{reflux} is the area of the reflux drum and A_{sump} is the area of the sump,

$$h_{reflux} = \frac{M_1}{\rho_1^{liq}(x_{1,c}, T_1, P_1)\, A_{reflux}} \tag{21}$$

$$h_{sump} = \frac{M_{N_S}}{\rho_{N_S}^{liq}(x_{N_S,c}, T_{N_S}, P_{N_S})\, A_{sump}} \tag{22}$$

Middle-Vessel - Material Balances

The mode-specific component mass balance equations of the middle vessel are represented compactly as shown here,

$$\frac{dm_{mv,c}}{dt} = s_{n_s,c} + \alpha f_{charge,c} - f_{n_f,c} - \beta f_{discharge,c},\ c = \{\text{HVC}, \text{IVC}, \text{LVC}\} \quad (23)$$

where,

$m_{mv,c}$ is the liquid molar holdup of component c in the middle vessel

$f_{charge,c}$ is the liquid flowrate of component c in the charging stream (Figure 1)

$f_{discharge,c}$ is the liquid flowrate of component c in the discharge stream (Figure 1)

$$\alpha = \begin{cases} 1, & T_\mu = \mu_3 \\ 0, & else \end{cases}$$

$$\beta = \begin{cases} 1, & T_\mu = \mu_2 \\ 0, & else \end{cases}$$

From the material balances of the column and the middle-vessel, the vapour liquid equilibrium relationships, the tray hydraulics, and the PI controller equations, we can gather the following: the differential variables ($\boldsymbol{z}$) are all the liquid molar holdups ($m_{n,c}$ and $m_{mv,c}$) and the differential states in the controller equations. The discrete design variables ($\boldsymbol{p_d}$) are the number of stages (N_s), feed stage location (n_f), side stream stage location (n_s), and equipment sizes. The real-valued design variables ($\boldsymbol{p_r}$) are the reflux rate (L_1), and all the controller tuning parameters. The remaining variables are all algebraic variables ($\boldsymbol{y}$). The equations presented in this section were implemented in a software tool called CasADi (Andersson et al., 2019) using its Python front-end.

4. The boundary value problem formulation

As an IVP, the solution of the hybrid model describing the semicontinuous distillation process is obtained by carrying out numerical integration from t_0 where the values of $\boldsymbol{z}(t_0(\boldsymbol{p_d}, \boldsymbol{p_r}), \boldsymbol{p_d}, \boldsymbol{p_r})$, and $\boldsymbol{y}(t_0(\boldsymbol{p_d}, \boldsymbol{p_r}), \boldsymbol{p_d}, \boldsymbol{p_r})$ are specified. The integrator then uses an event detection algorithm (which is a bisection algorithm) during an integration step for finding the location of the state-dependent events, which trigger the mode transition to some desired degree of tolerance (Aspen Plus® Dynamics; Barton, 1992). After detecting the location of an event where the instantaneous mode transition occurs, the DAE equation system is reinitialized, and then the integration is continued (Aspen Plus® Dynamics; Barton, 1992).

In a general boundary value problem with DAEs (DAE-BVP), the solution of the DAE is specified at more than one point, called the multi-point DAE-BVPs, by specifying conditions called the boundary conditions at these points (Ascher and Petzold, 1998; Lamour et al., 2015). However, typically, in most applications, the boundary conditions are just specified at two points (boundaries), which are called the two-point DAE-BVPs (Ascher and Petzold, 1998; Lamour et al., 2015). Boundary conditions that enforce time-periodic behaviour are non-separable, which

means that the conditions specified at the boundaries are not independent (Lamour et al., 2015). For a semi-explicit index-1 DAE, it is enough to enforce the boundary conditions only on the differential states because the algebraic states can be uniquely determined using the algebraic equations based on the values of the differential states (Lamour et al., 2015).

$$\boldsymbol{z}(t, \boldsymbol{p_d}, \boldsymbol{p_r}) - \boldsymbol{z}(t + \Gamma(\boldsymbol{p_d}, \boldsymbol{p_c}), \boldsymbol{p_d}, \boldsymbol{p_r}) = \boldsymbol{0} \tag{24}$$

where $\Gamma(\boldsymbol{p_d}, \boldsymbol{p_c})$ is the period of oscillation. This formulation was extended to hybrid systems by Khan et al., 2011, where the authors provided rigorous mathematical definitions. Based on their framework, the time-periodic boundary condition for semicontinuous distillation is defined as follows,

$$\boldsymbol{z}^{(\mu_1)}(t_0(\boldsymbol{p_d}, \boldsymbol{p_r}), \boldsymbol{p_d}, \boldsymbol{p_r}) - \boldsymbol{z}^{(\mu_1)}(t_3(\boldsymbol{p_d}, \boldsymbol{p_r}), \boldsymbol{p_d}, \boldsymbol{p_r}) = \boldsymbol{0} \tag{25}$$

where $t_0(\boldsymbol{p_d}, \boldsymbol{p_r}) \coloneqq 0$, and we consider that the processing starts at the beginning of the mode μ_1, which is the separating mode. The BVP of the hybrid model of the semicontinuous distillation system (hybrid-BVP) can thus be defined as follows,

$$\begin{aligned}
\dot{\boldsymbol{z}}^{(\mu_i)}(t, \boldsymbol{p_d}, \boldsymbol{p_r}) = & \begin{bmatrix} \boldsymbol{\Psi}_{cc}\left(\boldsymbol{z}^{(\mu_i)}, \boldsymbol{y}^{(\mu_i)}(t, \boldsymbol{p_d}, \boldsymbol{p_r}), \boldsymbol{p_d}, \boldsymbol{p_r}\right) \\ \boldsymbol{\Psi}_{mv}^{(\mu_i)}\left(\boldsymbol{z}^{(\mu_i)}, \boldsymbol{y}^{(\mu_i)}(t, \boldsymbol{p_d}, \boldsymbol{p_r}), \boldsymbol{p_d}, \boldsymbol{p_r}\right) \end{bmatrix} \\
\boldsymbol{0} = & \begin{bmatrix} \boldsymbol{\Phi}_{cc}\left(\boldsymbol{z}^{(\mu_i)}, \boldsymbol{y}^{(\mu_i)}(t, \boldsymbol{p_d}, \boldsymbol{p_r}), \boldsymbol{p_d}, \boldsymbol{p_r}\right) \\ \boldsymbol{\Phi}_{mv}^{(\mu_i)}\left(\boldsymbol{z}^{(\mu_i)}, \boldsymbol{y}^{(\mu_i)}(t, \boldsymbol{p_d}, \boldsymbol{p_r}), \boldsymbol{p_d}, \boldsymbol{p_r}\right) \end{bmatrix} \qquad i = \{1, 2, 3\} \\
0 = & \ \Omega_{\mu_1}^{\mu_2}(t, \boldsymbol{p_d}, \boldsymbol{p_r}) \\
0 = & \ \Omega_{\mu_2}^{\mu_3}(t, \boldsymbol{p_d}, \boldsymbol{p_r}) \\
0 = & \ \Omega_{\mu_3}^{\mu_1}(t, \boldsymbol{p_d}, \boldsymbol{p_r}) \\
0 = & \ \boldsymbol{\Theta}_{\boldsymbol{z}_{\mu_i}}^{\mu_j}(t, \boldsymbol{p_d}, \boldsymbol{p_r}) \\
0 = & \ \boldsymbol{\Theta}_{\boldsymbol{y}_{\mu_i}}^{\mu_j}(t, \boldsymbol{p_d}, \boldsymbol{p_r}) \\
0 = & \ \boldsymbol{z}^{(\mu_1)}(t_0(\boldsymbol{p_d}, \boldsymbol{p_r}), \boldsymbol{p_d}, \boldsymbol{p_r}) - \boldsymbol{z}^{(\mu_1)}(t_3(\boldsymbol{p_d}, \boldsymbol{p_r}), \boldsymbol{p_d}, \boldsymbol{p_r})
\end{aligned} \tag{26}$$

where,

$$\boldsymbol{z}^{(\mu_1)}(t_0(\boldsymbol{p_d}, \boldsymbol{p_r}), \boldsymbol{p_d}, \boldsymbol{p_r}) = \boldsymbol{z_0}(\boldsymbol{p_d}, \boldsymbol{p_r})$$

The value of $\boldsymbol{z_0}(\boldsymbol{p_d}, \boldsymbol{p_r})$ is particularly picked to coincide with the location of the event that satisfies the transition condition $\Omega_{\mu_3}^{\mu_1}(t, \boldsymbol{p_d}, \boldsymbol{p_r})$, i.e., $h_{mv}^{(\mu_1)}(t_0(\boldsymbol{p_d}, \boldsymbol{p_r}), \boldsymbol{p_d}, \boldsymbol{p_r}) = h_{mv}^{u}$. This selection, called the phase-locking condition (Seydel, 2010), limits the initial state value to a particular point on the periodic orbit (Khan et al., 2011). As a consequence of the periodic boundary condition, $h_{mv}^{(\mu_1)}(t_3(\boldsymbol{p_d}, \boldsymbol{p_r}), \boldsymbol{p_d}, \boldsymbol{p_r})$ is therefore implicitly specified.

4.1 Single shooting method for obtaining the solution of the hybrid-BVP

The shooting method is an ideal way of solving BVPs of ordinary differential equations and differential-algebraic equations. The main philosophy behind the shooting method is to transform the BVP to a family of IVPs, whose initial values are unknown. The goal is to find the initial value that satisfies the boundary conditions. In this paper, we use this method, specifically, the single shooting method for solving the hybrid-BVP (15).

We treated the hybrid-BVP as having four independent DAE-BVPs linked together through the transition functions $\boldsymbol{\Theta}_{\boldsymbol{z}_{\mu_i}}^{\mu_j}(t, \boldsymbol{p_d}, \boldsymbol{p_r})$ and $\boldsymbol{\Theta}_{\boldsymbol{y}_{\mu_i}}^{\mu_j}(t, \boldsymbol{p_d}, \boldsymbol{p_r})$ to apply the single shooting method. The four DAEs correspond to the dynamic models of the system in the four epochs defined in section 3. Since we pick the initial value to coincide with the event location, the time interval of the fourth epoch is zero, and thus we can safely ignore this epoch. Hence, three DAE-BVPs are mathematically defined here,

DAE-BVP 1:

$$\begin{aligned}
\dot{\boldsymbol{z}}^{(\mu_1)}(t, \boldsymbol{p_d}, \boldsymbol{p_r}) = & \begin{bmatrix} \boldsymbol{\Psi}_{cc}\left(\boldsymbol{z}^{(\mu_1)}, \boldsymbol{y}^{(\mu_1)}(t, \boldsymbol{p_d}, \boldsymbol{p_r}), \boldsymbol{p_d}, \boldsymbol{p_r}\right) \\ \boldsymbol{\Psi}_{mv}^{(\mu_1)}\left(\boldsymbol{z}^{(\mu_1)}, \boldsymbol{y}^{(\mu_1)}(t, \boldsymbol{p_d}, \boldsymbol{p_r}), \boldsymbol{p_d}, \boldsymbol{p_r}\right) \end{bmatrix} \\
\boldsymbol{0} = & \begin{bmatrix} \boldsymbol{\Phi}_{column}\left(\boldsymbol{z}^{(\mu_1)}, \boldsymbol{y}^{(\mu_1)}(t, \boldsymbol{p_d}, \boldsymbol{p_r}), \boldsymbol{p_d}, \boldsymbol{p_r}\right) \\ \boldsymbol{\Phi}_{mv}^{(\mu_1)}\left(\boldsymbol{z}^{(\mu_1)}, \boldsymbol{y}^{(\mu_1)}(t, \boldsymbol{p_d}, \boldsymbol{p_r}), \boldsymbol{p_d}, \boldsymbol{p_r}\right) \end{bmatrix} \\
x_{mv,IVC}^{desired} = & \; x_{mv,IVC}^{(\mu_1)}(t_1(\boldsymbol{p_d}, \boldsymbol{p_r}), \boldsymbol{p_d}, \boldsymbol{p_r}) \\
\boldsymbol{z_0}(\boldsymbol{p_d}, \boldsymbol{p_r}) = & \; \boldsymbol{z}^{(\mu_1)}(t_0(\boldsymbol{p_d}, \boldsymbol{p_r}), \boldsymbol{p_d}, \boldsymbol{p_r}) \\
\boldsymbol{y_0}(\boldsymbol{p_d}, \boldsymbol{p_r}) = & \; \boldsymbol{y}^{(\mu_1)}(t_0(\boldsymbol{p_d}, \boldsymbol{p_r}), \boldsymbol{p_d}, \boldsymbol{p_r})
\end{aligned} \tag{27}$$

where $\boldsymbol{y_0}(\boldsymbol{p_d}, \boldsymbol{p_r})$ is the value of the algebraic state that is consistent with the DAE at $t_0(\boldsymbol{p_d}, \boldsymbol{p_r})$. This DAE-BVP is applicable in the time interval $[t_0(\boldsymbol{p_d}, \boldsymbol{p_r}), t_1(\boldsymbol{p_d}, \boldsymbol{p_r})]$.

DAE-BVP 2:

$$\begin{aligned}
\dot{\boldsymbol{z}}^{(\mu_2)}(t, \boldsymbol{p_d}, \boldsymbol{p_r}) = & \begin{bmatrix} \boldsymbol{\Psi}_{cc}\left(\boldsymbol{z}^{(\mu_2)}, \boldsymbol{y}^{(\mu_2)}(t, \boldsymbol{p_d}, \boldsymbol{p_r}), \boldsymbol{p_d}, \boldsymbol{p_r}\right) \\ \boldsymbol{\Psi}_{mv}^{(\mu_1)}\left(\boldsymbol{z}^{(\mu_2)}, \boldsymbol{y}^{(\mu_2)}(t, \boldsymbol{p_d}, \boldsymbol{p_r}), \boldsymbol{p_d}, \boldsymbol{p_r}\right) \end{bmatrix} \\
\boldsymbol{0} = & \begin{bmatrix} \boldsymbol{\Phi}_{cc}\left(\boldsymbol{z}^{(\mu_2)}, \boldsymbol{y}^{(\mu_2)}(t, \boldsymbol{p_d}, \boldsymbol{p_r}), \boldsymbol{p_d}, \boldsymbol{p_r}\right) \\ \boldsymbol{\Phi}_{mv}^{(\mu_2)}\left(\boldsymbol{z}^{(\mu_2)}, \boldsymbol{y}^{(\mu_2)}(t, \boldsymbol{p_d}, \boldsymbol{p_r}), \boldsymbol{p_d}, \boldsymbol{p_r}\right) \end{bmatrix} \\
h_{mv}^{l} = & \; h_{mv}^{(\mu_2)}(t_2(\boldsymbol{p_d}, \boldsymbol{p_r}), \boldsymbol{p_d}, \boldsymbol{p_r}) \\
\boldsymbol{z}^{(\mu_1)}(t_1(\boldsymbol{p_d}, \boldsymbol{p_r}), \boldsymbol{p_d}, \boldsymbol{p_r}) = & \; \boldsymbol{z}^{(\mu_2)}(t_1(\boldsymbol{p_d}, \boldsymbol{p_r}), \boldsymbol{p_d}, \boldsymbol{p_r})
\end{aligned}$$

$$\boldsymbol{y}^{(\mu_1)}(t_1(\boldsymbol{p_d},\boldsymbol{p_r}),\boldsymbol{p_d},\boldsymbol{p_r}) = \quad \boldsymbol{y}^{(\mu_2)}(t_1(\boldsymbol{p_d},\boldsymbol{p_r}),\boldsymbol{p_d},\boldsymbol{p_r}) \tag{28}$$

This DAE-BVP is applicable in the time interval $[t_1(\boldsymbol{p_d},\boldsymbol{p_r}), t_2(\boldsymbol{p_d},\boldsymbol{p_r})]$.

DAE-BVP 3:

$$\dot{\boldsymbol{z}}^{(\mu_3)}(t,\boldsymbol{p_d},\boldsymbol{p_r}) = \quad \begin{bmatrix} \boldsymbol{\Psi}_{cc}\left(\boldsymbol{z}^{(\mu_3)},\boldsymbol{y}^{(\mu_3)}(t,\boldsymbol{p_d},\boldsymbol{p_r}),\boldsymbol{p_d},\boldsymbol{p_r}\right) \\ \boldsymbol{\Psi}_{mv}^{(\mu_3)}\left(\boldsymbol{z}^{(\mu_3)},\boldsymbol{y}^{(\mu_3)}(t,\boldsymbol{p_d},\boldsymbol{p_r}),\boldsymbol{p_d},\boldsymbol{p_r}\right) \end{bmatrix}$$

$$\boldsymbol{0} = \quad \begin{bmatrix} \boldsymbol{\Phi}_{cc}\left(\boldsymbol{z}^{(\mu_3)},\boldsymbol{y}^{(\mu_3)}(t,\boldsymbol{p_d},\boldsymbol{p_r}),\boldsymbol{p_d},\boldsymbol{p_r}\right) \\ \boldsymbol{\Phi}_{mv}^{(\mu_3)}\left(\boldsymbol{z}^{(\mu_3)},\boldsymbol{y}^{(\mu_3)}(t,\boldsymbol{p_d},\boldsymbol{p_r}),\boldsymbol{p_d},\boldsymbol{p_r}\right) \end{bmatrix}$$

$$h_{mv}^{u} = \quad h_{mv}^{(\mu_3)}(t_3(\boldsymbol{p_d},\boldsymbol{p_r}),\boldsymbol{p_d},\boldsymbol{p_r})$$

$$\boldsymbol{z}^{(\mu_2)}(t_2(\boldsymbol{p_d},\boldsymbol{p_r}),\boldsymbol{p_d},\boldsymbol{p_r}) = \quad \boldsymbol{z}^{(\mu_3)}(t_2(\boldsymbol{p_d},\boldsymbol{p_r}),\boldsymbol{p_d},\boldsymbol{p_r})$$

$$\boldsymbol{y}^{(\mu_2)}(t_2(\boldsymbol{p_d},\boldsymbol{p_r}),\boldsymbol{p_d},\boldsymbol{p_r}) = \quad \boldsymbol{y}^{(\mu_3)}(t_2(\boldsymbol{p_d},\boldsymbol{p_r}),\boldsymbol{p_d},\boldsymbol{p_r})$$

$$\boldsymbol{z_0}(\boldsymbol{p_d},\boldsymbol{p_r}) = \quad \boldsymbol{z}^{(\mu_3)}(t_3(\boldsymbol{p_d},\boldsymbol{p_r}),\boldsymbol{p_d},\boldsymbol{p_r}) \tag{29}$$

This DAE-BVP is applicable in the time interval $[t_2(\boldsymbol{p_d},\boldsymbol{p_r}), t_3(\boldsymbol{p_d},\boldsymbol{p_r})]$.

The single shooting method is an iterative procedure that involves integration and solving a system of non-linear algebraic equations. In brief, in this method, first, the DAEs in (27), (28), and (29) are integrated numerically to obtain solutions $\boldsymbol{z}^{(\mu_i)}(t,\boldsymbol{p_d},\boldsymbol{p_r})$ and $\boldsymbol{y}^{(\mu_i)}(t,\boldsymbol{p_d},\boldsymbol{p_r})$, for $i = \{1,2,3\}$, that satisfy the guessed initial conditions $\boldsymbol{z_0}(\boldsymbol{p_d},\boldsymbol{p_r})$ and $\boldsymbol{y_0}(\boldsymbol{p_d},\boldsymbol{p_r})$. These solutions are used to solve a system of non-linear algebraic equations formed by the boundary conditions imposed at the end of the time interval in which the DAE-BVP system is valid to improve the initial guess. The process is repeated until the desired convergence tolerance is obtained. The initial guess for $\boldsymbol{z_0}(\boldsymbol{p_d},\boldsymbol{p_r})$ and $\boldsymbol{y_0}(\boldsymbol{p_d},\boldsymbol{p_r})$ was selected such that it is the state of the hypothetical continuous distillation system described in the introduction section, for chosen $\boldsymbol{p_d}$ and $\boldsymbol{p_r}$ of the semicontinuous distillation system. Based on our experience in simulating semicontinuous distillation systems, convergence to a limit cycle is generally possible when this state is used as the initial state at t = 0.

To have a fixed horizon of integration ($[0,1]$) during the numerical integration process, some well-know tricks were applied to reformulate the DAEs (Ascher and Petzold, 1998). Specifically, we apply a change of variable by changing the independent variable t to τ. The change of variable for the three DAE-BVPs is as follows,

DAE-BVP 1: $\tau = {}^{t}/_{t_1(\boldsymbol{p_d},\boldsymbol{p_r})}$ (30)

DAE-BVP 2: $\tau = {}^{t}/_{t_2(\boldsymbol{p_d},\boldsymbol{p_r})}$ (31)

DAE-BVP 3: $\tau = {}^{t}/_{t_3(\boldsymbol{p_d},\boldsymbol{p_r})}$ (32)

The differential equation systems of the three BVPs were each augmented by adding the following differential equations because of the reformulation,

DAE-BVP 1: $\frac{dt_1(\boldsymbol{p_d},\boldsymbol{p_r})}{d\tau} = 0$ (33)

DAE-BVP 2: $\frac{dt_2(\boldsymbol{p_d},\boldsymbol{p_r})}{d\tau} = 0$ (34)

DAE-BVP 3: $\frac{dt_3(\boldsymbol{p_d},\boldsymbol{p_r})}{d\tau} = 0$ (35)

Appropriate modifications were also made to the differential equation part of the differential-algebraic equation systems to change $\frac{d\boldsymbol{z}^{(\mu_i)}}{dt}$ to $\frac{d\boldsymbol{z}^{(\mu_i)}}{d\tau}$.

5. Application of the single shooting method

The single shooting method for semicontinuous distillation design that was described in the previous section was applied to two case studies, both involving the separation of hexane, heptane, and octane. Details of the two case studies are provided in the table (Table 2). The properties of the components in the liquid mixture (T_c^{cr}, P_c^{cr}, Z_c^{Ra}, A_c, B_c, C_c, D_c, E_c) were taken from Aspen Physical Property database and Perry and Green, 2013. The initial guesses of the differential states and the algebraic states for chosen values of N_s, n_f, n_s, $x_{1,HVC}^{desired}$, and $x_{N_s,LVC}^{desired}$ for the two case studies, were obtained by simulating the hypothetical continuous distillation system in Aspen Plus V10. The values of the number of trays and reflux ratio values can be obtained from the modified Fenske-Underwood equations (Phimister and Seider, 2000). The cross-sectional areas of the tray (A_{Tray}), the reflux drum (A_{reflux}) and the sump (A_{sump}) were then used to calculate the liquid molar hold-ups on the stages based on the steady-state liquid flowrates leaving a stage.

Table 2: Some details of the systems (Case 1 and Case 2) used for demonstrating the application of the single shooting method. The system parameters in Case 2 were taken from Madabhushi and Adams, 2019.

	CASE 1	**CASE 2**
TERNARY MIXTURE	Hexane, Heptane, Octane	Hexane, Heptane, Octane
$\boldsymbol{N_s}$	5	40
$\boldsymbol{n_f}$	3	24
$\boldsymbol{n_s}$	2	13
$\boldsymbol{x_{1,HVC}^{desired}}$	0.65	0.95
$\boldsymbol{x_{N_s,LVC}^{desired}}$	0.65	0.95
$\boldsymbol{x_{mv,IVC}^{desired}}$	0.37	0.95

$\boldsymbol{A_{Tray}}$ (m^2)	0.657	0.657
$\boldsymbol{A_{reflux}}$ (m^2)	0.805	2.350
$\boldsymbol{A_{sump}}$ (m^2)	0.368	2.746
$\boldsymbol{P_1}$ (atm)	1.0	1.0
Stage pressure drop (atm)	0.0805	0.0067

To find the initial guess of the transition times, $t_1(\boldsymbol{p_d}, \boldsymbol{p_r})$, $t_2(\boldsymbol{p_d}, \boldsymbol{p_r})$, and $t_3(\boldsymbol{p_d}, \boldsymbol{p_r})$ at which the transition conditions, $\Omega_{\mu_1}^{\mu_2}(t, \boldsymbol{p_d}, \boldsymbol{p_r})$, $\Omega_{\mu_2}^{\mu_3}(t, \boldsymbol{p_d}, \boldsymbol{p_r})$, and $\Omega_{\mu_3}^{\mu_1}(t, \boldsymbol{p_d}, \boldsymbol{p_r})$ are satisfied, the non-linear optimization solver IPOPT (Wächter and Biegler, 2006) was used. The objective function of the non-linear optimization problem solved using IPOPT is the Euclidean norm of the residuals of the transition conditions, while these conditions were posed as constraints of the optimization problem.

Once the initial guesses are obtained, to find the zeroes of the transition conditions and the periodicity conditions in (27), (28), (29) for improving the initial guess, the non-linear optimization solver IPOPT (Wächter and Biegler, 2006) was again used. The objective function of the non-linear optimization problem posed to IPOPT is the Euclidean norm of the residuals of these conditions, while the constraints are the conditions mentioned above. Additionally, this optimization problem includes decision variables bounds to ensure that a physically unrealistic solution is not obtained. The numerical integrator that is used to integrate the DAEs is IDAS (Hindmarsh et al., 2005), which is a differential-algebraic equation system integrator equipped with the forward and adjoint sensitivity analysis modules. CasADi software has control over the sensitivity analysis method that IDAS uses to compute the derivative information. Furthermore, in the checkpointing scheme that is used in the backward integration of the adjoint sensitivity system in IDAS, the number of steps per checkpoint was picked to be 1000 to ensure convergence. The optimization problem that is used to determine the initial guess of the mode transition times was solved to optimality with the default values of the IPOPT solver parameters. Below, we present the sketch of the algorithm for applying the single shooting method for semicontinuous distillation design.

Algorithm: Single shooting method for semicontinuous distillation design

 # User Inputs to Algorithm

$\boldsymbol{p_d}$ ← **user_input** (N_s, n_f, n_s, A_{Tray}, A_{reflux}, A_{sump})

$\boldsymbol{p_r}$ ← **user_input** (L_1, $\{\boldsymbol{K_{p,k}}\}$, $\{\boldsymbol{K_{I,k}}\}$) (where $\boldsymbol{k}$ = Distillate concentration controller, Bottoms concentration controller, Reflux Drum level controller, Sump level controller, Side stream flowrate controller)

constants ← **user_input** ($x_{1,HVC}^{desired}$, $x_{N_s,LVC}^{desired}$, $h_{reflux}^{desired}$, $h_{sump}^{desired}$, $x_{mv,IVC}^{desired}$, h_{mv}^{l}, h_{mv}^{u}, $\{Z_c^{Ra}, c = 1 \text{ to } 3\}$, $\{P_c^{cr}, c = 1 \text{ to } 3\}$, $\{T_c^{cr}, c = 1 \text{ to } 3\}$,

$\{A_c, c = 1 \text{ to } 3\}$, $\{B_c, c = 1 \text{ to } 3\}$, $\{C_c, c = 1 \text{ to } 3\}$,
$\{D_c, c = 1 \text{ to } 3\}$, $\{E_c, c = 1 \text{ to } 3\}$)

 # Set index i to zero
$i \leftarrow 0$

 # User guesses for the mode transition times based on user's experience
user_input (t_1^i, t_2^i, t_3^i)

 # Set the initial guesses for the differential states associated with the integral term of the PI controllers (I_k^i) to zero

for k = {Distillate concentration controller, Bottoms concentration controller, Reflux Drum level controller, Sump level controller, Side stream flowrate controller}
$I_k^i \leftarrow 0$
end for

 # Solve non-linear algebraic equations of the hypothetical continuous distillation system analog to get the initial guesses for $m_{n,c}^i$, $m_{mv,c}^i$, and $\boldsymbol{y_0^i}(\boldsymbol{p_d}, \boldsymbol{p_r})$

$[m_{n,c}^i, m_{mv,c}^i, \boldsymbol{y_0^i}(\boldsymbol{p_d}, \boldsymbol{p_r})]$ = **Solve** (*Hypothetical continuous distillation system equations*)

 # Set the initial guesses that will be used for solving the BVPs in the next step to be the results of the previous step
$\boldsymbol{z_0}(\boldsymbol{p_d}, \boldsymbol{p_r}) \leftarrow (m_{n,c}^i, m_{mv,c}^i, I_k^i, t_1^i, t_2^i, t_3^i)$ (this is $\boldsymbol{z_0^i}(\boldsymbol{p_d}, \boldsymbol{p_r})$)
$\boldsymbol{y_0}(\boldsymbol{p_d}, \boldsymbol{p_r}) \leftarrow \boldsymbol{y_0^i}(\boldsymbol{p_d}, \boldsymbol{p_r})$

 # Solve the relaxed and reformulated boundary value problems DAEBVP-1, DAEBVP-2, DAEBVP-3 (which do not include periodic boundary conditions) to get a better initial guess for $t_1(\boldsymbol{p_d}, \boldsymbol{p_r})$, $t_2(\boldsymbol{p_d}, \boldsymbol{p_r})$, and $t_3(\boldsymbol{p_d}, \boldsymbol{p_r})$. *These new and better guesses will improve the convergence properties of the single shooting method in the final step.*

while norm (residual vector of mode transition conditions) > Desired tolerance

$[\boldsymbol{z}^{(\mu_1)}(1, \boldsymbol{p_d}, \boldsymbol{p_r}), \boldsymbol{y}^{(\mu_1)}(1, \boldsymbol{p_d}, \boldsymbol{p_r})]$ = **Integrate** (reformulated DAEBVP-1 DAEs, $\boldsymbol{z_0}(\boldsymbol{p_d}, \boldsymbol{p_r}), \boldsymbol{y_0}(\boldsymbol{p_d}, \boldsymbol{p_r})$)
$[\boldsymbol{z}^{(\mu_2)}(1, \boldsymbol{p_d}, \boldsymbol{p_r}), \boldsymbol{y}^{(\mu_2)}(1, \boldsymbol{p_d}, \boldsymbol{p_r})]$ = **Integrate** (reformulated DAEBVP-2 DAEs, $\boldsymbol{z}^{(\mu_2)}(0, \boldsymbol{p_d}, \boldsymbol{p_r}), \boldsymbol{y}^{(\mu_2)}(0, \boldsymbol{p_d}, \boldsymbol{p_r})$)
$[\boldsymbol{z}^{(\mu_3)}(1, \boldsymbol{p_d}, \boldsymbol{p_r}), \boldsymbol{y}^{(\mu_3)}(1, \boldsymbol{p_d}, \boldsymbol{p_r})]$ = **Integrate** (reformulated DAEBVP-3 DAEs, $\boldsymbol{z}^{(\mu_3)}(0, \boldsymbol{p_d}, \boldsymbol{p_r}), \boldsymbol{y}^{(\mu_3)}(0, \boldsymbol{p_d}, \boldsymbol{p_r})$)
$i \leftarrow i + 1$

$[t_1^i(\boldsymbol{p_d}, \boldsymbol{p_r}), t_2^i(\boldsymbol{p_d}, \boldsymbol{p_r}), t_3^i(\boldsymbol{p_d}, \boldsymbol{p_r})]$ = **Solve** $\left(\begin{bmatrix} \Omega_{\mu_1}^{\mu_2}(t, \boldsymbol{p_d}, \boldsymbol{p_r}) \\ \Omega_{\mu_3}^{\mu_1}(t, \boldsymbol{p_d}, \boldsymbol{p_r}) \\ \Omega_{\mu_2}^{\mu_3}(t, \boldsymbol{p_d}, \boldsymbol{p_r}) \end{bmatrix} = \boldsymbol{0} \right)$

$\boldsymbol{z_0}(\boldsymbol{p_d}, \boldsymbol{p_r}) \leftarrow \boldsymbol{z_0^i}(\boldsymbol{p_d}, \boldsymbol{p_r})$

$\boldsymbol{y_0}(\boldsymbol{p_d}, \boldsymbol{p_r}) \leftarrow \boldsymbol{y_0^i}(\boldsymbol{p_d}, \boldsymbol{p_r})$ (obtained based on $\boldsymbol{z_0^i}(\boldsymbol{p_d}, \boldsymbol{p_r})$)

end while

 # Single shooting: *Solve the reformulated boundary value problems DAEBVP-1, DAEBVP-2, DAEBVP-3 to find the initial/final point of the limit cycle*

while norm (residual vector of boundary conditions) > Desired tolerance

$[\boldsymbol{z}^{(\mu_1)}(1, \boldsymbol{p_d}, \boldsymbol{p_r}), \boldsymbol{y}^{(\mu_1)}(1, \boldsymbol{p_d}, \boldsymbol{p_r})]$ = **Integrate** (reformulated DAEBVP-1 DAEs, $\boldsymbol{z_0}(\boldsymbol{p_d}, \boldsymbol{p_r}), \boldsymbol{y_0}(\boldsymbol{p_d}, \boldsymbol{p_r})$)

$[\boldsymbol{z}^{(\mu_2)}(1, \boldsymbol{p_d}, \boldsymbol{p_r}), \boldsymbol{y}^{(\mu_2)}(1, \boldsymbol{p_d}, \boldsymbol{p_r})]$ = **Integrate** (reformulated DAEBVP-2 DAEs, $\boldsymbol{z}^{(\mu_2)}(0, \boldsymbol{p_d}, \boldsymbol{p_r}), \boldsymbol{y}^{(\mu_2)}(0, \boldsymbol{p_d}, \boldsymbol{p_r})$)

$[\boldsymbol{z}^{(\mu_3)}(1, \boldsymbol{p_d}, \boldsymbol{p_r}), \boldsymbol{y}^{(\mu_3)}(1, \boldsymbol{p_d}, \boldsymbol{p_r})]$ = **Integrate** (reformulated DAEBVP-3 DAEs, $\boldsymbol{z}^{(\mu_3)}(0, \boldsymbol{p_d}, \boldsymbol{p_r}), \boldsymbol{y}^{(\mu_3)}(0, \boldsymbol{p_d}, \boldsymbol{p_r})$)

$i \leftarrow i + 1$

$[\boldsymbol{z_o^i}(\boldsymbol{p_d}, \boldsymbol{p_r})]$ = Solve $\left(\begin{bmatrix} \Omega_{\mu_1}^{\mu_2}(t, \boldsymbol{p_d}, \boldsymbol{p_r}) \\ \Omega_{\mu_3}^{\mu_1}(t, \boldsymbol{p_d}, \boldsymbol{p_r}) \\ \Omega_{\mu_2}^{\mu_3}(t, \boldsymbol{p_d}, \boldsymbol{p_r}) \\ \boldsymbol{z}^{(\mu_1)}(\boldsymbol{t_0}(\boldsymbol{p_d}, \boldsymbol{p_r}), \boldsymbol{p_d}, \boldsymbol{p_r}) - \boldsymbol{z}^{(\mu_1)}(\boldsymbol{t_3}(\boldsymbol{p_d}, \boldsymbol{p_r}), \boldsymbol{p_d}, \boldsymbol{p_r}) \end{bmatrix} = \boldsymbol{0} \right)$

$\boldsymbol{z_0}(\boldsymbol{p_d}, \boldsymbol{p_r}) \leftarrow \boldsymbol{z_0^i}(\boldsymbol{p_d}, \boldsymbol{p_r})$

$\boldsymbol{y_0}(\boldsymbol{p_d}, \boldsymbol{p_r}) \leftarrow \boldsymbol{y_0^i}(\boldsymbol{p_d}, \boldsymbol{p_r})$ (obtained based on $\boldsymbol{z_0^i}(\boldsymbol{p_d}, \boldsymbol{p_r})$)

end while

 # the limit cycle is now stored in $\boldsymbol{z}(\boldsymbol{p_d}, \boldsymbol{p_r})$ *and* $\boldsymbol{y}(\boldsymbol{p_d}, \boldsymbol{p_r})$

Analysis of the results from many unsuccessful trials pointed to the observation that the side stream controller's integral term increases monotonically during the cycle. We manually reset this term to the initial value only at the beginning of a new cycle, because, overall, we found this to result in better system performance in terms of cost (Madabhushi and Adams, 2018). Because of this reason, the differential state associated with the side stream controller's integral term had to be dropped from the periodicity constraints enforced on DAE BVP-3. In Case 1, the optimization problem that was used to determine the point on the limit cycle was solved to optimality using IPOPT to a tolerance of 0.0001. The maximum absolute residual error of the differential state vector is less than this tolerance, while this error is slightly greater than tolerance (which is 0.0002) for the algebraic state vector.

When the algorithm failed to converge to the desired convergence tolerance, the controller tuning parameters and the reflux rate were varied until it is met using a trial and error method. Also, at the same time, by varying these design variables the top and bottoms product mass-averaged product purities were ensured to be met. In Figure 4, we present the two-dimensional phase plot between two differential states of Case 1. Convergence to tighter tolerances was found to be difficult, and after many tests, the reason could not be clearly surmised. But it is recognized that it could be due to a combination of numerical errors and the control system. To control the integration errors, the absolute and relative tolerance in the IDAS integrator were both chosen to be 0.00005. An initial step size of 0.001 and a maximum step size of 0.05 was selected. The mass-averaged product purities of the top and bottoms products were found to be 0.65.

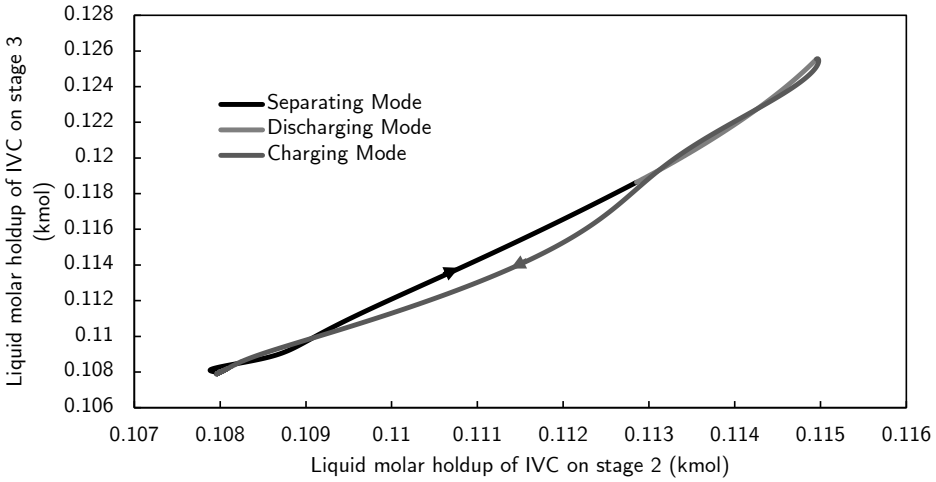

Figure 4: Two-dimensional phase plot illustrating the periodic orbit of the differential states $m_{2,1}(t)$ and $m_{3,1}(t)$ (in Case 1) which was obtained using the single shooting method.

Just as in Case 1, the controller tuning parameter values were varied to ensure convergence of the optimization problem that was used to determine the point on the limit cycle in Case-2. This problem was solved using IPOPT by using a convergence tolerance of 0.0001. The maximum absolute residual error of the differential state vector is less than this tolerance (0.00003), while this error is greater than tolerance (0.003) for the algebraic state vector. However, after analyzing the relative residual error of the algebraic state vector, which is 0.000008, we found that the result is acceptable for all practical purposes. The mass-averaged product purities of the top and bottoms products were found to be 0.96 and 0.951, respectively. The phase plot illustrating the periodic behaviour of this system is presented in Figure 5.

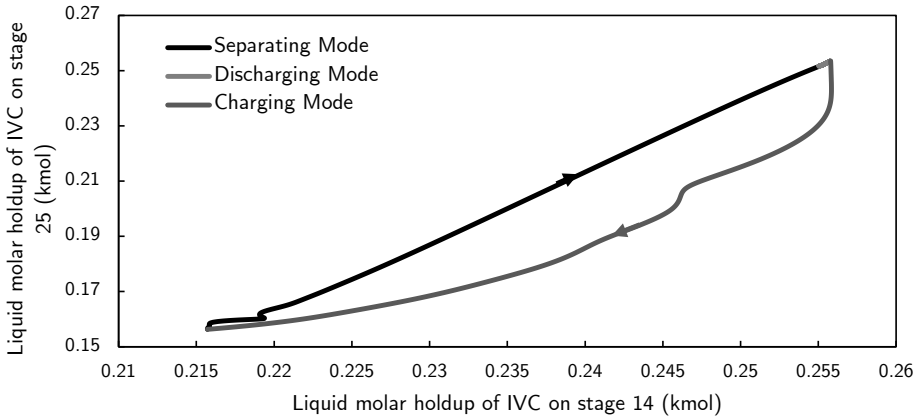

Figure 5: Two-dimensional phase plot illustrating the periodic orbit of the differential states $m_{14,1}(t)$ and $m_{25,1}(t)$ (in Case 2) which was obtained using the single shooting method.

A comparison of the phase plot in Figure 5 with the the phase plot obtained from Aspen Plus Dynamics when using a rigorous model illustrates important differences (Figure 6). From a cursory glance, qualitatively the shape and orientation of the cycles obtained from Aspen Plus Dynamics and the limit cycle found in this study is almost similar, although quantitatively they are very different. Further analysis points that this could be because of two reasons, firstly, a rigorous column model is used in Aspen to model the system as opposed to a simple model that was used in this study. Secondly, we observed that the for a certain period during the cycle the rate of material is recycled to the middle-vessel through the side stream is less in case of the Aspen model when compared to the CasADi (simple) model used in this study (Figure 7). Therefore, there is less material holdup in the column leading to a smaller span of the limit cycle (Figure 6) found in the current study.

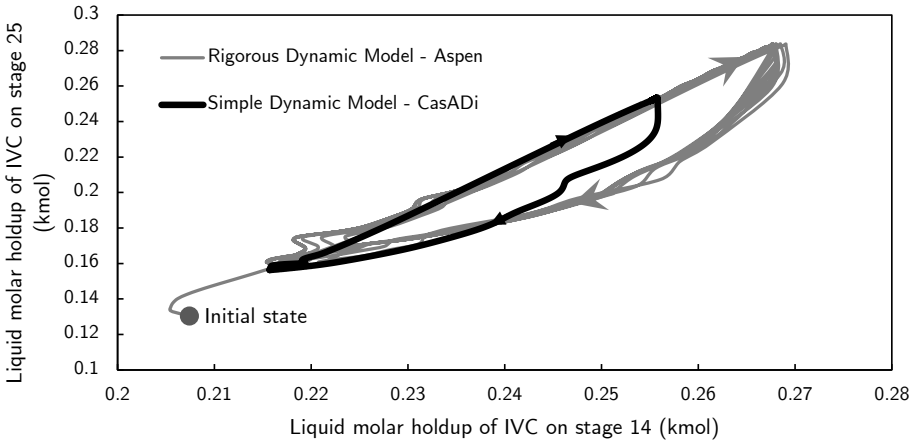

Figure 6: Plot illustrating the quantitative and qualitative differences in the cycles found using the rigorous model (10 cycles) and the limit cycle found using the simple model and the single shooting method.

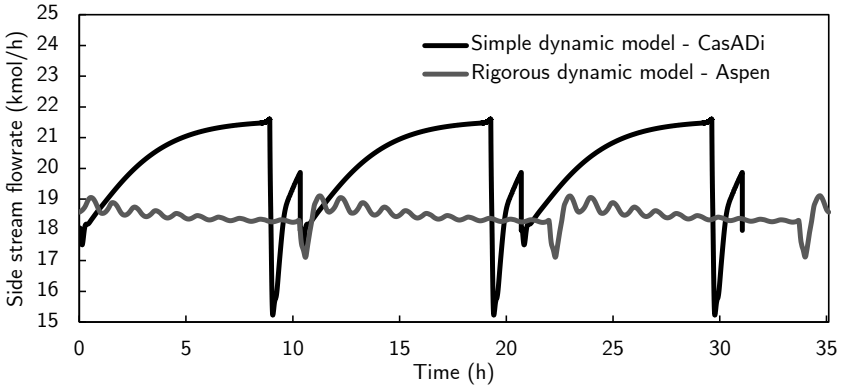

Figure 7: Plot illustrating the quantitative difference in the side stream flowrates.

A plot showing the dynamics of the mole fraction of the components in the middle vessel is presented as Figure 8. Since the focus of this article is to demonstrate the application of the algorithm for design, we do not check the feasibility of the column operation in terms of meeting the flooding, weeping, and weir loading limits in the cases. However, these limits can be easily met by adjusting the cross-sectional area of the trays (A_{Tray}) in the distillation column. Most importantly, the side stream pump and valve can be sized after the designing the system based on the trajectory of the side stream flowrate, which is in stark contrast to the backstepping design methodology.

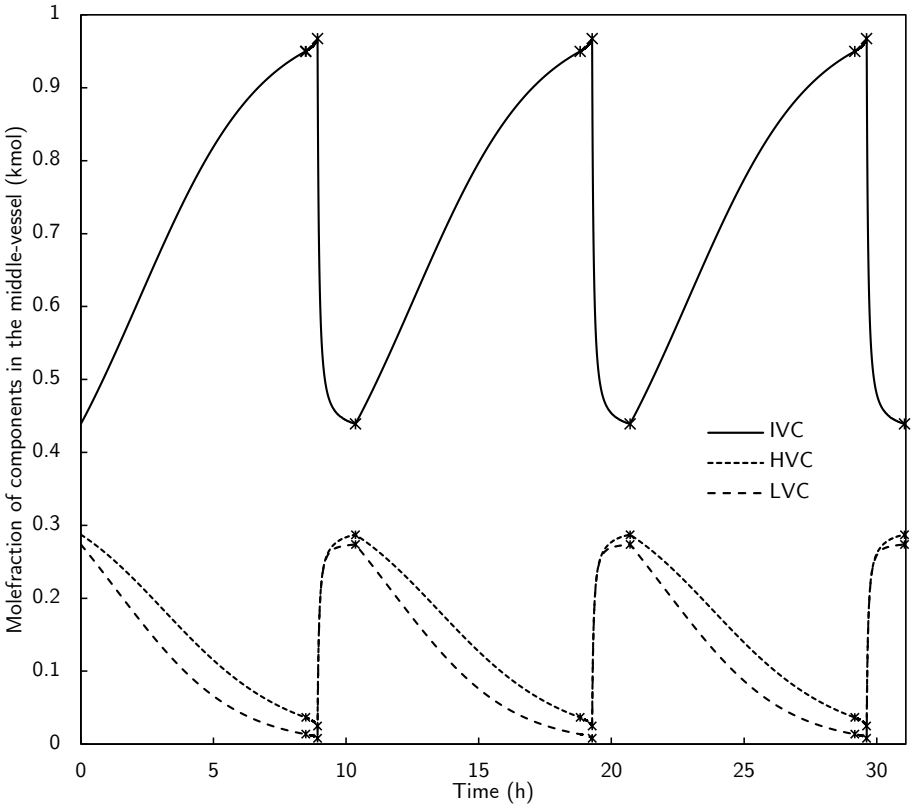

Figure 8: Plot illustrating the mole fraction dynamics of the components in the middle vessel. The stars indicate the time at which mode transitions occur.

6. Conclusion and Future work

This paper presents the application of the single shooting method for use in the design of semicontinuous distillation of ternary mixtures. The existing design methodologies were based on heuristics, and neither provided a guarantee on the optimality of the design obtained nor helped in identifying the precise location of the limit cycle. In this article, the proposed algorithm was applied to two case studies, both involving the separation of hexane, heptane, and octane, to demonstrate its use in determining the location of the limit cycle accurately to the desired convergence tolerance. We envision to incorporate the proposed single shooting algorithm in a gradient-based optimization framework to find the optimal semicontinuous distillation design for the separation of a given mixture in the future. The python files of this study are available on LAPSE: http://psecommunity.org/LAPSE:2020.0029.

Acknowledgment

This work was supported by the McMaster Advanced Control Consortium (MACC) and the Ontario Research Fund, grant number RE09-058.

Nomenclature

Abbreviations

HVC	High volatile component
LVC	Low volatile component
IVC	Intermediate volatile component
DAE	Differential Algebraic Equations
SP	Setpoint
PV	Process variable
DAE-BVP	Boundary value problem involving differential-algebraic equations
hybrid-BVP	Boundary value problem involving the hybrid model

Greek symbols

ρ_n^{liq}	Density of liquid on tray n
θ_i	i^{th} epoch in the hybrid model
μ_i	Mode i in the hybrid model
$\boldsymbol{\Psi}_{cc}$	Differential equations of the column and the control system
$\boldsymbol{\Phi}_{cc}$	Algebraic equations of the column and the control system
$\boldsymbol{\Psi}_{mv}^{(\mu_i)}$	Differential equations of the middle-vessel in mode μ_i
$\boldsymbol{\Phi}_{mv}^{(\mu_i)}$	Algebraic equations of the middle-vessel in mode μ_i
$\Omega_{\mu_i}^{\mu_j}$	The condition required to transition from mode μ_i to mode μ_j at t_i
$\boldsymbol{\Theta}_{\boldsymbol{z}_{\mu_i}^{\mu_j}}$	Transition functions of the hybrid model related to the differential variables
$\boldsymbol{\Theta}_{\boldsymbol{y}_{\mu_i}^{\mu_j}}$	Transition functions of the hybrid model related to the algebraic variables
ζ	Binary number
ς	Binary number

α	Binary Number
β	Binary Number
Γ	Period of oscillation
τ	Dummy time variable

Other Symbols

$\boldsymbol{p_d}$	Vector of design variables that take discrete values (discrete design variables)
$\boldsymbol{p_r}$	Vector of design variables that take real values (real design variables)
$\boldsymbol{z}$	Vector of differential state variables
$\boldsymbol{z_0}$	Vector that specifies the initial state of the differential variables
$\boldsymbol{y}$	Vector of algebraic state variables
$\boldsymbol{y_0}$	Vector that specifies the initial state of the algebraic variables
t_i	Time at which there is a switch in the model equations of the middle-vessel, $i = 1, 2, 3$
$x_{1,HVC}(t)$	Mole fraction of HVC on stage 1
$x_{1,HVC}^{desired}$	Desired mole fraction of HVC on stage 1
$x_{mv,IVC}^{(\mu_1)}$	Mole fraction of the intermediate volatile component in the middle-vessel in mode μ_1
$x_{mv,IVC}^{desired}$	Desired purity value of the intermediate volatile component in the middle-vessel
$x_{N_s,LVC}(t)$	Mole fraction of HVC on stage N_s
$x_{N_s,LVC}^{desired}$	Desired mole fraction of HVC on stage N_s
$h_{mv}^{(\mu_2)}$	Height of the liquid in the middle-vessel in mode μ_2
h_v^l	Predetermined lower limit of height of the liquid in the middle-vessel
h_{mv}^u	Predetermined upper limit of height of the liquid in the middle-vessel
$h_{reflux}(t))$	Height of liquid in the reflux drum
$h_{reflux}^{desired}$	Desired height of liquid in the reflux drum
$h_{sump}(t)$	Height of liquid in the sump
$h_{sump}^{desired}$	Desired height of liquid in the sump

n	Stages
n_f	Feed stage location
n_s	Side stream stage
c	Components
N_s	Total number of stages
$m_{n,c}$	Liquid molar holdup of component c on stage n
M_n	Total molar holdup of liquid on stage n
$l_{n,c}$	Liquid flowrate of component c leaving stage n
L_n	Total flowrate of liquid leaving stage n
$v_{n,c}$	Vapour molar flowrate of component c entering stage n
V_n	Total flowrate of vapour leaving stage n
S	Side stream flowrate
d	Distillate flowrate
b	Bottoms flowrate
F	Feed flowrate to the column
V_{N_s}	Reboil rate
d_c	Distillate molar flowrate of component c leaving stage 1
f_c	Molar flowrate of component c in the liquid feed
s_c	Molar flowrate of component c in the liquid side stream
b_c	Bottoms molar flowrate of component c leaving the stage N_s
K_c	Phase equilibrium ratio of component c on stage n
$y_{n,c}$	Mole fraction of component c in the vapour leaving stage n
$x_{n,c}$	Mole fraction of component c in the liquid leaving stage n
T_n	Temperature of the stage n
P_n	Pressure of the stage n
A_c	Antoine parameter for component c
B_c	Antoine parameter for component c

C_c	Antoine parameter for component c
D_c	Antoine parameter for component c
E_c	Antoine parameter for component c
A_{Tray}	Tray cross-sectional area
A_{reflux}	Cross-sectional area of the reflux drum
A_{sump}	Cross-sectional area of the sump
h_{weir}	Weir height
L_{weir}	Weir length
g	gravitational constant
R_{gas}	Ideal gas constant
T_c^{cr}	Critical temperature of component c
P_c^{cr}	Critical pressure of component c
Z_c^{Ra}	Rackett compressibility factor of component c
u	Manipulated variable
u_{bias}	Controller bias
K_p	Proportional gain
K_i	Integral gain
e	error (Setpoint – Process Variable value at time t)
I	differential state of the integral term of the PI controller
$m_{mv,c}$	Liquid molar holdup of component c in the middle vessel
$f_{charge,c}$	Liquid flowrate of component c in the charging stream
$f_{discharge,c}$	Liquid flowrate of component c in the discharge stream
T_μ	Mode trajectory of the hybrid model

References

Adams II, T.A., Pascall, A., 2012. Semicontinuous Thermal Separation Systems. Chem. Eng. Technol. 35, 1153–1170. https://doi.org/10.1002/ceat.201200048

Adams, T.A., Pascall, A., 2012. Semicontinuous Thermal Separation Systems. Chem. Eng. Technol. https://doi.org/10.1002/ceat.201200048

Andersson, J.A.E., Gillis, J., Horn, G., Rawlings, J.B., Diehl, M., 2019. CasADi: a software framework for nonlinear optimization and optimal control. Math. Program. Comput. https://doi.org/10.1007/s12532-018-0139-4

Annakou, O., Mizsey, P., 1995. Rigorous investigation of heat pump assisted distillation. Heat Recover. Syst. CHP 15, 241–247. https://doi.org/10.1016/0890-4332(95)90008.

Ascher, U.M., Petzold, L.R., 1998. Computer methods for ordinary differential equations and differential-algebraic equations, Computer Methods for Ordinary Differential Equations and Differential-Algebraic Equations. https://doi.org/10.1137/1.9781611971392

Aspen Plus ® Dynamics [WWW Document]. AspenTech Inc. URL https://www.aspentech.com/en/products/pages/aspen-plus-dynamics (accessed 11.23.19a).

Bansal, V., Perkins, J.D., Pistikopoulos, E.N., 2002. A case study in simultaneous design and control using rigorous, mixed-integer dynamic optimization models. Ind. Eng. Chem. Res. https://doi.org/10.1021/ie010156n

Barton, P.I., 1992. The modelling and simulation of combined discrete/continuous processes. Imperial College London.

Barton, P.I., Lee, C.K., 2004. Design of process operations using hybrid dynamic optimization, in: Computers and Chemical Engineering. https://doi.org/10.1016/j.compchemeng.2003.09.015

Flatby, P., Skogestad, S., Lundström, P., 1994. Rigorous Dynamic Simulation of Distillation Columns Based on UV-Flash. IFAC Proc. Vol. https://doi.org/10.1016/s1474-6670(17)48161-4

Galán, S., Feehery, W.F., Barton, P.I., 1999. Parametric sensitivity functions for hybrid discrete/continuous systems. Appl. Numer. Math. https://doi.org/10.1016/S0168-9274(98)00125-1

Gani, R., Ruiz, C.A., Cameron, I.T., 1986. A generalized model for distillation columns-I. Model description and applications. Comput. Chem. Eng. https://doi.org/10.1016/0098-1354(86)85001-3

Green, D.W., Southard, M.Z., 2019. Perry's Chemical Engineers' Handbook, 9th Edition, McGraw-Hill Education.

Hindmarsh, A.C., Brown, P.N., Grant, K.E., Lee, S.L., Serban, R., Shumaker, D.E., Woodward,

C.S., 2005. SUNDIALS: Suite of nonlinear and differential/algebraic equation solvers. ACM Trans. Math. Softw. https://doi.org/10.1145/1089014.1089020

Khan, K.A., Saxena, V.P., Barton, P.I., 2011. Sensitivity analysis of limit-cycle oscillating hybrid systems. SIAM J. Sci. Comput. https://doi.org/10.1137/100804632

Khayet, M., 2011. Membranes and theoretical modeling of membrane distillation: A review. Adv. Colloid Interface Sci. 164, 56–88. https://doi.org/10.1016/J.CIS.2010.09.005

Kiss, A.A., 2014. Distillation technology - still young and full of breakthrough opportunities. J. Chem. Technol. Biotechnol. https://doi.org/10.1002/jctb.4262

Kiss, A.A., 2013. Advanced Distillation Technologies. John Wiley & Sons, Ltd, Chichester, UK. https://doi.org/10.1002/9781118543702

Lamour, R., März, R., Weinmüller, E., 2015. Boundary-Value Problems for Differential-Algebraic Equations: A Survey. https://doi.org/10.1007/978-3-319-22428-2_4

Madabhushi, P.B., Adams, T.A., 2019. Finding Better Limit Cycles of Semicontinuous Distillation. 1. Back Stepping Design Methodology. Ind. Eng. Chem. Res. 58, 16654–16666. https://doi.org/10.1021/acs.iecr.9b02639

Madabhushi, P.B., Adams, T.A., 2018. Side stream control in semicontinuous distillation. Comput. Chem. Eng. https://doi.org/10.1016/j.compchemeng.2018.09.002

Madabhushi, P.B., Medina, E.I.S., Adams, T.A., 2018. Understanding the dynamic behaviour of semicontinuous distillation, in: Computer Aided Chemical Engineering. https://doi.org/10.1016/B978-0-444-64235-6.50148-0

Maleta, V.N., Kiss, A.A., Taran, V.M., Maleta, B. V., 2011. Understanding process intensification in cyclic distillation systems. Chem. Eng. Process. Process Intensif. 50, 655–664. https://doi.org/10.1016/j.cep.2011.04.002

Meidanshahi, V., Adams, T.A., 2016. Integrated design and control of semicontinuous distillation systems utilizing mixed integer dynamic optimization. Comput. Chem. Eng. https://doi.org/10.1016/j.compchemeng.2016.03.022

Parker, T.S., Chua, L.O., Parker, T.S., Chua, L.O., 1989. Locating Limit Sets, in: Practical Numerical Algorithms for Chaotic Systems. https://doi.org/10.1007/978-1-4612-3486-9_5

Pascall, A., Adams, T.A., 2013. Semicontinuous separation of dimethyl ether (DME) produced from biomass. Can. J. Chem. Eng. https://doi.org/10.1002/cjce.21813

Perry, R.H., Green, D.W., 2013. Perry's Chemical Engineers' Handbook, 8th Edition, Journal of Chemical Information and Modeling. https://doi.org/10.1017/CBO9781107415324.004

Petlyuk, F.B., 2004. Distillation Theory and Its Application to Optimal Design of Separation Units. Cambridge University Press, Cambridge. https://doi.org/10.1017/CBO9780511547102

Phimister, J.R., Seider, W.D., 2000. Semicontinuous, middle-vessel distillation of ternary mixtures. AIChE J. https://doi.org/10.1002/aic.690460804

Prokopakis, G.J., Seider, W.D., 1983. Dynamic simulation of azeotropic distillation towers. AIChE J. https://doi.org/10.1002/aic.690290622

Seydel, R., 2010. Practical Bifurcation and Stability Analysis, Interdisciplinary Applied Mathematics. https://doi.org/10.1007/978-1-4419-1740-9

Skogestad, S., 1997. Dynamics and control of distillation columns - A critical survey. Model. Identif. Control. https://doi.org/10.4173/mic.1997.3.1

Toftegàrd, B., Clausen, C.H., Jørgensen, S.B., Abildskov, J., 2016. New Realization of Periodic Cycled Separation. Ind. Eng. Chem. Res. https://doi.org/10.1021/acs.iecr.5b03911

Wächter, A., Biegler, L.T., 2006. On the implementation of an interior-point filter line-search algorithm for large-scale nonlinear programming. Math. Program. https://doi.org/10.1007/s10107-004-0559-y

Wijesekera, K.N., Adams, T.A., 2015a. Semicontinuous Distillation of Quintenary and N-ary Mixtures. Ind. Eng. Chem. Res. https://doi.org/10.1021/acs.iecr.5b03219

Wijesekera, K.N., Adams, T.A., 2015b. Semicontinuous distillation of quaternary mixtures using one distillation column and two integrated middle vessels. Ind. Eng. Chem. Res. https://doi.org/10.1021/ie504584y

Chapter 5

Conclusions and Future Work

5.1 Conclusions

Distilling ternary mixtures through semicontinuous distillation has been a topic of research for the past twenty years. During this time, strides were made to make the process a competing alternative to batch or continuous distillation in terms of economics. Simultaneously, the application of this technology for the separation of several ternary chemical mixtures was demonstrated through computer simulations. In almost all these studies, the process was designed using the sequential design methodology, which had its basis in heuristics. In this thesis, the use of two of them, perhaps the essential ones, was challenged.

Until recently, the recycle rate of the material pumped to the middle vessel through the column side stream was given by the "Ideal side draw recovery arrangement," which generated setpoint trajectories for a PI controller to follow. These setpoint trajectories, which were supposed to help in limiting the loss of intermediate volatile component through the distillate and bottoms streams, also restricted the rate of the recycled material. Therefore, in this thesis, the status quo, which was used for the last fifteen years, was replaced with a modified version by incorporating two key elements. First, the modified version allowed the faster recycling of material to the middle-vessel via the side stream, which implied that the intermediate volatile component in the middle-vessel reached the desired purity much faster. Consequently, the processing time was reduced, leading to a significant reduction in the separating cost.

Second, the trajectories obtained when using the modified version were found to be close to the trajectories obtained when minimizing the separating cost using a dynamic optimization routine. Therefore, instead of using the traditional control vector parametrization to find the side stream control trajectory that minimizes cost, for all practical purposes, it seems to be sufficient to use the modified model with the controller tuning parameters as decision variables. In terms of complexity, in a direct sequential dynamic optimization framework, optimizing only the controller parameters is a much simpler problem because of the reduced number of decision variables. Moreover, the dynamic optimization problems presented in Chapter 2 are not well-posed (because of software constraints), which led to several convergence issues such as QP subproblem and filter line search failures. The final time should not be an optimization decision variable since it is an implicit function of the design. Instead, the solution strategy provided in Chapter 4 should be followed.

Simulation experiments conducted shortly afterwards (presented in Chapter 3) showed that sub-optimal designs were obtained from the sequential design methodology, mainly because the designs consist of side stream pump and valve sizes that restricted the maximum flowrate pumped to the middle-vessel. Therefore, to get a much higher impact from using the "Modified-Ideal side draw recovery arrangement" for side stream flowrate control, the back-stepping design methodology was proposed. The designs obtained from the procedure will have a larger side stream pump and valve than the best-known designs, which will allow faster recycling of material to the middle-vessel and thereby cost-benefits. Moreover, the designs obtained from this design procedure are guaranteed to have feasible column operation, i.e., the flooding, weeping, and weir loading limits were satisfied. Additionally, it features advanced capabilities in terms of classifying different kinds of steady-states that systems exhibit to restrict the domain for black-box optimization to a desirable region. At most, a CPU-week is required to obtain a substantially improved design in terms of cost using this new design methodology, while it takes almost a CPU-month to obtain a 'PSO optimized' design using the sequential design methodology. Particle swarm optimization, which does not mathematically guarantee solution

optimality, was typically used in both these design procedures to find the values of the design variables that minimized cost. Thus, it is advisable to test the solution obtained for local optimality (at least) by performing a neighbourhood search.

Although the back-stepping design procedure yielded cost-effective designs compared to the state-of-the-art, it has drawbacks. Firstly, a large number of simulations are still necessary to restrict the design space, thus requiring significant CPU times for design. Moreover, the black-box optimization routine used to find a better design in terms of cost does not guarantee the optimality of the design. Additionally, in this black-box optimization stage, a heuristic termination criterion is used to detect the convergence to a limit cycle for ending a semicontinuous distillation simulation run. A heuristic termination criterion is necessary because the convergence to a limit cycle was ascertained by visual observation by tracking the trajectories of some state variables. Therefore, to address the issues, the single shooting method for semicontinuous distillation design was demonstrated in Chapter 4, which is a direct method for finding the limit cycle.

5.2 Future Work

The single shooting method was found to be an very good alternative for semicontinuous distillation design compared to the heuristic-based design procedures, and thus future work should be focused on improving it further. The convergence of the algorithm presented in Chapter 4 to a desired mass-average product purity was ensured by varying the controller tuning parameters and the reflux rate using a trial and error method. A manual guess and check procedure is not an efficient way of making the algorithm meet the desired specification. Therefore, the immediate goal should be to automate this process by incorporating it as one of the constraints in the optimization problem that was used to find the limit cycle.

In the current form, this method can be used to simulate the periodic steady-states of the process for different design variable values and extract useful information such as flowrate, heating duty and cooling duty trajectories and cycle time. However, to find the optimal semicontinuous distillation design, this method could be used in conjunction with any of the gradient-based optimization methods for dynamic optimization. This optimal design problem will be an optimization problem in the finite-dimensional space if PI controllers are used for manipulating the control variables to meet the setpoints. However, when the optimal control trajectories also have to found, it will be an optimization problem in the infinite-dimensional space, although this level of sophistication may be unnecessary, judging from the dynamic optimization results obtained in Chapter 2. Furthermore, the full design space of this process consists of integer variables; therefore, it may be ideal to first consider the dynamic optimization of the design by fixing the integer-valued parameters before solving the mixed-integer dynamic optimization problem.

The single shooting method of finding the process limit cycle is ideal for use in a closed-loop economic model predictive control framework to find the optimal control trajectories (in real-time) that ensure limit cycle operation despite process uncertainties. Since optimal control trajectories have to be computed in real-time, a linear time-varying model should perhaps be identified for use in the MPC framework from an implementation point of view. Furthermore, the design of the control system, i.e., finding controller tuning parameters to meet a control performance criterion, is still based on a guess and check procedure. Therefore, there is an immediate need to devise a method to address this issue. Perhaps the best approach may be to incorporate this requirement as an additional criterion when finding the optimal design. Furthermore, with the explosion in high-performance parallel computing, viewing the hybrid system as a sequence of boundary value problems in the different modes (Chapter 4) is particularly advantageous as it opens up avenues for parallelization and thereby reducing CPU time. With so many different valuable avenues, it is better to focus more on the areas mentioned above in future research.

In a much broader context, semicontinuous distillation as a technology is still

a concept that needs considerable research focus from the experimental front. Although there is a vast body of literature that is in support of this process from an economic perspective, there is no knowledge about the start-up procedure. Also, plant-wide dynamic simulation studies after the inclusion of semicontinuous distillation are necessary to ascertain safety and develop plant start-up guidelines.